

POLITECNICO DI TORINO

MECHANICAL AND AEROSPACE ENGINEERING DEPARTMENT



Master's Degree in Aerospace Engineering

**Conceptual design of hydrogen-powered
high-speed aircraft in low supersonic regime**

Professors:

Dr. Davide Ferretto

Prof.ssa Nicole Viola

Student:

Emanuele SUNZERI

OCTOBER 2023

*"To all the stars that have illuminated my path,
and those I have yet to reach."*

Abstract

The thesis aims to create a methodology capable of generating a conceptual design for a liquid hydrogen-powered supersonic civilian aircraft at Mach 2, validating it through parameter variations, specifically using Mach 1.5 and Mach 2.5. The methodology begins with a statistical analysis of aircraft concepts that do not yet exist due to both regulations that do not permit them and the fact that liquid hydrogen as aircraft fuel is a developing technology. Afterward, all aerodynamic aspects, fuel weight considerations, and operational empty weight are calculated. The verification of wing loading and thrust-to-weight ratio requirements is then carried out, concluding with the design of the tanks, which is crucial for an aircraft of this type because LH2 has a much lower density compared to conventional fuels, necessitating larger storage space. These calculations are iterated until the total calculated mass is similar to that of the previous iteration. At that point, using the obtained data, various graphs and preliminary aircraft designs are developed. A strong point of the methodology is that the user can choose input data according to their preferences, allowing for the generation of different configurations. In the thesis, 5 different configurations are also analyzed (one for design point and the other for validation), varying the Mach number and the number of passengers. The method used for the calculations is the same as for conventional aircraft, with appropriate modifications to meet the requirements imposed by this new technology.

Contents

1	Introduction	5
1.1	Why Liquid Hydrogen as a fuel?	5
1.1.1	Property of LH2	6
1.1.2	Cost of LH2 compared to conventional fuel	8
1.2	Why fly supersonic?	10
1.3	Thesis outline	12
2	Reference Aircraft and Initial Point of design	15
2.1	Reference Aircraft	15
2.2	Project's requirement	23
2.3	Input Data	24
2.3.1	Requirements	24
2.3.2	Mission profile	24
2.3.3	Aerodynamics	25
2.3.4	Fuel Weight	25
2.3.5	Operative Empty Weight	25
2.3.6	W/S Requirements Verification	28
2.3.7	T/W Requirements Verification	29
2.3.8	Tank sizing	29
3	Structure of methodology	31
3.1	General functioning	33

4	Statistical Analysis and Mission Profile	35
4.1	Statistical Analysis	35
4.1.1	Definition of MTOW	36
4.1.2	Definition of others parameters	37
4.2	Mission profile	39
5	Aerodynamics	42
5.1	Lift	42
5.1.1	Subsonic	43
5.1.2	Supersonic	45
5.2	Drag	46
5.2.1	Subsonic	46
5.2.2	Supersonic	55
5.3	Aerodynamic efficiency	57
5.4	Aerodynamics output	57
6	Fuel Weight and Operative Empty Weight	63
6.1	Fuel weight	63
6.1.1	Raymer's method	64
6.2	Operative empty weight	66
6.3	Output data	68
6.3.1	Fuel weight	68
6.3.2	Operative empty weight	69
7	Performance requirements verification	71
7.1	Wing Loading Requirements	72
7.2	Thrust to weight ratio requirements	73
7.3	Matching Chart	78
7.4	Output Data	79
7.4.1	Wing Loading Requirements	79
7.4.2	Thrust to weight ratio requirements	80
7.4.3	Matching chart	80

8 Tank sizing	88
8.1 Underfloor Tank Configuration	88
8.2 Rear Tank and Aircraft Length Definition	92
8.2.1 Rear Tank	92
8.2.2 Aircraft Length	92
8.3 Layers Thickness of Structural and Insulation Material	94
8.3.1 Structural design	94
8.3.2 Insulation design	96
8.3.3 Sizing Procedure	98
8.4 Output data	100
8.5 End Convergence Loop	106
9 Aircraft center of gravity and comparison of configuration	108
9.1 Aircraft center of gravity	108
9.2 Comparison of configuration	109
9.2.1 Configuration A: 80 pax and Mach 2	109
9.2.2 Configuration B: 60 pax and Mach 2	112
9.2.3 Configuration C: 100 pax and Mach 2	114
9.2.4 Configuration D: 80 pax and Mach 1.5	116
9.2.5 Configuration E: 80 pax and Mach 2.5	118
10 Conclusion and future trend	121
List of Figure	124
List of Tables	128
Bibliography	131

Chapter 1

Introduction

1.1 Why Liquid Hydrogen as a fuel?

In the last decades, aeronautics's industry tried to reach better aircraft performance, specially about energy efficiency end environmental sustainability. At a time when global attention is increasingly focused on climate change and reducing greenhouse gas emissions, innovation in aviation has become crucial to addressing the challenges posed by this industry. Indeed, as mentioned in [20], the projection of CO₂ production is growing significantly, as can also be seen in the following image. It is therefore important to take action to counteract this phenomenon.

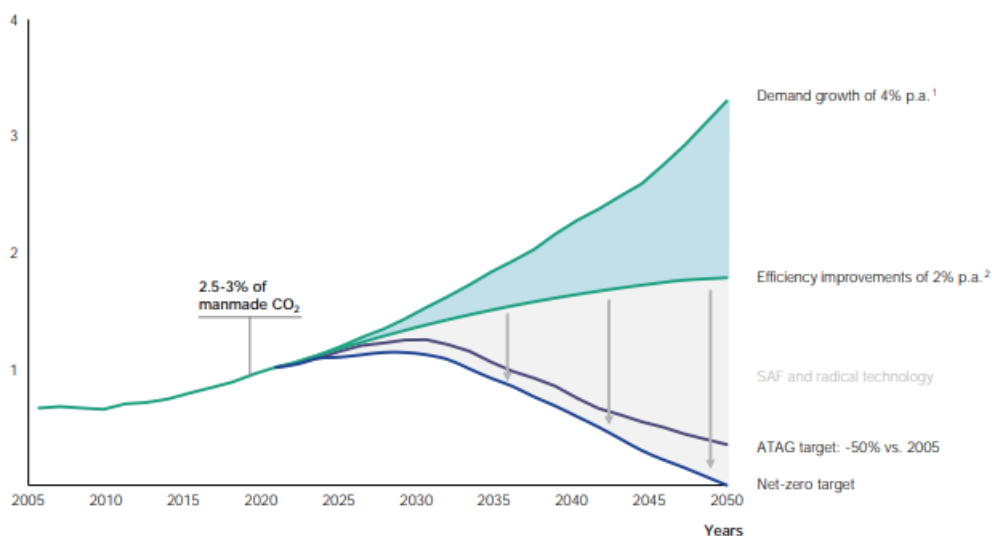


Figure 1.1: Projection of CO₂ emissions from aviation (from [20])

Among many innovations underway, the adoption of hydrogen as an aviation fuel has captured the imagination of developer. Hydrogen, known for its exceptional energy properties and producing only water as a by-product of combustion, has proven to be a promising candidate for creating a sustainable alternative to fossil fuels in aviation.

In this perspective, this thesis focuses on the development of a methodology capable of generating concepts for a supersonic aircraft powered by liquid hydrogen, as a function of various input parameters, the main ones being: Mach, number of passengers and the Range. Such an aircraft would represent a significant evolution in the aviation scenario, combining the speed and efficiency of supersonic flight with the environmental benefits of hydrogen as a fuel. The main challenge in this context is to balance aerodynamic performance and propulsion with the peculiarities of hydrogen, such as energy density management, flammability and on-board distribution.

Through an in-depth analysis of existing technologies, technological challenges and opportunities for innovation, this thesis aims to create a program capable of analyzing the primary aspects of the design of this aircraft, considering aspects related to propulsion systems, the aerodynamic optimization, the determination of the various weights and also the design of the hydrogen tanks, which are decisive in terms of size.

Ultimately, this thesis not only aims to advance the knowledge of the feasibility of a hydrogen supersonic aircraft, but also to contribute to the global debate on the evolution of aviation towards more environmentally friendly solutions. The ultimate goal is to imagine a future in which speed and technological innovation are combined with sustainability, paving the way (especially from the regulatory point of view) for an aviation sector capable of flying through the skies with less environmental impact.

1.1.1 Property of LH2

Liquid hydrogen (LH2) is a form of hydrogen that occurs in a liquid state at extremely low temperatures, close to absolute zero (-273.15°C or 0 K) and moderate pressures. It has been considered a promising candidate as an aviation fuel due to its unique properties and low emission of pollutants. Here is an overview of the main properties of liquid hydrogen used as fuel for an aircraft:

- **High Energy Density:** Despite its low density, hydrogen has an exceptionally

high energy potential. This means that a small amount of liquid hydrogen can store a large amount of energy, making it ideal for aircraft applications that require high power and performance.

- **Zero Emissions:** Combustion of liquid hydrogen produces only water as a by-product. This makes it one of the cleanest fuels available, in contrast to fossil fuels which emit carbon dioxide (CO₂) and other air pollutants.
- **High Burn Rate:** Hydrogen has a very high burn rate, which can translate into better engine performance and higher thermal efficiency.
- **High flame temperature:** Hydrogen has a very high flame temperature compared to other fuels, which can improve combustion cycle efficiency and reduce emissions of nitrogen oxides (NO_x), known air pollutants.
- **Light Weight:** Hydrogen is the lightest element in the universe, which results in greater weight efficiency for aircraft payload and fuel consumption. However, it is important to account for the additional weight of insulated tanks and the structures required to handle liquid hydrogen.
- **Intake Air Cooling:** The evaporation of liquid hydrogen can be used to cool the engine's intake air, improving overall efficiency and performance.
- **Complex thermal management:** Due to the low storage temperatures of liquid hydrogen, storage and distribution systems require advanced thermal insulation to prevent thermal energy loss. This complex thermal management can present an engineering challenge.
- **Flammability:** Hydrogen is highly flammable, requiring special precautions in the design of storage, distribution and safety systems on board aircraft.

In summary, liquid hydrogen offers a number of properties that make it attractive as an aviation fuel, especially for the purpose of reducing greenhouse gas emissions and improving environmental sustainability. However, the adoption of this technology brings technological and logistical challenges, requiring insights into materials engineering, systems safety and aeronautical design.

1.1.2 Cost of LH2 compared to conventional fuel

In addition to the environmental aspects, it is crucial to consider the production costs, including infrastructure, associated with both of these fuels.

Liquid Hydrogen (LH2): Liquid hydrogen, as already mentioned, is considered an environmentally friendly energy source in the aviation industry since its combustion produces only water vapour. However, the production, distribution and use of LH2 involves significant costs. The production of LH2 requires the use of energy for the electrolysis of water or the reforming of natural gas. These processes can be expensive and are highly dependent on the price of the energy used.

A crucial aspect of the cost of liquid hydrogen is the infrastructure required for its transportation and storage. Liquid hydrogen requires extremely low temperatures to remain liquid, so a highly specialized cold chain is required. This implies significant investments in cryogenics and thermal insulation technologies in airport and refueling infrastructure. Such investments can significantly affect the total cost of producing and distributing LH2. There are projections that make this aspect clear, indeed it is estimated that by 2050 the cost will be comparable to that of conventional fuel.

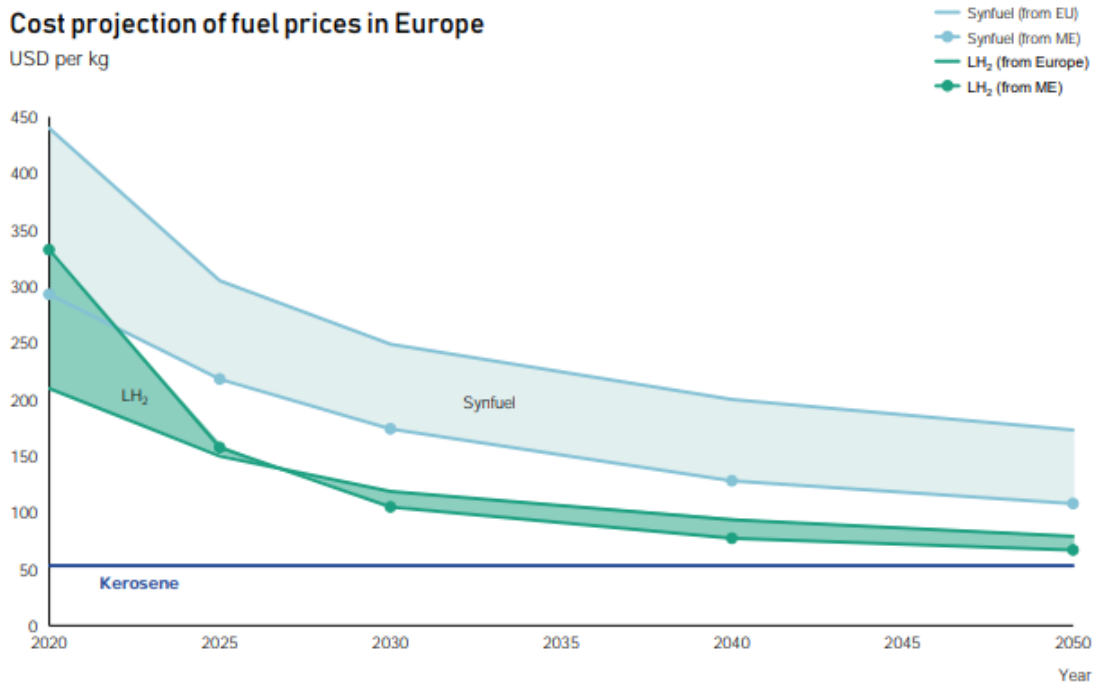


Figure 1.2: Cost projection of landed costs at EU airports (from [20])

A-1 Jet Fuel: Jet A-1 is the conventional fuel widely used in commercial aviation. Its production involves crude oil refining processes, which can vary according to fluctuations in oil prices. However, oil refining is an established technology and existing infrastructure can be used for its production and distribution. This can help keep Jet A-1 production costs relatively stable, despite oil price fluctuations.

Cost Comparison: While the LH2 offers environmental benefits, its production costs are often higher than the Jet A-1. The infrastructure suitable for the production, storage and distribution of liquid hydrogen requires considerable investment, increasing operating costs for airlines. Furthermore, the energy supply for electrolysis or reforming can represent a significant part of the total costs. All this is also to be included in the airport environment, going to have to create a new regulation to keep everything safe. On the other hand, the Jet A-1, being based on existing oil refining technologies, can benefit from economies of scale and infrastructure already in place. However, it should be noted that Jet A-1 costs may fluctuate based on crude oil price fluctuations and changes in global energy policies. In the following image, the LCC (Life Cycle Cost) of an aircraft using traditional fuel are compared with those of one using LH2 (Liquid Hydrogen) and another using synthetic fuel. It is evident that opting for an LH2 configuration is the most effective choice for reducing harmful emissions.

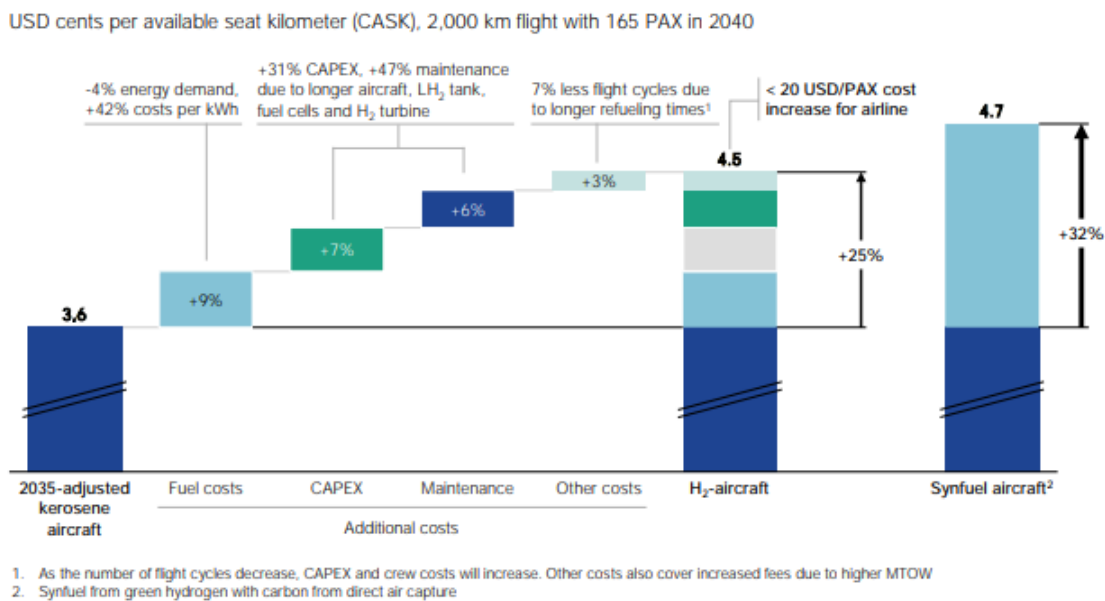


Figure 1.3: Cost comparison of H2 short-range aircraft versus kerosene and synfuel aircraft (from [20])

In conclusion, the cost of production including infrastructure plays a major role in choosing between LH2 and Jet A-1 in the aviation industry. Liquid hydrogen represents a greener solution, but currently entails higher production costs due to technological and infrastructural needs. Meanwhile, the Jet A-1 offers stability and cost familiarity, but carries with it environmental concerns related to greenhouse gas emissions. Deciding between these options requires a balance between environmental sustainability and economic feasibility.

1.2 Why fly supersonic?

Civil aviation has undergone continuous evolution over the years, prompting developers to explore new frontiers to improve the efficiency, speed and comfort of air travel. Supersonic flight, involving speeds exceeding Mach 1 (the speed of sound), has emerged as a potential innovation in the aviation industry. However, there are significant benefits and challenges to be faced when considering the integration of supersonic flight into civil aviation.

Benefits of Supersonic Flight:

- **High Speed:** The most obvious advantage of supersonic flight is speed. Supersonic aircraft can dramatically reduce travel time between distant destinations. This could be especially beneficial for business travelers or for emergency situations that require a quick response.
- **Reduction of Travel Time:** The increased speed of supersonic flight could allow faster transoceanic and transcontinental travel, opening up new possibilities for connecting cities and markets.
- **Time Efficiency:** Traveling faster reduces the need for long overnight layovers or extended disruptions, improving flight efficiency.
- **Exclusive Travel Experience:** Supersonic flight could offer a premium and luxurious travel experience, attracting a segment of passengers willing to pay more to save time and enjoy high-quality services on board.

- **Promotion of Innovation:** The development of technologies for supersonic flight could stimulate innovation in various sectors of aeronautical and aerospace engineering, contributing to the general progress of the industry.

Disadvantages of Supersonic Flight:

- **High Fuel Consumption:** Supersonic flights require increased fuel consumption due to aerodynamic drag and the energy required to overcome the sound barrier. This could increase greenhouse gas emissions and operating costs. In fact, precisely for this reason, in this thesis we opt for LH2 to overcome this disadvantage.
- **Environmental Impact:** Increased fuel consumption translates into an increase in CO2 emissions and possible pollution of the atmosphere. This could thwart global efforts to reduce aviation's environmental impact. Similar considerations to the previous point regarding LH2.
- **Elevated Sound Levels:** The sonic boom generated by supersonic aircraft when breaching the sound barrier can cause acoustic disturbance on the ground, limiting flight routes and airport access in densely populated areas.
- **High Costs:** The development, certification and production of supersonic aircraft require considerable investment, increasing production costs compared to conventional aircraft.
- **Regulations and Norm:** Supersonic flight requires specific regulations to manage noise, pollution and flight paths, which could complicate the process of integration into the existing airport environment.
- **Route Limitations:** Due to noise and regulations, supersonic aircraft may be limited in their choice of routes, limiting their operational flexibility. In fact, the ban on flying over the emerged lands at supersonic speeds is mentioned.

In conclusion, supersonic flight represents a double sword for the civil aviation industry. While it offers opportunities to reduce travel times and foster innovation, it also

presents significant environmental, noise, cost and regulatory challenges. The integration of supersonic flight will require a careful and balanced assessment of advantages and disadvantages, taking into account the needs of passengers, the environment and the aviation industry as a whole.

1.3 Thesis outline

- Chapter 1: A brief presentation is shown about Liquid Hydrogen like a fuel, about why supersonic aircraft are investigated and the reasons for this choice of fuel.
Bibliography: [20],[9], [7].
- Chapter 2: An overview of each reference aircraft where characteristics and parameters are shown. After, the requirements of project are presented and an overview of input data.
Bibliography: [5], [6], [12], [3], [2].
- Chapter 3: The general outline and operation of the Matlab program are presented.
- Chapter 4: In this chapter, the method used for developing the statistical analysis is explained. Following that, the mission profile definition is provided.
Bibliography: [15]
- Chapter 5: The chosen aerodynamic model (Lift and Build Up) is presented along with comments on the outputs.
Bibliography: [15], [21].
- Chapter 6: The two mass parameters are calculated, the fuel and operative empty weight. A state of art methodology is adopted. As far as OEW is concerned, a state of art methodology, adjusted for LH2 propellant implementation, is adopted by Raymer method.
Bibliography: [15]
- Chapter 7: Verification of requirement about wing loading and thrust to weight ratio. After these creation of Matching chart.
Bibliography: [15], [13]

- Chapter 8: In the chapter, you will find the procedure for sizing LH2 tanks, leading to the final definition of the aircraft's dimensions.

Bibliography: [\[11\]](#)

- Chapter 9: The Center of Gravity first estimation is treated and a comparison of all configurations are made.
- Chapter 10: Conclusion and future trends are analyzed

Chapter 2

Reference Aircraft and Initial Point of design

2.1 Reference Aircraft

In this section, the aircraft chosen for the statistical foundation, necessary to determine the initial data for the design, are listed. Specifically, aircraft that do not yet exist physically but only as projects have been selected, as hydrogen-powered planes do not yet exist. The database primarily encompasses supersonic aircraft in order to maintain a strong coherence with the initial data. The parameters listed in the database of reference aircraft for both categories are:

- Payload
- Maximum Take Off Weight (MTOW)
- Net Thrust
- Wing Surface
- Specific Fuel Consumption (SFC)
- Specific Impulse (ISP)
- Mach Number

- Propellant Mass (PM)
- Propellant Mass Fraction (PMF)

NASA Concept

One subsonic and one supersonic concept are taken as references ([6][5]).

The Subsonic Concept completes the study conducted by NASA's Langley Research Center in 1972. The analyzed concept represents a short-range (2780 km) configuration with a capacity of 130 passengers. This study explores both internal and external LH2 tank solutions and compares them with a conventionally fueled aircraft. The external tanks are not competitive and result in an increase in total aircraft drag. Another goal of the study is to determine a crossover point that highlights the advantages of innovative fuel compared to conventional fuel. While this benefit is more pronounced in long-range aircraft, the reference short configuration is at or near the crossover point.

The Supersonic Concept is a study carried out by Lockheed-California Company for NASA-Ames Research Center. It aims to investigate the feasibility of using LH2 fuel in the advanced design of supersonic transport concepts. This study is divided into two phases: the first phase involves a parametric analysis to determine an optimal configuration in alignment with project goals, while the second phase analyzes the selected configuration to establish a design concept for the vehicle structure, cryogenic fuel tanks, and tank thermal protection system. At the conclusion of both phases, estimates are made for weights and costs, in addition to evaluating environmental compatibility in terms of noise, sonic boom overpressure, and exhaust emissions.

To validate the concept, a comparison with conventional aircraft is conducted.

Specifications			
	Unit	Subsonic	Supersonic
Payload	[kg]	12973	28032
MTOW	[tons]	50	190
Thrust	[kN]	90	1305
Wing Surface	[m ²]	90	836
SFC	[kg/daN/h]	0.215	0.439
ISP	[s]	17068	7444
Mach		0.85	2.7
Propellant Mass	[kg]	3900	42774
Propellant mass fraction	[%]	7.8	22.51
Range	[km]	9260	7778

Table 2.1: Specifications of NASA Concept

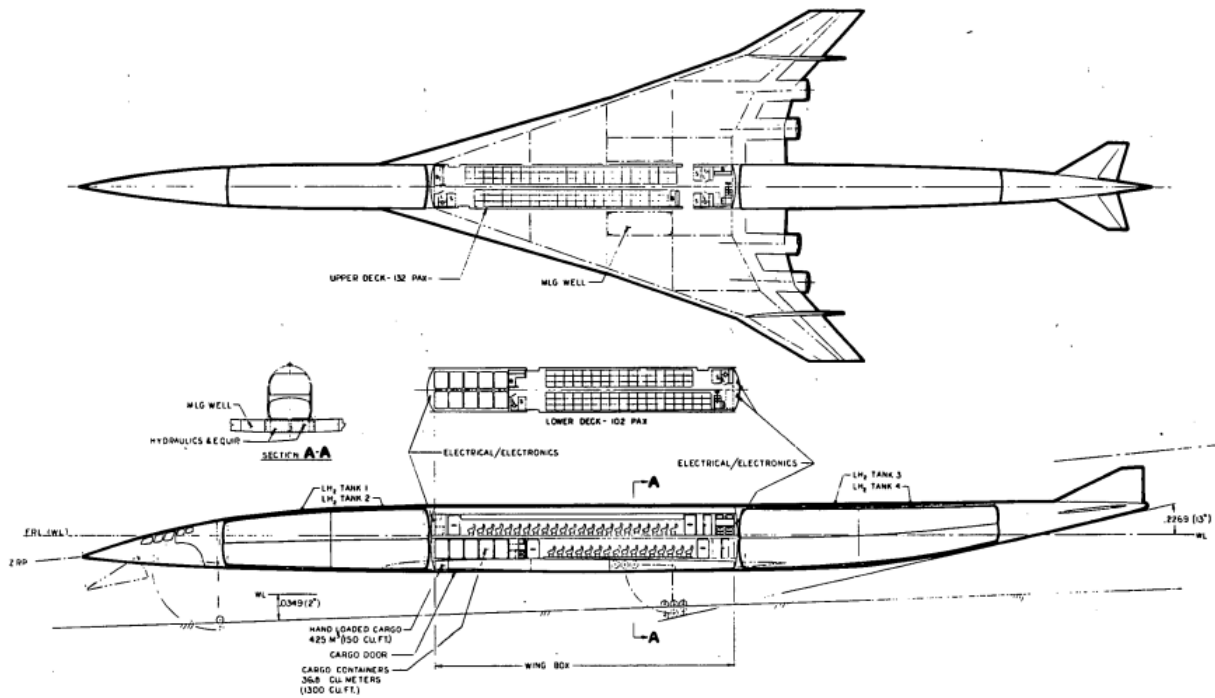


Figure 2.1: NASA Supersonic concept (from [5])

Lapcat A2

LAPCAT was an EU Project coordinated by the European Space Agency (ESA) and funded for two consecutive editions (LAPCAT and LAPCAT II) from 2005 to 2013. The primary objective was to carry out the preliminary design of a suitable hypersonic cruiser concept through iterative design loops. Various aircraft configurations were proposed, and trade studies were conducted to select the optimal platform architecture. The LAPCAT A2 is a Mach 5 vehicle designed for antipodal flights (>16000 km). The A2 adopts a conventional wing-body configuration. Its fuselage comprises an external aeroshell reinforced with ceramic composite materials, insulation, an actively cooled screen, a carbon fiber reinforced polymer (CFRP) structure, and a hydrogen tank made of welded aluminum. Moreover, it is equipped with four Scimitar precooled engines. The Scimitar engine is derived from the Sabre space plane engine, initially developed for Single-Stage-To-Orbit (SSTO) launcher applications, but with a design for extended operational life. This engine draws upon existing gas turbine, rocket, and subsonic ramjet technologies. The aircraft has a Maximum Take-Off Weight (MTOW) of approximately 400 tons, with a maximum seating capacity of 300 passengers. In the following table, we can observe its specifications, as reported by [12].

Specifications		
	Unit	Lapcat A2
Payload	$[kg]$	29000
MTOW	$[tons]$	400
Thrust	$[kN]$	1488
Wing Surface	$[m^2]$	900
SFC	$[kg/daN/h]$	0.9
ISP	$[s]$	1800
Mach		5
Propellant Mass	$[kg]$	198000
Propellant mass fraction	$[\%]$	49.5
Range	$[km]$	2000

Table 2.2: Specifications of Lapcat A2



Figure 2.2: Lapcat A2

Twin Tail Boom Configuration

This concept has been developed by Cranfield University through a PhD project that analyzes various unconventional configurations. The chosen configuration is a Twin Tail Boom. The conceptual design aims to create a medium-range hydrogen aircraft to determine its mass, dimensions, and performance characteristics. This project was undertaken as part of the aerospace systems design course at Politecnico of Torino [3].

Specifications		
	Unit	Twin Tail Boom
Payload	[<i>kg</i>]	18260
MTOW	[<i>tons</i>]	110
Thrust	[<i>kN</i>]	121
Wing Surface	[<i>m</i> ²]	337
SFC	[<i>kg/daN/h</i>]	0.207
ISP	[<i>s</i>]	17712
Mach		0.8
Propellant Mass	[<i>kg</i>]	31500
Propellant mass fraction	[%]	28.64
Range	[<i>km</i>]	7964

Table 2.3: Specifications of Twin Tail Boom Configuration

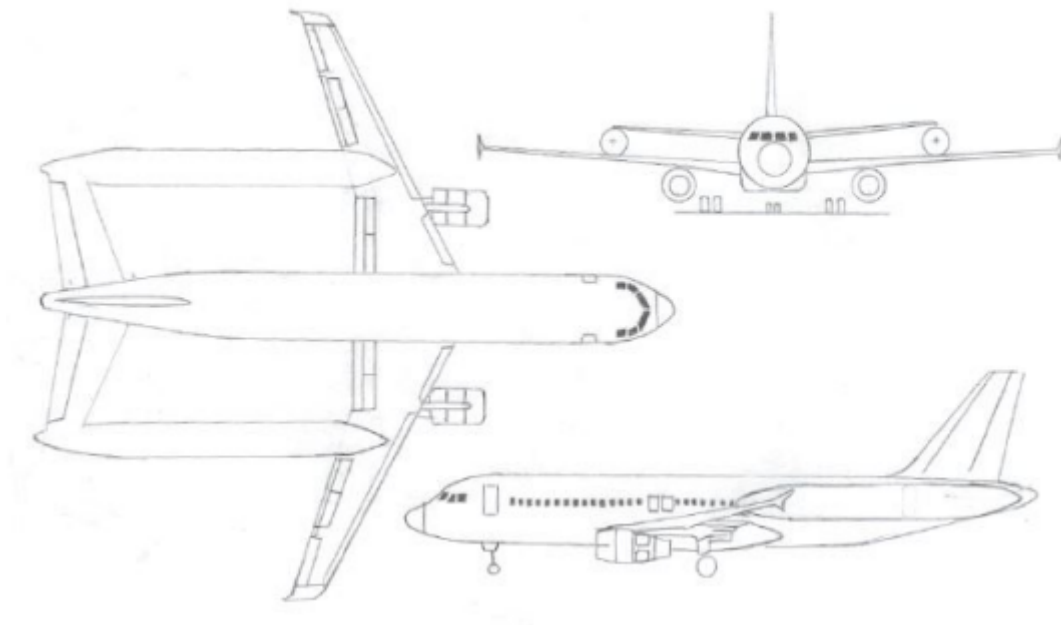


Figure 2.3: Twin Tail Boom Configuration (from [3])

Hydr.a.

From a project carried out during the Aerospace Systems Design course of the academic year 2022/2023, we discuss a hydrogen-powered supersonic aircraft designed by a group of students [2]. Below are the specifications:

Specifications		
	Unit	Hydr.a.
Payload	[<i>kg</i>]	10000
MTOW	[<i>tons</i>]	108
Thrust	[<i>kN</i>]	540
Wing Surface	[<i>m</i> ²]	341
SFC	[<i>kg/daN/h</i>]	0.28
ISP	[<i>s</i>]	13106
Mach		1.7
Propellant Mass	[<i>kg</i>]	17500
Propellant mass fraction	[%]	16.2
Range	[<i>km</i>]	6500

Table 2.4: Specifications of Hydr.a. (from [2])

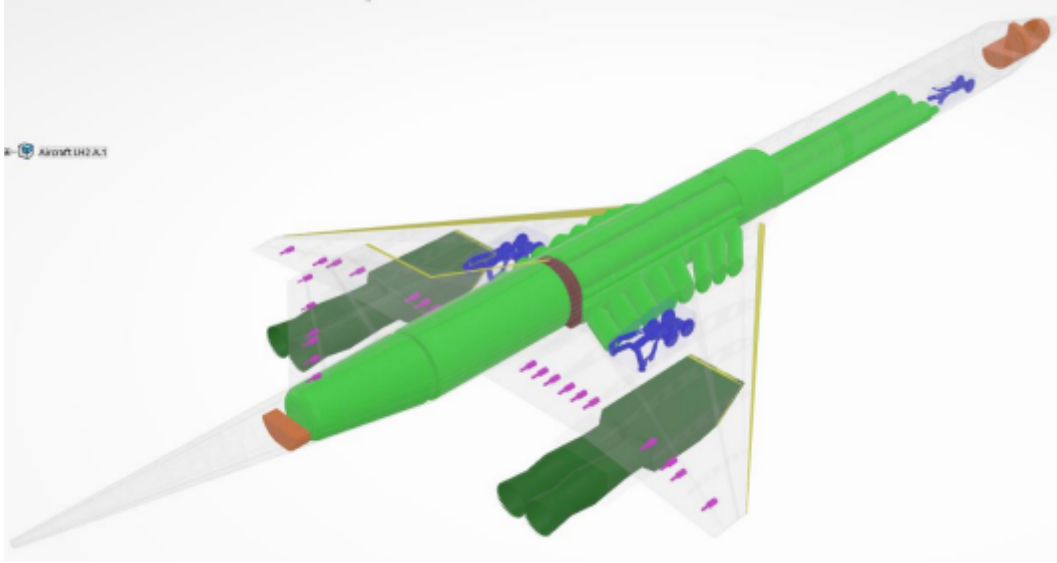


Figure 2.4: Hydr.a. (from [2])

Two concept of LH2 low boom

From the same Hydr.a. document [2], data related to two low boom supersonic aircraft concepts are extracted, which help increase the range of Mach numbers present in the database. Their specifications are as follows:

Specifications			
	Unit	Concept 1	Concept 2
Payload	$[kg]$	11103	12000
MTOW	$[tons]$	156	171
Thrust	$[kN]$	534	600
Wing Surface	$[m^2]$	680	900
SFC	$[kg/daN/h]$	0.21	0.26
ISP	$[s]$	17475	14114
Mach		1.57	1.6
Propellant Mass	$[kg]$	32386	45359
Propellant mass fraction	$[\%]$	20.78	26.46
Range	$[km]$	9819	10871

Table 2.5: Specifications of Low boom Concept

2.2 Project's requirement

In this section, the requirements of the aircraft to be designed are discussed. It needs to be a supersonic aircraft powered by LH2 (liquid hydrogen), of civilian type as it should transport passengers, and finally, it should have a medium-range capability. For this study, several assumptions have been made, listed below:

- It is hypothesized that LH2 is already produced for aircraft fuel purposes.
- The existence of an engine suitable for liquid hydrogen is assumed.
- It is assumed that regulations exist concerning the airport environment, including refueling, storage, and other related aspects.
- Maintenance aspects are not taken into consideration.
- Aerodynamic aspects related to the sonic boom are not explored in depth.
- The database includes aircraft powered by sources other than hydrogen due to a lack of specific references.

The concept is developed to operate at its design point but for validation of methodology is used variation of two variable. The performance requirements are therefore presented in the table 2.6, including potential variations. Furthermore, as a requirement, the aircraft must take off and land at existing airports, which implies consistent runway lengths.

Requirements			
	Unit	Design's point	Variation for validation
Passenger capacity		80	60 - 100
Mach		2	1.5 - 2.5
Range	[<i>km</i>]	6000	
Fuel		LH2	

Table 2.6: Requirements

2.3 Input Data

To input the initial data into the program, an Excel file called "Input data" is used, containing all the data that the user needs to input. These are divided into various sections, as listed below.

2.3.1 Requirements

The user needs to enter the data related to the requirements. In the document, these data will be changed according to the table 2.6 to analyze multiple configurations.

Passengers	80
Mach	2
Range [km]	6000

Table 2.7: Requirement

2.3.2 Mission profile

The user needs to input data related to the mission profile. In this case, for a better analysis, the missed approach is introduced by default. It is necessary to input the duration and altitude of this phase.

Phase	Time duration [min]	Final Altitude [m]
Taxi	10	0
Take Off	1	122
Subsonic climb	15	4572
Subsonic Cruise	30	7315
Supersonic Climb	25	18288
Supersonic cruise	150	18288
Supersonic Descent	25	7315
Subsonic Cruise (Descent)	30	3000
Subsonic Descent	15	1524
Climb Missed Approach	15	3000
Cruise Missed Approach	20	3000
Descent Missed Approach	15	122
Landing	1	0
Taxi out	10	0

Table 2.8: Mission profile

2.3.3 Aerodynamics

In table 2.9, all the required data regarding the aerodynamic aspect should be inserted.

2.3.4 Fuel Weight

Subsonic Cruise descent Mach	0,75
------------------------------	------

Table 2.10: Fuel Weight

2.3.5 Operative Empty Weight

A and B data is selected from the image 2.5, the other are set like in a figure.

Regime	Subsonic Mach	0,8
	Supersonic Mach	2
	Alpha Subsonic [deg]	5
	Alpha Supersonic [deg]	2,5
	Airfoil aerodynamic efficiency	0,95
	Wing Sweep Angle [deg]	59,04
	Wing span [m]	30
	Wing Root chord [m]	25
Percentage Wing Wetted Area	Subsonic [decimal]	0,9
	Supersonic [decimal]	0,95
	Percentage of laminar flow on the Wing [%]	40
	Tail Root chord [m]	10
	Tail Height [m]	6,25
Percentage Tail Wetted Area	Subsonic [decimal]	0,9
	Supersonic [decimal]	0,98
	Percentage of laminar flow on the Tail [%]	40
	Engine Length [m]	5
	Engine External Diameter [m]	2
Percentage Nacelle Wetted Area	Subsonic [decimal]	0,7
	Supersonic [decimal]	0,8

	Thrust Available for single Engine	90
	Percentage of laminar flow on the Nacelle/Engines [%]	20
	Aircraft length [m]	60
Fuselage Diameter [m]	Internal	3
	External	3,5
Percentage Fuselage Wetted Area	Subsonic [decimal]	0,8
	Supersonic [decimal]	0,9
	Percentage of laminar flow on the Fuselage [%]	20
	Roughness factor [m]	5,18E-07
	Chordwise Location of the Airfoil Maximum Thickness (x/c)	0,5
	Profile Thickness on Chord Ratio (t/c)	0,05
Percentage of Miscellaneous drag	Subsonic [decimal]	0,05
	Supersonic [decimal]	0,05
Percentage of leakages and protuberance drag [%]	Subsonic [decimal]	0,05
	Supersonic [decimal]	0,05
Viscosity	Value	1,63E-05
	Altitude referred	5000
Viscosity	Value	1,46E-05
	Altitude referred	10000

Table 2.9: Aerodynamics

A	1,02
B	-0,06
Kvs	1
Kmaterial	1

Table 2.11: Operative Empty Weight

$W_e/W_0 = AW_0^C K_{vs}$	A	C
Sailplane—unpowered	0.86	-0.05
Sailplane—powered	0.91	-0.05
Homebuilt—metal/wood	1.19	-0.09
Homebuilt—composite	0.99	-0.09
General aviation—single engine	2.36	-0.18
General aviation—twin engine	1.51	-0.10
Agricultural aircraft	0.74	-0.03
Twin turboprop	0.96	-0.05
Flying boat	1.09	-0.05
Jet trainer	1.59	-0.10
Jet fighter	2.34	-0.13
Military cargo/bomber	0.93	-0.07
Jet transport	1.02	-0.06

K_{vs} = variable sweep constant = 1.04 if variable sweep
 = 1.00 if fixed sweep

Figure 2.5: Operative Empty Weight parameters

2.3.6 W/S Requirements Verification

Length of Runway [m]	4500
Mach turn	0,5
Altitude Turn [m]	1500

Table 2.12: T/S Requirements Verification

2.3.7 T/W Requirements Verification

Take off Runway length [m]	4500
TOP [lb/ft] (take off parameter)	250
Cl take off	1,95
Climb angle (gamma) [deg]	5

Table 2.13: T/W Requirements Verification

2.3.8 Tank sizing

Margin empty space between internal fuselage and wing [%]	1
Margin of width between fuselage and tank [%]	3
Margin of length between fuselage and tank [%]	1
Margin between wing and rear tank [%]	1
Margin between passenger compartment and rear tank [%]	1
Max Pressure in tank [Mpa]	0.2
Strength limit of tank material [MPa]	800
Young modulus of tank material [MPa]	50000
Thermal conductivity of insulation material [W/(m*K)]	0,0003
Density of insulation material [kg/m3]	30
Operative temperature to sizing the insulation thickness [°C] (max 30,15°C)	30

Table 2.14: Tank sizing

Chapter 3

Structure of methodology

The methodology consists of several standalone functions, where the outputs of one function affect the subsequent ones since these outputs become inputs for one or more subsequent functions. The choice to divide it into multiple functions, thus separating the major topics, allows for autonomous work, possibly improving or modifying a single aspect while maintaining the program's functionality.

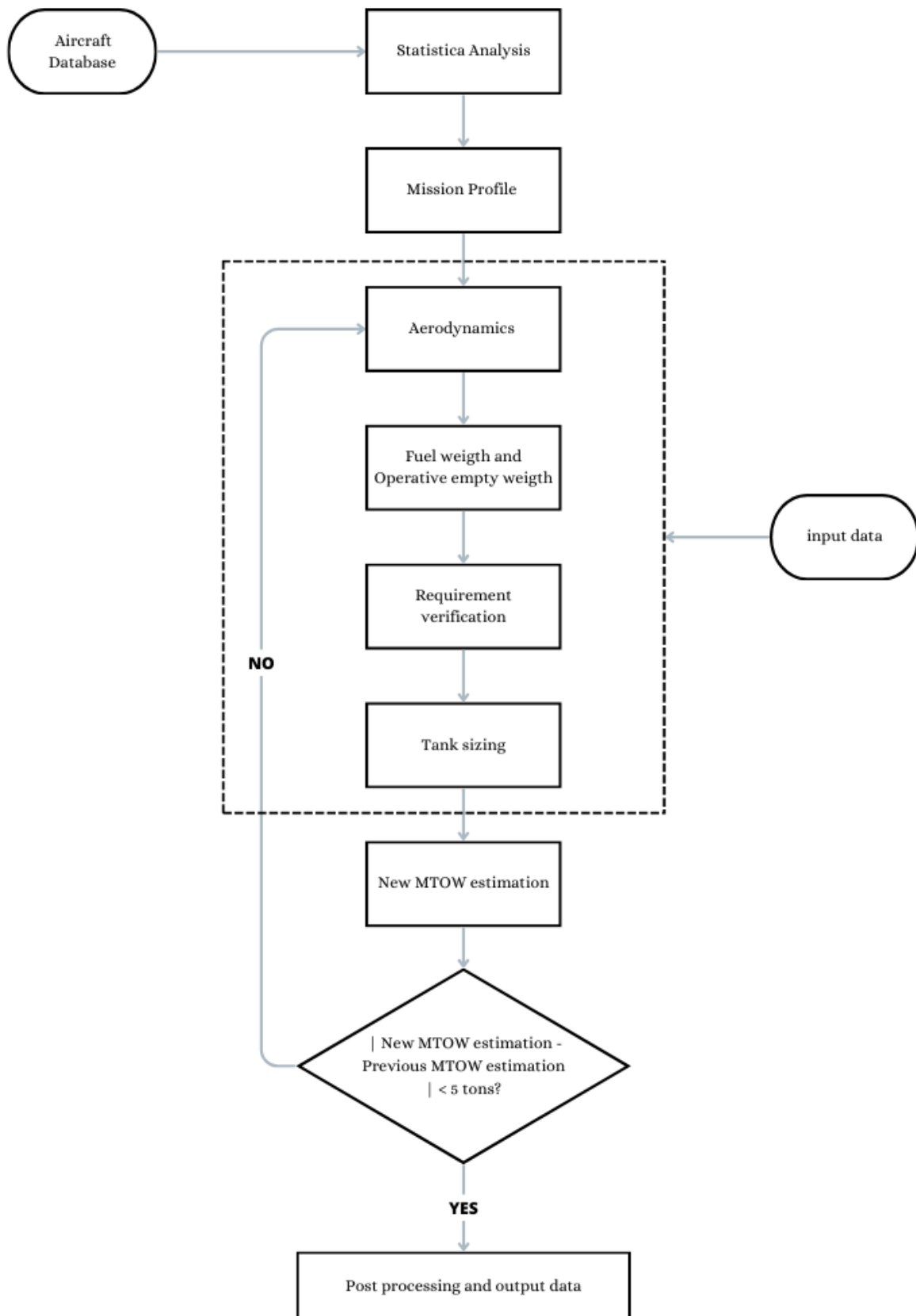


Figure 3.1: Structure of the methodology

3.1 General functioning

In the figure 3.1, the overall operation of the methodology is outlined. The purpose of this chapter is to explain how works, while the explanations of individual functions will be provided in the following chapters. The methodology starts by reading a Database containing various prototypes of aircraft similar to the one you want to design (2.1). Subsequently, using the data acquired from it, a statistical analysis is performed to find the initial iteration data for the program (4.1). The next step is the definition of the mission profile, where flight altitudes and travel times are specified. This is done using user-provided inputs specified in the 'Input data', which contains all the data that the user needs to input for each major project area. After that, within the dashed rectangle, the actual design process takes place. Each function is responsible for sizing specific aspects, and the entire process is iterated multiple times. This is the convergence loop based on MTOW, the maximum takeoff weight, with the stopping condition being that the difference between two consecutively calculated weights is less than 5 tons. Inside the convergence loop, you'll find the following functions:

- Aerodynamics (5)
- Fuel weight and operative empty weight (6)
- Requirement verification (7)
 - W/S Requirement (7.1)
 - T/W Requirement (7.2)
- Tank sizing (8)

At this point, if the difference between the calculated weight in the previous iteration and the weight calculated in the last iteration is less than five tons, the convergence loop terminates, and you proceed to post-processing. In the post-processing phase, graphs and data for the complete aircraft are generated and returned. If the difference is still greater than five tons, the convergence loop continues, and another iteration is performed.

Chapter 4

Statistical Analysis and Mission Profile

The starting point of the project is the statistical analysis of the aircraft listed in the second chapter. Three different approaches will be used, and then an average will be taken to obtain the initial values, to be added to the user's input values. Clearly, the output data won't be final; they can vary significantly, especially due to the fact that the database, due to the lack of aircraft of this type, is heterogeneous. After that, the definition of the mission profile is addressed.

4.1 Statistical Analysis

As previously mentioned, the statistical analysis is the first step of the project, through which high-level parameters are defined by means of linear regression of the data provided in the reference aircraft database (remembering that these are concepts and have not been constructed). The data derived from this phase will serve as inputs for the subsequent stages, where they might be subject to variations through iterative cycles. Particularly, values such as weight, propulsion, and geometry are determined. The data obtained from this phase can describe the state of the art of this type of aircraft.

The adopted logical process is as follows: it begins with the reading of high-level requirements (number of passengers, Mach, and range) which, through functions described later, will determine the maximum takeoff weight (MTOW); subsequently, using this driver, other parameters will be defined (net thrust, wing area, SFC, ISP, propellant mass, and its fraction relative to the total weight).

4.1.1 Definition of MTOW

To achieve a good result from the statistical analysis, it is necessary to consider the three high-level requirements, namely the number of passengers, Mach number and the range. First and foremost, it calculates the payload weight using the formula:

$$Payload = Passenger * (C_{wp} + C_{wl}) \quad (4.1)$$

where C_{wp} is the weight of each passengers (assumed as 80 kg) and C_{wl} is the weight of one luggage (assumed as 35 kg). The values are referred to a current experience of transportation aircraft line.

For a better result, it is advisable to use a linear regression that depends on all three project requirements. This way, a result is obtained that takes into account the contribution of all three terms. Otherwise, if a regression is performed depending on only one requirement at a time, the values could be far apart from each other. To achieve this, the following formulas are used:

$$\frac{MTOW}{Range} = p_{00} + p_{10} * \left(\frac{Payload}{Range}\right) + p_{01} * \left(\frac{Mach}{Range}\right) \quad (4.2)$$

where p_{00} , p_{10} and p_{01} are the result from Matlab function *fit*. The results are shown in the table 4.1 for same value of Mach=2 and in the table 4.2 for the same value of Passengers=80.

	Unit	Design Point	Passengers=60	Passengers=100
MTOW	tons	137	136	139

Table 4.1: $MTOW = f(Mach, Range)$ at Mach=2

	Unit	Design Point	Mach=1.5	Mach=2.5
MTOW	tons	137	112	163

Table 4.2: $MTOW = f(Mach, Range)$ at Passengers=80

4.1.2 Definition of others parameters

Once the value of MTOW is found, the values of the other parameters are now calculated through linear regression, as shown below:

$$Variable = p_1 * MTOW + p_2 \quad (4.3)$$

where p_1 and p_2 are the result from Matlab function *fit*, where the data from within the database are extracted. These parameters are:

- Net Thrust [kN]
- Wing Surface [m^2]
- SFC (Specific Fuel Consumption) [$kg/daN/h$]
- Isp (Specific Impulse) [s]
- Propellant Mass [kg]
- Propellant Mass Fraction [%]

The results are shown in the table 4.3 for same value of Mach=2 and in the table 4.4 for the same value of Passengers=80.

	Unit	Design Point (A)	Pax=60 (B)	Pax=100 (C)
MTOW	tons	137	136	139
Net Thrust	kN	535	531	540
Wing Surface	m^2	513	510	516
SFC	$kg/daN/h$	0.298	0.296	0.301
Isp	s	14171	14226	14117
Prop. Mass	kg	34894	34228	35560
Prop. Mass fraction	%	21.15	21.02	21.27

Table 4.3: Other parameters at Mach=2

	Unit	Design Point (A)	Mach=1.5 (D)	Mach=2.5 (E)
MTOW	tons	137	112	163
Net Thrust	kN	535	430	640
Wing Surface	m^2	5138	457	569
SFC	$kg/daN/h$	0.298	0.245	0.352
Isp	s	14171	15354	12989
Prop. Mass	kg	34894	20545	49242
Prop. Mass fraction	%	21.15	18.45	23.84

Table 4.4: Other parameters at Passengers=80

Observing these results, first and foremost, it's evident that the data values are quite close when it comes to the variation in passengers. For instance, the Net Thrust increases with the rise in velocity or with an increase in the number of passengers, as expected. The same reasoning extends to the other data, thus confirming the validity of the utilized model. Regarding the variation in Mach, being more significant, it won't yield similar results but all will be proportionally either directly or inversely related to the increase in the value.

The intention behind varying the requirements is not to compare changes in individual data points, but to compare five different configurations and observe how the relationships between the data can be explained by providing validity to the program within the range of requirement data.

These available data, lead to have the initial aircraft data both at the design point and in its vicinity. In the two tables (4.3, 4.4), a total of five initial aircraft are available. During the course of the thesis, the design of these aircraft will be carried out. However, if desired, other combinations of high-level requirements could also be explored.

For convenience, we will refer to these 5 configurations using letters, as indicated in the tables (4.3, 4.4).

4.2 Mission profile

The next step to undertake is the definition of the mission profile, as it is necessary to know the flight altitudes, for instance, to calculate air characteristics (which vary with altitude) that will be used in subsequent calculations. The importance of this step also concerns estimating the required propellant, as Raymer's Method is based on different mission phases. The profile must be chosen carefully; in fact, we cannot create a mission profile for a conventional subsonic aircraft that goes beyond 11,000 meters. Thus, by analyzing the case studied in the thesis, it becomes evident that the profile should have the following phases:

- Warm Up
- Take Off
- Subsonic Climb
- Subsonic Cruise
- Supersonic Climb
- Supersonic Cruise-Climb
- Supersonic Descent
- Subsonic Cruise-Descent
- Subsonic Descent

- Missed Approach: Climb, Cruise, Descent
- Landing
- Taxi Out

The missed approach has been included because, in a project, the worst-case scenario must be taken into account; the same encompasses an initial ascent phase to altitude, a holding phase, a subsequent descent, which concludes the mission and is followed by the landing phase.

Therefore, considering a failed landing, it is necessary to ensure that the aircraft has sufficient fuel to attempt landing again, as stipulated by aviation regulations. As stated in the section 2.3.2, the user needs to input the duration in minutes of the phase and its final altitude through the dedicated Excel file. However, an approximation of constant cruise altitude has been used, whereas in reality, due to autopilot modes, the aircraft's altitude might vary for time or fuel optimization. Another necessary observation pertains to defining the landing phase: the initiation of this phase is synchronized with the obstacle predefined by regulations and concludes when the aircraft comes to a stop. The same consideration applies to the take-off phase. In the figure 4.1, you can observe the mission profile selected in the section 2.3.2 using the input data. Additionally, during this phase, the flight time is straightforwardly calculated, amounting to approximately six hours.

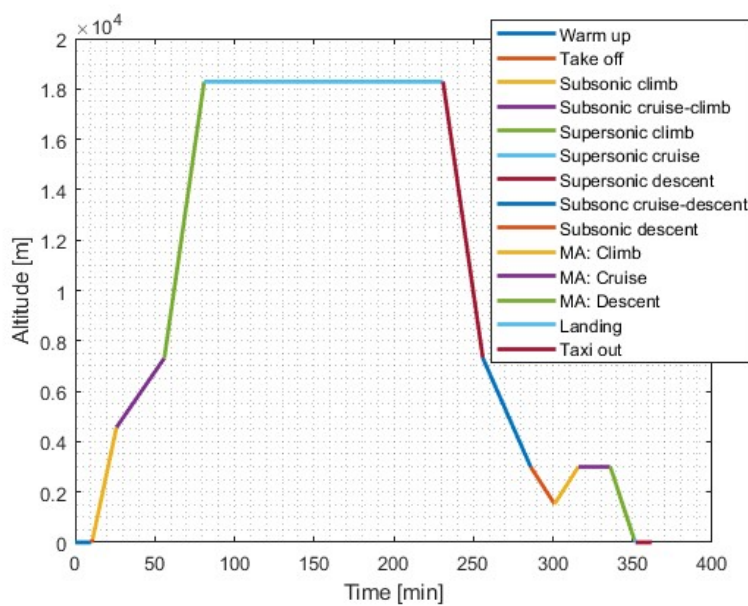


Figure 4.1: Mission profile with missed approach

Chapter 5

Aerodynamics

In this chapter, the aerodynamic study is addressed with the aim of determining the lift and drag coefficients, and hence the efficiency of the aircraft, both in subsonic and supersonic conditions. We will observe that the methodologies proposed will vary depending on whether the aircraft has a speed greater or lesser than that of sound. Efficiency is important to calculate, especially for the subsequent phase where the required fuel weight for the mission will be determined. It is calculated as the ratio between the two coefficients mentioned earlier and depends on various factors: geometry, air characteristics, and more. The analysis method chosen is 'Lift and Drag Buildup' which is the most complete approach for aerodynamic parameters estimation. For the subsequent calculations, numerous inputs will be required, as highlighted in the section [2.3.3](#), and they will be analyzed as they are encountered. This analytical and semi-empirical method exhibits a high degree of result fidelity.

5.1 Lift

For the study of lift, we begin with the assumption of linearity of the C_l -Alpha curve up to angles of attack equal to the stall angle. This assumption holds for many flight phases, such as cruise, but not during take-off, for instance. As this is a concept study, this fact is overlooked, and thus, we consistently consider this assumption to be valid. Consequently, we calculate:

$$C_L = C_{l\alpha} * \alpha \quad (5.1)$$

5.1.1 Subsonic

For calculating the lift coefficient in subsonic conditions, according to Equation 4.1, we require the slope of this curve. To find it, it's necessary to perform the following calculation:

$$C_{L\alpha} = \frac{2 * \pi * AR}{2 + \sqrt{4 + (\frac{AR * \beta}{\eta})^2 * (1 + (\frac{\tan \Lambda [\text{rad}]}{\beta})^2)}} * \frac{S_{\text{exposed}}}{S_{\text{ref}}} * F \quad (5.2)$$

where:

- Aspect Ratio [AR]:

$$AR = \frac{\text{Wing Span}^2}{\text{Wing Surface}} \quad (5.3)$$

- β : it's a function of Mach number of Subsonic cruise:

$$\beta = \sqrt{1 - M^2} \quad (5.4)$$

where M is Mach number of subsonic cruise.

- Λ : It's the Wing sweep angle measured in radians.
- η : it's the wing profile aerodynamic efficiency. Value of 0.95 is assumed when the lift curve (in function of Mach Number) of airfoil is unknown.
- Fuselage Lift Factor [F]: It's a parameter that describes the shape, structure, or characteristics of an object. In this case the formula is:

$$F = 1.07 * (1 + \frac{\text{External Diameter Of Fuselage}}{\text{Wing Spane}})^2 \quad (5.5)$$

- Surface ratio $\frac{S_{\text{exposed}}}{S_{\text{ref}}}$: To determine this value, various methodologies can be employed, and it can vary significantly in supersonic aircraft. There are no reference values available in the literature. The chosen method is referred to as the "Dummy" method: In this approach, the exposed outer surface of the delta wing facing the air-flow is approximated as a triangle, while the section covered by the fuselage is

treated as a rectangular shape. The parameters considered are the wingspan, the fuselage's external diameter, and the root chord of the wing. The calculated exposed surface pertains to half of the wing (either top or bottom), thus to obtain the total plan form area, it needs to be doubled. The segment covered by the fuselage is subsequently added.

$$S_{exposed,i} = \frac{Exposed\ Length * Root\ Chord}{2} \quad (5.6)$$

$$S_{covered} = Length\ Covered * Root\ Chord \quad (5.7)$$

$$S_{ref} = 2 * S_{exposed,i} + S_{covered} \quad (5.8)$$

$$S_{ratio} = \frac{2 * S_{exposed,i}}{S_{ref}} \quad (5.9)$$

With all the inputs in place, the results for the first iteration of the code are presented in table 5.1, as well as the results for the last iteration in table 5.2 , for each configuration defined in the section 4.1.2.

First Iteration					
	A (Design Point)	B	C	D	E
C_L	0.174	0.174	0.174	0.184	0.165

Table 5.1: Subsonic C_L first iteration

Final Iteration					
	A (Design Point)	B	C	D	E
C_L	0.25745	0.27179	0.2503	0.19134	0.32217

Table 5.2: Subsonic C_L final iteration

It's possible to observe that in the subsonic case, the values of the lift coefficient vary slightly among configurations without a discernible pattern. This is due to the different geometries arising from the statistical analysis, as modifying the number of passengers affects the payload, which is a driving factor in the analysis, similar to the Mach number.

5.1.2 Supersonic

For calculating the lift coefficient in supersonic regime, Raymer [15] recommends using the formula 5.10, which represents the ideal case.

$$C_{L\alpha} = \frac{4}{\sqrt{M^2 - 1}} \quad (5.10)$$

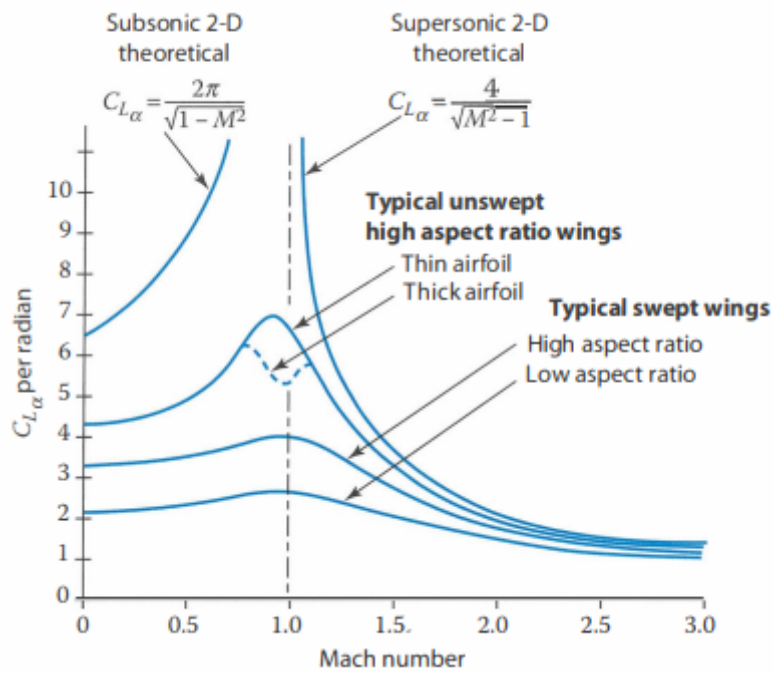


Figure 5.1: $C_{L\alpha} = f(Mach)$ [15]

In the image 5.1, you can observe the trend of the curve slope in relation to the cruise Mach number. In the subsonic portion of the graph, there's a significant difference between the 2D theory and reality, as the curves are quite distant. On the contrary, in the supersonic part, the higher the Mach number, the more similar the two theories become. This observation justifies the use of the theory solely for the supersonic case.

With all the inputs in place, the results for the first iteration of the code are presented in table 5.3, as well as the results for the last iteration in table 5.4, for each configuration defined in the section 4.1.2.

First Iteration					
	A (Design Point)	B	C	D	E
C_L	0.101	0.101	0.101	0.156	0.0762

Table 5.3: Supersonic C_L first iteration

Final Iteration					
	A (Design Point)	B	C	D	E
C_L	0.101	0.101	0.101	0.156	0.0762

Table 5.4: Supersonic C_L final iteration

In the supersonic case, differences between configurations are only noticeable when the supersonic flight Mach number varies. Particularly, we observe that between the design configuration A and the two configurations where the Mach numbers D and E change (with values of 1.5 and 2.5 respectively), the lift coefficient decreases with increasing flight velocity at the same angle of attack.

5.2 Drag

Similarly to the section dedicated to lift, in this one, we proceed with calculating the drag coefficient. This is more complex to compute due to the fact that there are multiple terms resulting from different phenomena that contribute to aerodynamic drag. Moreover, various parts of the aircraft also have different impacts.

5.2.1 Subsonic

For calculating the drag coefficient in the subsonic regime, the formula 5.11 is used, which turns out to be less complex than its counterpart for the supersonic regime.

$$C_D = C_{D0} + C_{D,DTL} \quad (5.11)$$

where:

- C_{D0} is called Parasite Drag.
- $C_{D,DTL}$ is called Drag Due to Lift.

Parasite Drag

$$C_{D0} = \frac{\sum(C_{f,i} * FF_i * Q_i * S_{wet,i})}{S_{ref}} + C_{D,misc} + C_{D,L\&P} \quad (5.12)$$

The terms within the summation are calculated for the main aircraft components generating drag: wing, tail, fuselage, and engine nacelle. For simplicity, the other two terms, miscellaneous drag ($C_{D,misc}$) and leakage and protuberance drag ($C_{D,L\&P}$), are considered as a percentage (assigned in the input) of the previously described term. This simplification is adopted to avoid complicating the method further. The term "miscellaneous drag" considers objects that aren't streamlined and create disruption in the airflow. The contribution from "leakages and protuberances" includes items like antennas, hinges for control surfaces, as well as protruding rivets or panel misalignment. Additionally, "leakages" account for the aircraft's tendency to draw in air in high-pressure areas through gaps, which adds resistance, and to expel air in low-pressure areas, promoting flow separation.

Now the procedure for obtain the first term of summation, $C_{f,i}$, by calculating the flat plate friction coefficient:

- **Reynolds Number estimation.** The transition from laminar to turbulent airflow is identified through the cut-off Reynolds number. Therefore, it's necessary to calculate all these values for the aforementioned main components. The transition also takes into account the roughness of the surface and factors such as the presence of rivets. However, in a high-level analysis, the specific details of rivets and various materials used won't be considered. This parameter remains unaffected by surface ratios or reference surfaces, thus its value remains fixed regardless of configuration changes.

$$Re = \frac{\rho * V * l}{\mu} \quad (5.13)$$

$$Re_{cut-off} = 38.21 * (l/k)^{1.053} \quad (5.14)$$

$$l = \begin{cases} MAC [tail, wing] \\ length [fuselage, nacelle] \end{cases} \quad (5.15)$$

- **C_f estimation.** The coefficient in question is calculated for each main component as previously mentioned. The friction coefficient is determined for both turbulent and laminar flow cases. The values obtained will not depend on the surface but solely on the Reynolds number. In fact, it is subsequently multiplied by the wetted area of the respective main component to which it pertains.

$$C_{f,laminar} = \frac{1.328}{\sqrt{Re}} \quad (5.16)$$

$$C_{f,turbolent} = \frac{0.455}{(\log(\min(Re, Re_{cut-off})))^{2.58} * (1 + 0.144 * M^2)^{0.65}} \quad (5.17)$$

- **Weighted C_f estimation.** With the knowledge of the laminar and turbulent flow percentages present in each main component (provided by the user in the input file), we can now proceed to calculate the weighted friction coefficient using the following formula 5.18:

$$C_{f,i} = \%_{laminarflow} * C_{f,laminar} + \%_{turbolentflow} * C_{f,turbolent} \quad (5.18)$$

In the following, we list the steps to derive the necessary terms for the $C_{f,i}$ calculation procedure:

- **Density, ρ .** Density calculation is performed using the International Standard Atmosphere (ISA) formula 5.19 for the troposphere. These equations are valid only for subsonic flight, as supersonic flight takes place in the stratosphere, and its calculations will be presented later. Considering that altitude can be constant or variable based on the flight phases, the average density value within the phase is used 5.30.

$$\rho_i = 1.226 * (1 - 0.0000226 * z[m])^{4.256} \quad (5.19)$$

$$\rho = \frac{\sum_{z_{star}}^{z_{end}} * \rho_i}{\#\rho} \quad (5.20)$$

- *Speed, V.* Velocity is a function of the Mach number and altitude. The speed of sound is determined by the air temperature and other air parameters (such as γ). Similar to density, the velocity is also averaged within the flight phase to account for variations.

$$V = M * a \quad (5.21)$$

$$a = \sqrt{\gamma * R * T} \quad (5.22)$$

$$\begin{cases} \gamma = \frac{C_p}{C_v} \\ R = C_p - C_v \\ T = f(\text{altitude}) \end{cases} \quad (5.23)$$

The specific heat at constant pressure and at constant volume are calculated as linear combinations of temperature with coefficients as described below:

$$C_p = a + b * T \quad (5.24)$$

$$C_v = a' + b * T \quad (5.25)$$

$$\begin{cases} a = 0.228 \left[\frac{\text{kcal}}{\text{kgK}} \right] \\ a' = 0.159 \left[\frac{\text{kcal}}{\text{kgK}} \right] \\ b = 3.6 * 10^{-5} \left[\frac{\text{kcal}}{\text{kgK}} \right] \end{cases} \quad (5.26)$$

For the temperature, we once again apply the ISA formulas:

$$T = \begin{cases} T_0 + T_z * z \\ T_{trp} \end{cases} \quad (5.27)$$

$$\begin{cases} T_0 = 288[K] \\ T_z = -6.5 \left[\frac{K}{\text{km}} \right] \\ T_{trp} = 216[K] \end{cases} \quad (5.28)$$

where T_0 is the sea level temperature, T_z the temperature gradient and T_{trp} is the tropopause temperature.

- *Dynamic viscosity, μ* . For dynamic viscosity, we employ a linear regression between two points, provided as input by the user, considering subsonic flight. Similar to density, an average is taken within the flight phase.

$$\mu_i = \mu_{start} + \mu_{end} * \frac{z_i - z_{star}}{z_{end} - z_{start}} \quad (5.29)$$

$$\mu = \frac{\sum_{z_{star}}^{z_{end}} * \mu_i}{\#\mu} \quad (5.30)$$

- *Skin roughness value, k* . This term takes into account the surface roughness and its impact on the airflow. Without simplifications, each surface should have a different k value, as even the non-uniform presence of rivets leads to a change in this value. For simplicity, a single value is adopted for the entire aircraft, which can be chosen from the table 5.2 provided in Raymer [15].

Surface	k , ft	k , m
Camouflage paint on aluminum	3.33×10^{-5}	1.015×10^{-5}
Smooth paint	2.08×10^{-5}	0.634×10^{-5}
Production sheet metal	1.33×10^{-5}	0.405×10^{-5}
Polished sheet metal	0.50×10^{-5}	0.152×10^{-5}
Smooth molded composite	0.7×10^{-5}	0.052×10^{-5}

Figure 5.2: Skin roughness [15]

For the study, Smooth molded composite are choose.

- *Mean aerodynamic chord, MAC* . It is assumed that the mean aerodynamic chord is located at one-third of the wingspan (or height in the case of the tail). It is then scaled with respect to half the wingspan or height, and the root chord.

$$Position = \frac{1}{3} * (Half\ Wing\ Span\ or\ Tail\ Height) \quad (5.31)$$

$$MAC = Position * \frac{Root\ Chord}{(Half\ Wing\ Span\ or\ Tail\ Height)} \quad (5.32)$$

We now proceed to analyze the other terms of the formula 5.12 for calculating the parasite drag coefficient.

Form Factor, FF

The form factor is calculated using the Stratford criterion, which is valid up to the divergence Mach number. It represents the contribution of the resistance generated by the separation of airflow over a surface. The form factor of the tail in Equation 5.33 is increased by 10% to account for the drag rise caused by the hinges, which create a gap between the tail structure and the flight control surface.

- *Wing and Tail*

$$FF = \left(1 + \frac{0.6}{\frac{x}{c}} * \frac{t}{c} + 100 * \left(\frac{t}{c}\right)^4\right) * (1.34 * M^{0.18} * (\cos(\Lambda[\text{rad}])))^{0.28} \quad (5.33)$$

- *Fuselage*

$$FF = 1 + \frac{60}{f^3} + \frac{f}{400} \quad (5.34)$$

- *Engine*

$$FF = 1 + \frac{0.35}{f} \quad (5.35)$$

where:

- $\frac{x}{c}$ is the chordwise location at maximum thickness
- $\frac{t}{c}$ is the profile thickness ratio
- M is the Mach number in the phase
- Λ is the sweep angle of wing and tail
- $f = \frac{l}{d}$ is the length to diameter ratio of fuselage and nacelles

Interference drag, Q

The interference factor takes into account the interference that arises between the elements and their contours. In the figure 5.3, typical values adopted in the study are shown. [21]

Component	Interference factor, Q
Nacelle or external store mounted directly on the fuselage or wing	1.5
Nacelle or external store mounted less than one diameter away from the fuselage or wing	1.3
Nacelle or external store mounted more than one diameter away from the fuselage or wing	1
Wing-tip mounted missiles	1.25
High-wing, mid-wing, well-filletted low wing	1
Undiluted low wing	1.1 – 1.4
Fuselage	1
Conventional tail	1.04 – 1.05
V-tail	1.03
H-tail	1.08

Figure 5.3: Interference Factor

Wetted area, S_{wet}

The wetted area is estimated differently based on the main component for which we want to calculate it. The calculations share the fact that it is a percentage (provided as input by the user) of the previously calculated exposed area. Not all of the surface is affected by the flow. Below is the calculation for each component:

- *Wing.* For the wing, the exposed surface is the one calculated in the lift section using the equation 5.7. This is then multiplied by four to account for both the upper and lower surfaces of both wings.

$$S_{wet} = 4 * S_{exposed} * \% \text{ Wetted Surface} \quad (5.36)$$

- *Tail.* With the simplification to a triangular geometry, an additional 5% is added to counteract this strong simplification. Then, it is multiplied by 2 to account for both the upper and lower surfaces.

$$S_{wet} = 2 * S_{triangle} * 2 * \% \text{ Wetted Surface} \quad (5.37)$$

- *Fuselage and Nacelle.* For the fuselage and nacelle, a cylindrical geometry is considered. For the nacelle, it is necessary to multiply by the number of required engines.

$$S_{cylinder} = 2 * \pi * Radius * Length \quad (5.38)$$

$$S_{wet,fuselage} = S_{cylinder} * \% \text{ Wetted Surface} \quad (5.39)$$

$$S_{wet,nacelle} = \# \text{ Engine} * S_{cylinder} * \% \text{ Wetted Surface} \quad (5.40)$$

The contribution of the drag coefficient from parasite drag can now be calculated.

Drag Due to Lift

Drag due to lift encompasses viscous separation arising from the shift of the flow separation point, variations in parasitic drag resulting from fluctuations in flow velocity around the wing and induced drag. To calculate this contribution, the equation is used 5.41:

$$C_{D,DTL} = K * C_L^2 \quad (5.41)$$

where C_L was calculated in section 5.1 and K coefficient is calculated with *Leading edge suction method*, based on the variation of the coefficient caused by the lift coefficient. In fact in supersonic profiles, they exhibit a negative pressure gradient at the leading edge, which generates a suction force in the forward direction (5.4).

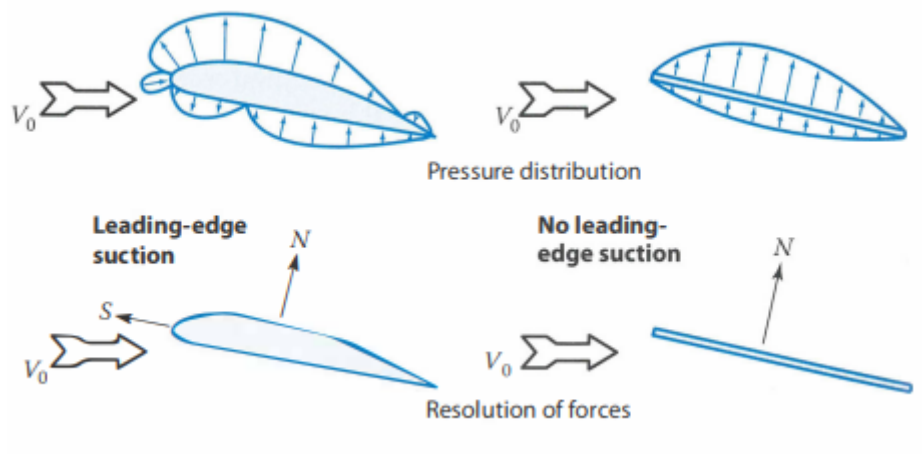


Figure 5.4: Leading edge suction [15]

$$K = S * K_{100} + (1 + S) * K_0 \quad (5.42)$$

$$K_{100} = \frac{1}{\pi * AR} \quad (5.43)$$

$$K_0 = \frac{1}{C_{L\alpha}} \quad (5.44)$$

$$S = 0.85 \text{ or } 0.95 \tag{5.45}$$

K_{100} and K_0 They respectively represent 100% and 0% of the suction, where the first one assume $s = 1$ according to d'Alembert's paradox.

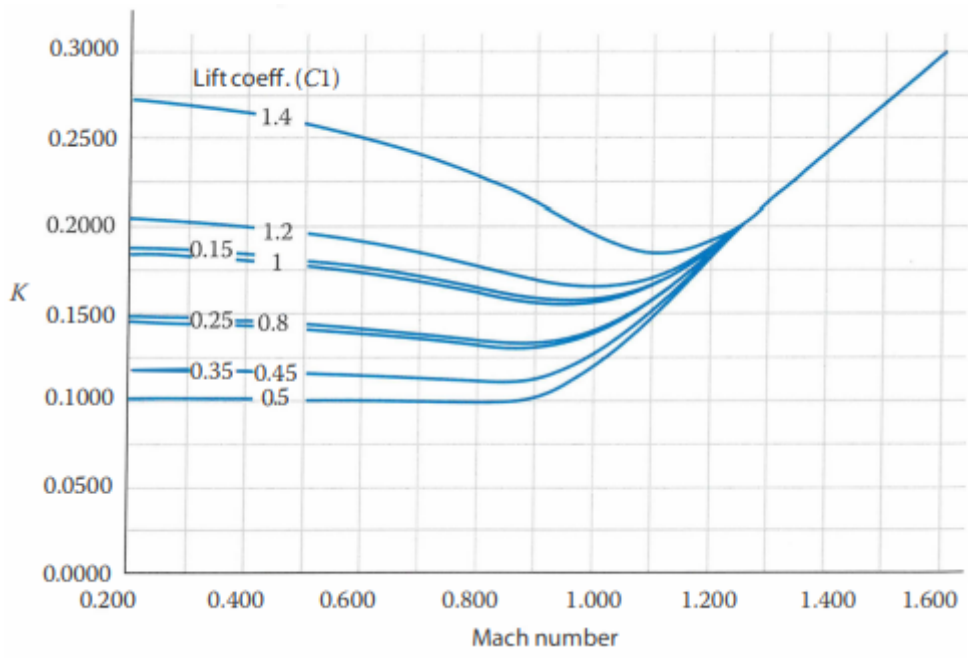


Figure 5.5: $K = f(Mach)$ [15]

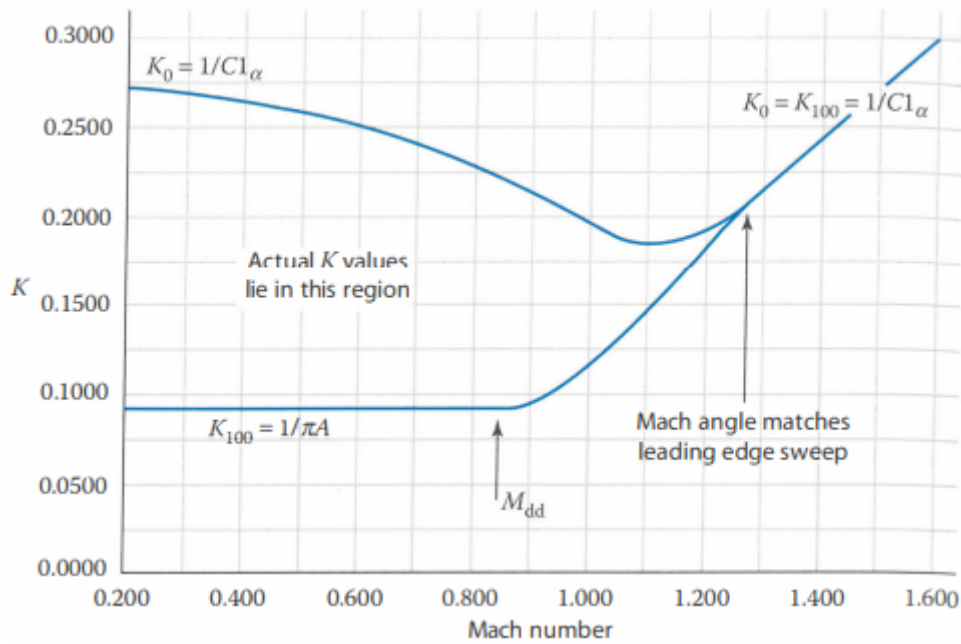


Figure 5.6: $K = f(Mach)$ [15]

In the figures 5.5 and 5.6 it is possible observe trend of K coefficient in function of

Mach and C_L .

5.2.2 Supersonic

The calculation of the supersonic drag coefficient is similar to that in subsonic conditions, with the addition of a term in the parasitic drag coefficient and other variations described subsequently. We begin again with:

$$C_D = C_{D0} + C_{D,DTL} \quad (5.46)$$

In this section, only the changes will be reported, the procedure remains the same as in the subsonic case.

Parasite Drag

The expression for parasitic drag is similar to the subsonic case: there is no contribution from the form factor and interference coefficient, but the wave drag term is added. As in the subsonic case, the terms of miscellaneous and leakages drag correspond to a percentage of the other two terms.

$$C_{D0} = \frac{\sum(C_{f,i} * S_{wet,i})}{S_{ref}} + C_{D,wave} + C_{D,misc} + C_{D,L\&P} \quad (5.47)$$

Similarly to the subsonic case, the terms in the summation are calculated for each main component (wing, tail, fuselage, and nacelle).

Flat plate friction coefficient

The difference compared to the subsonic case is indeed the flight regime, where it is assumed to be completely turbulent.

- **Reynolds Number.** Here the cut-off Reynolds number is adopted since the flow is entirely turbulent. Therefore, the expression for the calculation will change, becoming a function of the Mach number (using the one in supersonic cruise).

$$Re_{cut-off} = 44.62 * (l/k)^{1.053} * M_{1.16} \quad (5.48)$$

- **C_f estimation.** Since the flow is completely turbulent, the friction coefficient will be given only by the $C_{f,turbulent}$:

$$C_{f,turbulent} = \frac{0.455}{(\log(Re_{cut-off}))^{2.58} * (1 + 0.144 * M^2)^{0.65}} \quad (5.49)$$

Wetted surface, S_{wet}

The equations remain the same as in the previous section 5.2.1, so we use the equation 5.36 for the wing, the equation 5.37 for the tail and the equation 5.39 and 5.40 for fuselage and nacelles respectably. The only difference lies in the input percentages, which will be the ones relevant to the supersonic case.

Wave drag $C_{D,wave}$

During a shock wave, a resistance arises due to pressure, and this term precisely accounts for this aspect. This coefficient is of paramount importance as it has a significant impact on the total resistance. Moreover, as evident from the equation, it depends on the volume distribution of the body in the x-y plane.

$$\left(\frac{D}{q}\right)_{wave} = E_{WD} * (1 - 0.2 * (M - 1.2)^{0.57} * (1 - \frac{\pi * \Lambda[deg]^{0.77}}{100})) * \left(\frac{D}{q}\right)_{Sears-Haack} \quad (5.50)$$

$$\left(\frac{D}{q}\right)_{Sears-Haack} = \frac{9}{2} * \pi * \left(\frac{A_{max}}{l}\right)^2 \quad (5.51)$$

where:

- **Wave drag efficiency Factor E_{WD} .** It is a semi-empirical value dependent on the aircraft configuration, and these values can be observed in the table 5.5.

Configuration	E_{WD}
Blended delta wing	1.2
Supersonic fighter	1.8-2.2
Poor supersonic design	2.5-3.0

Table 5.5: E_{WD} [21]

For the study, the first value in the table is used.

- **Maximum cross sectional area A_{max} .** The maximum cross-sectional area considered for the aircraft is located at the attachment points of the main landing gear, typically where one of the main frames is situated. This term encompasses three contributions related to the fuselage, engines, and wing. Regarding the engines, they are assumed to have a cylindrical shape. The cross-sectional surface of the wing exhibits a complex geometry due to the curvature of profiles employed for a delta wing. For the sake of simplicity, a 25% increase in the total area is assumed.

$$A_{fuselage} = \pi * \left(\frac{Diameter}{2}\right)^2 \quad (5.52)$$

$$A_{engine} = \# Engine \pi * \left(\frac{Diameter}{2}\right)^2 \quad (5.53)$$

$$A_{wing} = 25\%A_{max} \quad (5.54)$$

After, it is necessary refer $\left(\frac{D}{q}\right)_{wave}$ to an adimensional coefficient:

$$C_{D,wave} = \frac{\left(\frac{D}{q}\right)_{wave}}{S_{ref}} \quad (5.55)$$

Drag Due to Lift

For this term, we refer equally to the section, with the variation that for the subsonic case, the coefficient K according to the leading edge suction method changes its formula:

$$K = S * K_0 + (1 + S) * K_0 \quad (5.56)$$

5.3 Aerodynamic efficiency

Once the lift and drag coefficients have been calculated, we can finally proceed with the calculation of the aerodynamic efficiency by taking the ratio between the two.

$$E = \frac{C_L}{C_D} \quad (5.57)$$

5.4 Aerodynamics output

In this section, we will use the aerodynamic calculation results based on the inputs presented in the previous section 2.9, with the only variation being the high-level requirements as presented in the table 2.6.

Preliminary aerodynamics outputs						
		A (Design Point)	B	C	D	E
First it.	AR	1.75	1.76	1.75	1.97	1.58
	Wing MAC [m]	8.33	8.33	8.33	8.33	8.33
	Tail MAC [m]	3.33	3.33	3.33	3.33	3.33
	Tail sweep [deg]	57.99	57.99	57.99	57.99	57.99
	Engine estimated	6	6	6	6	7
Last it.	AR	2.02	2.10	1.98	1.61	2.40
	Wing MAC [m]	12.70	12.40	12.90	10.10	15.14
	Tail MAC [m]	4.7975	4.68	4.87	3.82	5.72
	Tail sweep [deg]	57.79	57.79	57.79	57.79	57.79

Table 5.6: Preliminary aerodynamics outputs

The table 5.6 presents the initial output parameters provided by the program. Regarding the first iteration, it is observed that significant variations occur only when the Mach number changes. These values vary between the first and the last iteration, as the program recalculates multiple times until a certain condition is satisfied, which will be discussed later. Similar observations can be made for the last iteration as well.

Subsonic lift output						
		A (Design Point)	B	C	D	E
First iteration	$C_{L\alpha}$	1.994	2.000	1.989	2.112	1.886
	C_L	0.174	0.174	0.174	0.184	0.165
Last iteration	$C_{L\alpha}$	2.950	2.625	2.538	1.894	3.315
	C_L	0.229	0.243	0.221	0.165	0.289

Table 5.7: Subsonic lift output

In the data regarding the lift coefficients shown in the table 5.7, it is observed that

the C_L decreases as the number of passengers increases (in the order B, A, C), while it increases with an increase in Mach number (in the order D, A, E).

Supersonic lift output						
		A (Design Point)	B	C	D	E
First iteration	$C_{L\alpha}$	2.309	2.309	2.309	3.578	1.746
	C_L	0.101	0.101	0.101	0.156	0.076
Last iteration	$C_{L\alpha}$	2.309	2.309	2.309	3.578	1.746
	C_L	0.101	0.101	0.101	0.156	0.076

Table 5.8: Supersonic lift output

For the supersonic lift (as shown in the table 5.8), it can be observed that the lift coefficient remains relatively constant with changes in the number of passengers, while it decreases as the Mach number increases (in the order D, A, E).

Subsonic drag output						
		A(Design Point)	B	C	D	E
First it.	C_{D0}	0.00078	0.00071	0.00078	0.000766	0.00080
	$C_{D,dtt}$	0.00646	0.00647	0.00646	0.00655	0.00634
	C_D	0.00724	0.00725	0.00724	0.00731	0.00714
Last it.	C_{D0}	0.00082	0.00087	0.00080	0.00075	0.00089
	$C_{D,dtt}$	0.00944	0.01019	0.00904	0.00631	0.01251
	C_D	0.010259	0.01106	0.00984	0.00706	0.01340

Table 5.9: Subsonic drag output

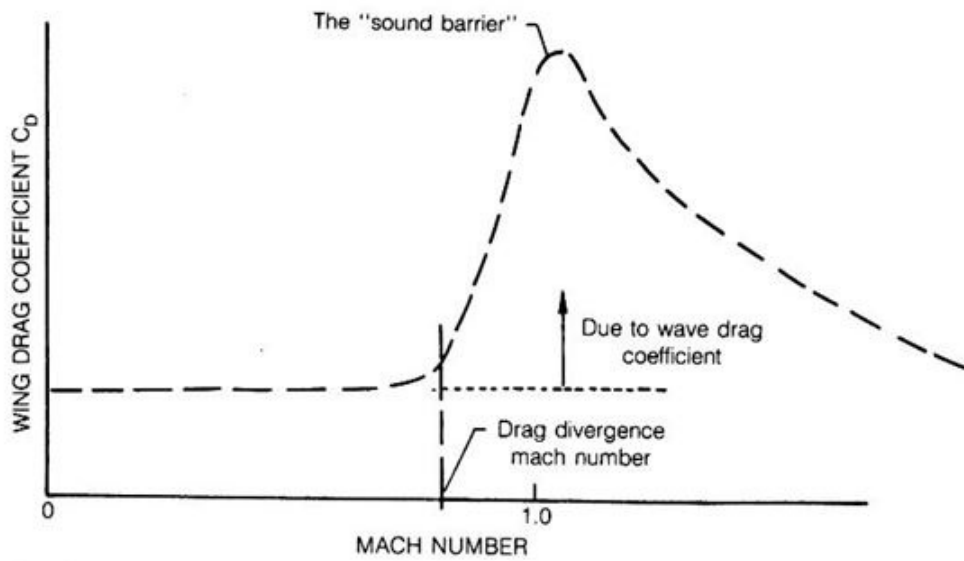
In the table 5.9, the data related to the subsonic drag coefficient is presented. It can be observed that with an increase in the number of passengers, the term experiences a slight decrease, while it shows an increase with an increase in the Mach number. This

variation can be attributed to the drag due to lift contribution, which follows the trend just described.

Supersonic drag output						
		A (Design Point)	B	C	D	E
First it.	C_{D0}	0.01738	0.01738	0.01738	0.01419	0.02095
	$C_{D,wave}$	0.01543	0.01543	0.01543	0.01248	0.01872
	$C_{D,dtl}$	0.00440	0.00440	0.00440	0.00681	0.00332
	C_D	0.02178	0.02178	0.02178	0.02100	0.02427
Last it.	C_{D0}	0.01008	0.01152	0.00928	0.01681	0.00698
	$C_{D,wave}$	0.00875	0.01004	0.00803	0.01485	0.00596
	$C_{D,dtl}$	0.00440	0.00440	0.00440	0.00681	0.00332
	C_D	0.01448	0.01592	0.01367	0.02362	0.01031

Table 5.10: Supersonic drag output

Regarding the data for supersonic drag coefficient in the table 5.10, it should be clarified that the contribution from wave drag is already accounted for within the parasitic drag term. However, it is presented separately as it is the reason behind the trends described below. It can be observed that there is a decrease in the drag coefficient with an increase in the number of passengers, as well as a decrease with an increase in the Mach number. As previously mentioned, these trends are influenced by the wave drag coefficient, while the drag due to lift coefficient remains relatively constant.

Figure 5.7: $C_D = f(Mach)$

While it may seem counter intuitive that resistance decreases as speed increases, observe the trend (Fig. 5.7) of the coefficient of resistance as the Mach number increases: approaching the Mach drag rise, there is a significant increase in resistance; this behavior persists in the transonic region, after which resistance starts to decrease.

		Aerodynamic efficiency				
		A (Design Point)	B	C	D	E
First iteration	Subsonic	24.02	24.07	23.98	25.21	23.04
	Supersonic	4.63	4.63	4.63	7.43	3.14
Last iteration	Subsonic	22.33	22.00	22.51	23.34	21.59
	Supersonic	6.96	6.33	7.37	6.61	7.39

Table 5.11: Aerodynamic efficiency

Finally, in the table 5.11, a comparison of aerodynamic efficiencies can be made. It is observed that for the subsonic efficiency, a slight increase with an increase in the number of passengers and a small decrease with an increase in the Mach number. For the supersonic efficiency, there is also an increase with an increase in the number of passengers and an increase with an increase in the Mach number.

Chapter 6

Fuel Weight and Operative Empty Weight

In this chapter, methods for estimating fuel mass and operational empty weight are described. For the estimation of fuel mass Raymer method are analyzed. The Raymer method is based on it: by using altitude and duration of different phases as variables, the necessary amount of fuel for each mission phase and the total amount are estimated. The operational empty weight is computed using an exponential relation adapted to the LH2 (liquid hydrogen) case. This weight parameter is the only one that doesn't benefit from the innovative propellant. While LH2 is lighter than hydrocarbon fuels, it occupies more space due to its need for lower temperatures to remain in a liquid state. As a result, larger and highly-integrated fuel tanks are required in the fuselage. This leads to a significant increase in this mass contribution.

6.1 Fuel weight

The evaluation of necessary propellant for complete the mission has an important impact on the development of concept. For the different mass and volume of LH2 respect to conventional propellants it is necessary allocate the tanks in a optimized configuration. For this motivation the algorithms must be modified respect to a conventional aircraft. While LH2 takes up more volume for us, however, we go on to save considerable weight. Raymer's method is chosen because he envisions the use of hydrogen as a fuel.

6.1.1 Raymer's method

This method is based on propellant calculation due to defined weight ratio between the final and initial mass of the aircraft, for each flight phase defined in the mission profile. In particular, Breguet's formulation 6.1 is used, but it needs to be modified because it considers that the values remain constant throughout the flight phase, an approximation that is possible to make only in the cruise phase. Standard values are then assumed for the other phases.

$$\frac{W_i}{W_{i-1}} = e^{-\frac{R*SFC}{V*\frac{L}{D}}} \quad (6.1)$$

Next, the different stages are analyzed.

Phase with constant value

In taxi, take off, Subsonic climb, supersonic climb and landing are assumed this value of ratio.

$$\frac{W_i}{W_{i-1} \text{ Taxi \& Warm up}} = 0.97 \quad (6.2)$$

$$\frac{W_i}{W_{i-1} \text{ Subsonic climb}} = 0.985 \quad (6.3)$$

$$\frac{W_i}{W_{i-1} \text{ Supersonic climb}} = 0.985 \quad (6.4)$$

$$\frac{W_i}{W_{i-1} \text{ Landing}} = 0.995 \quad (6.5)$$

Cruise phase

The weight ratio is calculated using Equation 6.1. The method also takes into account the amount of fuel required for descent following cruise when calculating the corresponding cruise phase. So, for example, calculating supersonic cruise also goes to include the descent from supersonic to subsonic, similarly for subsonic cruise and missed approach cruise.

The parameters of the Breguet formulation are listed below.

- *Speed [V]*. Velocity is calculated as a function of altitude and mach number according to the procedure already explained in the section on aerodynamics. Equations 5.21 through 5.28 are then recalled.
- *Range [R]*. The range is calculated as a function of the velocity at the point above and the phase duration time given as input in section 2.8.

$$R = V * t \quad (6.6)$$

- *Aerodynamic Efficiency [L/D]*. This value is derived from the aerodynamic analysis for subsonic and supersonic cruise calculated in the chapter on aerodynamics, the results of which are in the table 5.11. The subsonic cruise efficiency is assumed also for constant altitude leg of missed approach.
- *Specific Fuel Consumption [SFC]*. A "scaling" procedure is adopted for the SFC. The SFC statistic, found in Table 4.3 and 4.4, is used as a reference. This value is then scaled for a propulsive efficiency ratio. Equations 6.7 and 6.8 represent the procedure in which the propulsive efficiency dependence of two characteristics of the propellant: the calorific value per unit mass and the specific impulse. The propulsive efficiency parameter was chosen because it is absolutely relevant to of the (propulsive) application and is characteristic of the performance of the engine as a function of the propellant.

$$SFC = \frac{\eta_{cruise}}{\eta_{ref}} * SFC_{ref} \quad (6.7)$$

$$\eta = \frac{g}{H} * ISP * V \quad (6.8)$$

Supersonic Climb Phases

For this phase, Raymer suggests using a constant value as chosen, or you can make a variation to the Breguet formula. As for speed and its estimation, the approach remains unchanged, similarly for the range. However, aerodynamic efficiency is calculated as the arithmetic mean between that in subsonic and that in supersonic conditions:

$$E_{climb} = \frac{E_{subsonic} + E_{supersonic}}{2} \quad (6.9)$$

Regarding the estimated Specific Fuel Consumption (SFC), it is scaled differently than the previous one because it takes into account the throttle. This choice is made because to accelerate to supersonic speeds, it is necessary to increase thrust and thus adjust the throttle, unlike the cruising phase where it remains relatively constant. The following formula is used:

$$SFC = \frac{\Pi_{climb}}{\Pi_{cruise}} * SFC_{ref} \quad (6.10)$$

where the reference value is obtained from statistics, and a throttle setting of 80% is assumed during cruise, and 100% during climb. Since this is a phase with a Mach variation, the weight ratio is calculated as the average of multiple segments into which the phase is divided, as follows:

$$\frac{W_i}{W_{i-1}^{Climb}} = \frac{\sum_{Star\ altitude}^{Final\ Altitude} * \frac{W_i}{W_{i-1}}}{\# \frac{W_i}{W_{i-1}}} \quad (6.11)$$

Mission fuel weight

To calculate the total fuel weight, multiply all the weight ratios found to obtain the total mission weight. However, the choice to use LH2 (liquid hydrogen) results in a variation of the coefficient of reserve and trapped fuel ($C_{r\&t}$), ranging from 6% more for aircraft powered by hydrocarbon fuels to 30% for the design choice made.

$$W_{fuel} = C_{r\&t} * \left(1 - \frac{W_i}{W_{i-1}^{total}}\right) * MTOW \quad (6.12)$$

6.2 Operative empty weight

The Operational Empty Weight (OEW) is one of the components used to calculate the total weight of the aircraft, along with payload and fuel weight. Normally, this data should be initialized using statistics, but due to limited information about the specific aircraft design chosen, this could not be done. Nevertheless, it needs to be defined in order to calculate the Maximum Takeoff Weight (MTOW) because the result will later be compared to the statistical value. If the deviation is greater than five tons, a convergence cycle will be initiated specifically for MTOW.

What is presented here is a high-level approach, as there are no references available for this aircraft category. Raymer proposes an exponential formula as a function of MTOW found in statistics and other factors, which are shown in the figure 6.1.

$$\frac{OEW}{MTOW} = K_{vs} * K_{material} * A * MTOW^C \quad (6.13)$$

$W_e/W_0 = A W_0^C K_{vs}$	A	C
Sailplane—unpowered	0.86	-0.05
Sailplane—powered	0.91	-0.05
Homebuilt—metal/wood	1.19	-0.09
Homebuilt—composite	0.99	-0.09
General aviation—single engine	2.36	-0.18
General aviation—twin engine	1.51	-0.10
Agricultural aircraft	0.74	-0.03
Twin turboprop	0.96	-0.05
Flying boat	1.09	-0.05
Jet trainer	1.59	-0.10
Jet fighter	2.34	-0.13
Military cargo/bomber	0.93	-0.07
Jet transport	1.02	-0.06

K_{vs} = variable sweep constant = 1.04 if variable sweep
= 1.00 if fixed sweep

Figure 6.1: Parameters for OEW

For the study are assumed Jet transport coefficient with fixed sweep. $K_{material}$ is assumed 1 for metallic material, if the choose is composite material the coefficient has a value of 0.95.

6.3 Output data

6.3.1 Fuel weight

Constant weight ratio	
Phase	Value
Taxi and Take off	0.97
Subsonic climb	0.985
Supersonic climb	0.985
Subsonic climb (MA)	0.985
Landing	0.995

Table 6.1: Constant weight ratio

The values in the table 6.1 are recommended by Raymer [15].

Variable weight ratio						
	Phase	Design Point	B	C	D	E
First iteration	Sub. Cruise (A)	0.997	0.997	0.997	0.997	0.997
	Sup. Cruise	0.854	0.855	0.853	0.922	0.759
	Sub. Cruise (D)	0.998	0.998	0.998	0.998	0.998
	Missed app. Cruise	0.998	0.998	0.998	0.998	0.998
	Total fuel [kg]	38903	38378	39431	22606	64299
Last iteration	Sub. Cruise (A)	0.997	0.997	0.997	0.997	0.997
	Sup. Cruise	0.900	0.892	0.905	0.913	0.890
	Sub. Cruise (D)	0.997	0.997	0.997	0.997	0.997
	Missed app. Cruise	0.998	0.998	0.998	0.998	0.998
	Total fuel [kg]	46404	45128	47361	35822	56307

Table 6.2: Variable weight ratio

Observing the table, we can notice how the values vary. In particular, as the number of passengers (B, A, C) increases, there is a decrease in weight ratios because the aircraft, being heavier, consumes more. In fact, the total fuel increases as the number of passengers increases, albeit with small variations. When varying the Mach number, it is observed that with its increase (D, A, E), the weight ratios decrease only in supersonic cruise while they slightly increase in subsonic phases. Nevertheless, the fuel weight correctly increases as the Mach number increases.

6.3.2 Operative empty weight

		Operative empty weight				
		A (Design Point)	B	C	D	E
First iteration	OEW [kg]	105199	104276	105962	86846	123191
Last iteration	OEW [kg]	151882	141994	158325	127008	173402

Table 6.3: Operative empty weight

In the table 6.3, you can see the results of the empty operating weight, where it is noticeable that as the number of passengers increases, the empty operating weight increases significantly, and the same trend is observed as the Mach number increases. The values are very high, due to the fact that, as will be shown later, the dimensions of the aircraft are above average because the storage of LH2 (liquid hydrogen) requires high volumes, which result in a longer length of the aircraft.

Chapter 7

Performance requirements verification

The process of verifying requirements introduces performance constraints into the vehicle design procedure, encompassing aspects such as wing surface area, maximum take-off weight (MTOW), and thrust. These requirements fall into two main categories: the ratio of aircraft mass (e.g., MTOW) to wing surface area, known as wing loading, and the Thrust-to-MTOW ratio. The first category is pivotal within the convergence loop since it determines the final wing surface area. Conversely, the second category primarily pertains to propulsion and regulatory constraints, exerting a limited influence on the overall design methodology. Each requirement is linked to a specific phase of the mission: landing and instantaneous turns define the constraints related to wing loading, while takeoff, cruise, climb, and the second segment determine the constraints related to the thrust-to-weight ratio. To facilitate meaningful comparisons, all parameters are standardized with respect to MTOW and sea-level conditions. This standardization is crucial because each requirement is closely tied to a mission phase that exhibits distinct characteristics in terms of weight and air properties. At this stage, the conceptual design of the aircraft is nearly complete. The focus shifts to the verification of project and mission feasibility, involving a comprehensive assessment of key points and requirements, both from technical and operational perspectives.

7.1 Wing Loading Requirements

During the landing and instantaneous turn phases, specific wing loading values are imposed. Consequently, we need to determine a corresponding MTOW and wing surface area that satisfy these constraints. In theory, the most stringent requirement, which is the instantaneous turn, should be used for sizing purposes. However, in this project, the landing requirement is employed because, being a passenger transport aircraft, an instantaneous turn during cruise is not envisaged. This would be different for a military aircraft. The formulas that guide the estimation of wing loads for both of these requirements are elaborated upon below.

Landing

$$\frac{W}{S} = \frac{S_{LND} * SM - S_a}{5} * C_{L,max} * \frac{MTOW}{W_{lnd}} * \sigma \quad (7.1)$$

where the parameters represents:

- S_{LND} : is the length of destination airport and is an input (2.3.6).
- SM: is the safety margin assumed as 1.67.
- S_a : Is the obstacle clearance distance, a typical value that is different for the case.

$$S_a = \begin{cases} 304.8 \rightarrow 3^\circ \text{ Glidescope} \\ 182.88 \rightarrow \text{general aviation approach} \\ 137.16 \rightarrow \text{STOL } 7^\circ \text{ approach} \end{cases} \quad (7.2)$$

- $C_{L,max}$: is the maximum lift coefficient that is an input by user. Is the maximum between supersonic and subsonic phases.
- $\frac{MTOW}{W_{lnd}}$: is the weight ratio and their value are $\frac{1}{0.85}$.
- σ : is the density ratio, that is referred to the altitude of destination airport, using the ISA formulation.

$$\sigma = \frac{\rho_{SL}}{\rho_{LND}} \quad (7.3)$$

$$\rho_{LND} = 1.226 * (1 - 0.0000226 * z_{LND}[m])^{4.256} \quad (7.4)$$

Instantaneous turn

$$\frac{W}{S} = \frac{0.5 * \rho_{IT} * V^2 * C_{L,max}}{n * g} * \sigma \quad (7.5)$$

where:

- V: The speed is estimated using the procedure previously employed (Equations 5.21 through 5.28).
- $C_{L,max}$: Maximum lift coefficient defined in landing procedure.
- n: is the load factor and the formulation is below. $\dot{\psi}$ is the turn rate, fixed by certification (360°turn in two minutes).

$$n = \sqrt{1 + \left(\frac{V * \dot{\psi}}{g}\right)^2} \quad (7.6)$$

$$\dot{\psi} = 3 \frac{deg}{s} = 0.05236 \frac{rad}{s} \quad (7.7)$$

$$g = 9.81 \frac{m}{s^2} \quad (7.8)$$

- σ : The density ratio is as in the case of landing, but the reference values in this case are related to the altitude of the instantaneous turn.

7.2 Thrust to weight ratio requirements

The requirements of this section are derived from the climb, cruise, takeoff, and second segment phases. Unlike the previous section, now the most stringent requirement is the one with a higher value, with the aim of not over sizing the aircraft. For the supersonic analysis, the formulas used are the same as those detailed in the 'cruise' subsection, with the only difference being in the density ratio, for which formulas for the stratosphere will be employed. Additionally, a different wing loading value is used compared to the one calculated previously because the phases under consideration are far from sea level conditions; thus, the considered mass will also be different. So there will be a different reference mass than that of takeoff (MTOW). Instead, the wing area used is the same as determined by the subsonic landing requirements.

Cruise

$$\frac{T}{W} = \frac{0.5 * \rho * V^2 * C_{D0}}{\frac{W}{S}} * \sigma \quad (7.9)$$

where:

- V : The speed is estimated using the procedure previously employed (Equations 5.21 through 5.28).
- C_{D0} : The value of the aerodynamic drag coefficient is calculated in section 5.2.1 for subsonic and 5.2.2 for supersonic.
- $\frac{W}{S}$: For the subsonic analysis, the wing loading used is the *available* one, which is the wing area divided by the total mass. However, for the supersonic analysis, the weight is estimated as per the equations below. The wing area takes its value from the calculation in the previous section, and MTOW is initially defined from statistics and later updated in the convergence loop.

$$W_{supersonic\ analysis} = OEW + W_{fuel\ medium} + W_{payload} \quad (7.10)$$

$$W_{fuel\ medium} = \frac{W_{fuel\ Supersonic\ climb} + W_{fuel\ Supersonic\ cruise}}{2} \quad (7.11)$$

$$W_{fuel\ Supersonic\ climb} = \left(1 - \frac{W_i}{W_{i-1\ from\ Gound\ to\ Climb}}\right) * MTOW \quad (7.12)$$

$$W_{fuel\ Supersonic\ Cruise} = \left(1 - \frac{W_i}{W_{i-1\ from\ Gound\ to\ Cruise}}\right) * MTOW \quad (7.13)$$

- σ : The density ratio is calculated using the formulas provided below, taking the cruise altitude specified in the input in Section 2.8. The final result for density is the average, as cruise conditions, as known, are not exactly at a constant altitude.

$$\sigma = \frac{\rho_{SL}}{\rho_{CRS}} \quad (7.14)$$

$$\rho_{Sub,CRS} = 1.226 * (1 - 0.0000226 * z_{CRS}[m])^{4.256} \quad (7.15)$$

Take off

$$\frac{T}{W} = \frac{\frac{W}{S}}{TOP * \sigma * C_{L,to}} \quad (7.16)$$

where:

- $\frac{W}{S}$: The procedure is analogous to the one presented in the previous section for the cruise phase.
- TOP: The takeoff parameter is an input value that depends on the length of the runway. This length is defined in three different ways. The first is called *Ground roll*, in which the measurement starts when the aircraft is stationary on the runway and continues until the wheels of the landing gear leave the ground. The second is called *Over 50 ft*, and it starts from when the aircraft is stationary on the runway and extends until it clears the imaginary obstacle specified by regulations at a height of 50 feet above the runway. Finally, the third parameter is known as *Balance field length*, which begins at the same point and extends until reaching the *decision speed*. The decision speed is the velocity at which the takeoff can still be executed even in case of a failure. Typical values for these parameters are provided in the image.

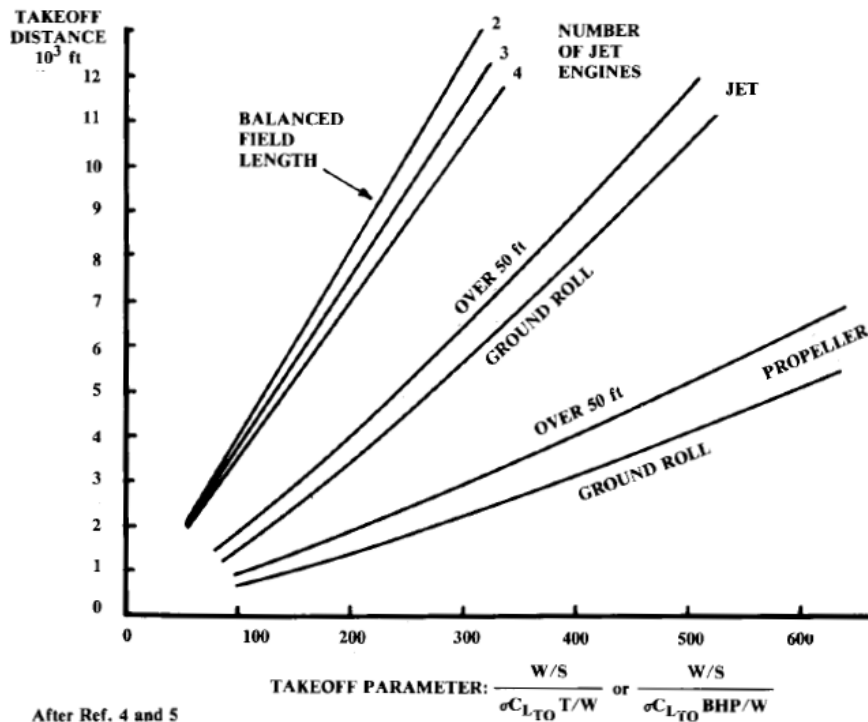


Figure 7.1: TOP [15]

- $C_{L,to}$: The lift coefficient at takeoff is calculated by increasing the value of the subsonic cruise lift coefficient by 40%.
- σ : The density ratio, being in the denominator, is inverted. Altitude is always defined by the inputs of the mission profile.

$$\sigma = \frac{\rho_{to}}{\rho_{SL}} \quad (7.17)$$

$$\rho_{Sub,CRS} = 1.226 * (1 - 0.0000226 * z_{TO}[m])^{4.256} \quad (7.18)$$

Climb

$$\frac{T}{W} = \left(\frac{T - D}{\frac{W}{S} * S * g} + 2 * C_{L,best} \gamma \right) * \sigma \quad (7.19)$$

The climb phase is a non-stationary phase, so it is more complicated to analyze. The parameters in the formula are:

- T: The thrust refers to the total available thrust, so it is obtained by multiplying the thrust of an individual engine by the number of engines, as defined in the table 5.6.
- D: For the calculation of drag, it is necessary to know the drag coefficient in this phase. To do so, the equilibrium equation along the trajectory axis as shown in the figure is used. The approximation of instantaneous climb is employed for estimating this value.

$$D = 0.5 * \sigma * V^2 * S * C_D \quad (7.20)$$

$$F - D = W * g * \sin(c) \quad (7.21)$$

where c is climb angle.

$$C_D = \frac{F - W * g * \sin(c)}{0.5 * \rho * V^2 * S} \quad (7.22)$$

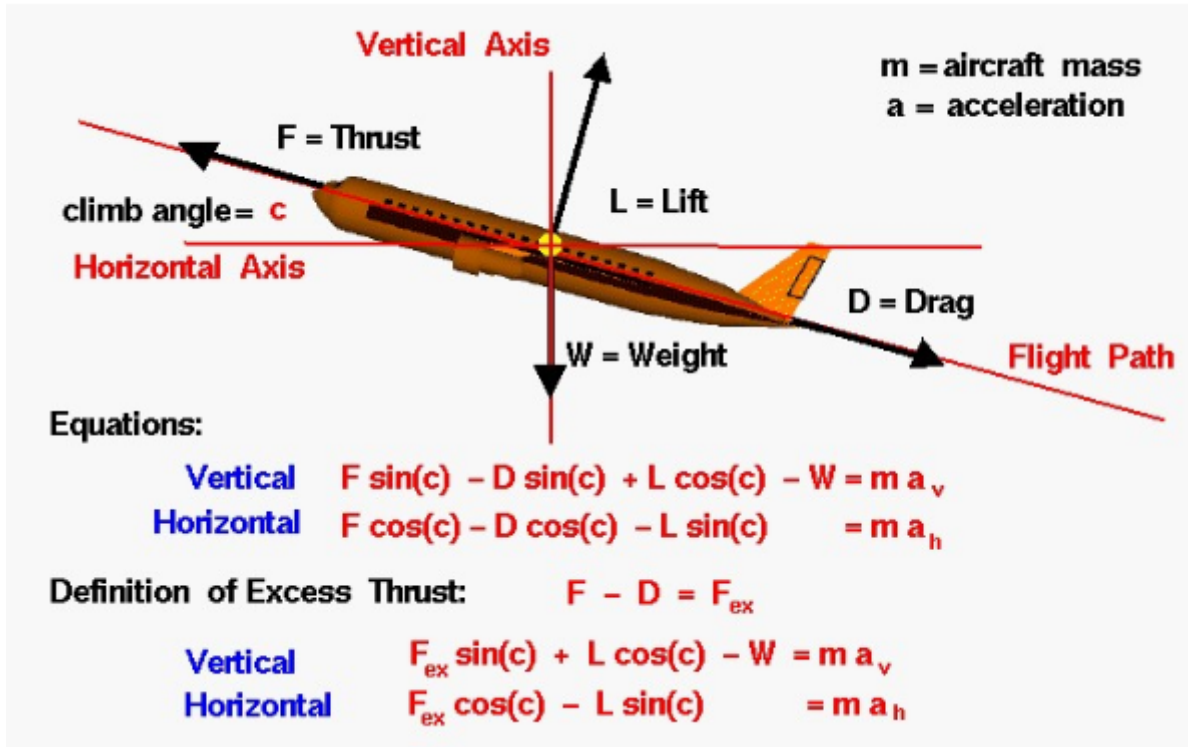


Figure 7.2: Equilibrium equations in climb [13]

- $\frac{W}{S}$: For the Wing loading the was used the same procedures used in cruise phase.
- $C_{L,best \gamma}$: The Lift coefficient for the best climb angle is calculated with the equation below. The parameters of this formula are computed in aerodynamic section 5.

$$C_{L,best \gamma} = \sqrt{\frac{C_{D0}}{\pi * AR * e}} \quad (7.23)$$

- σ : The density ratio has starting and ending altitudes defined by the data input for the mission profile, which are used to calculate the reference density. To obtain the density, ISA (International Standard Atmosphere) formulas for the troposphere are used. The final result for density is the average, as cruise conditions, as known, are not exactly at a constant altitude.

$$\sigma = \frac{\rho_{SL}}{\rho_{CLM}} \quad (7.24)$$

$$\rho_{Sub,CLM} = 1.226 * (1 - 0.0000226 * z_{CLM}[m])^{4.256} \quad (7.25)$$

Second segment

The requirement related to the second segment is derived from regulations. It takes into account that in the event of an engine failure, the aircraft must continue the mission safely with a maneuver that meets the minimum climb gradient specified by regulations, based on the aircraft's category. All the flight mechanics and aerodynamic parameters used are those derived from the takeoff and initial climb phases. This is because this requirement is applicable to both phases, serving as the initial segment of the climb, with a focus on operational and safety considerations.

$$\frac{T}{W} = \left(\frac{n_c}{n_c - 1} * \frac{C_D}{C_{L,to}} + \sin(\gamma) \right) * \sigma \quad (7.26)$$

where

- n_c : The number of necessary engines it is estimated during the preliminary aerodynamics calculation. Results are in table 5.6.
- C_D & C_L : The drag and lift coefficient are calculated in previous section, respectively in climb and take off.
- γ : The climb angle is an input of T/W Requirements Verification section (2.13).
- σ : The density ratio is between the sea-level density and that of the second segment, already calculated in the reference phases.

7.3 Matching Chart

The matching chart is a graph introduced by NASA that is useful for summarizing the data obtained in this chapter. It is a 2D representation of the aircraft's power as a function of wing configuration, specifically wing loading. This chart is valuable in defining what the design point is, particularly by analyzing the curves that are created by varying the wing loading, as seen in the T/W requirement section. In our case, the design point will be identified between the curves related to climb and the one related to wing loading during landing. The graph is presented with T/W on the y-axis and W/S on the x-axis. As can be observed in the section dedicated to the graph's outputs, all the

curves tend to intersect in a defined area. Within this area, we can find other possible design configurations based on the project's intent, meeting the project requirements. In addition, the chart is constrained on the x-axis by the designer with the goal of avoiding over sizing the wing area and constrained on the y-axis due to regulations. The matching chart is used for both the supersonic and subsonic regimes. In the former, all the phases described earlier pertain to the same regime, and the same applies to the chart for the supersonic regime. These charts refer to Maximum Takeoff Weight (MTOW) and sea level conditions.

7.4 Output Data

7.4.1 Wing Loading Requirements

Wing Loading Requirements						
		A (Design Point)	B	C	D	E
First it.	$\frac{W}{S}$ Landing	350.1	350.3	349.9	332.9	392.6
	$\frac{W}{S}$ Inst. turn	210.4	211.0	209.8	222.8	199.0
Last it.	$\frac{W}{S}$ Landing	325.2	330.4	322.1	337.8	312.6
	$\frac{W}{S}$ Inst. turn	210.4	211.0	209.8	222.8	199.0

Table 7.1: Wing Loading Requirements

In the table 7.1, we can observe that as the number of passengers (B, A, C) increases, the value decreases, creating a more stringent requirement. Similarly, the same trend is observed as the Mach number increases.

7.4.2 Thrust to weight ratio requirements

Thrust to weight Requirements						
		A (Design Point)	B	C	D	E
First it.	$\frac{T}{W} Sub. cruise$	0.105	0.105	0.105	0.111	0.101
	$\frac{T}{W} Sup. cruise$	0.219	0.221	0.216	0.108	0.389
	$\frac{T}{W} Take off$	0.114	0.113	0.114	0.104	0.121
	$\frac{T}{W} Sub. climb$	0.156	0.156	0.156	0.157	0.155
	$\frac{T}{W} Second seg.$	0.151	0.152	0.151	0.150	0.153
	$\frac{T}{W} Sup. climb$	0.681	0.682	0.680	0.655	0.706
Last it.	$\frac{T}{W} Sub. cruise$	0.091	0.094	0.089	0.080	0.101
	$\frac{T}{W} Sup. cruise$	0.106	0.119	0.098	0.095	0.120
	$\frac{T}{W} Take off$	0.139	0.141	0.138	0.144	0.134
	$\frac{T}{W} Sub. climb$	0.160	0.162	0.158	0.153	0.165
	$\frac{T}{W} Second seg.$	0.133	0.139	0.130	0.137	0.131
	$\frac{T}{W} Sup. climb$	0.591	0.622	0.574	0.659	0.549

Table 7.2: Thrust to weight Requirements

In the table 7.2, we can observe the results and notice that the phase with the highest thrust-to-weight ratio is the climb, both for the subsonic and supersonic regimes. Therefore, this will be the project requirement. For all phases, the trend of the value decreases slightly as the number of passengers increases. On the other hand, with an increase in the Mach number, we see an increase in the value for the cruise, subsonic climb, and second segment phases. For the remaining phases, there is a slight increase.

7.4.3 Matching chart

The following charts are created using the data obtained at the end of the convergence loop.

Subsonic

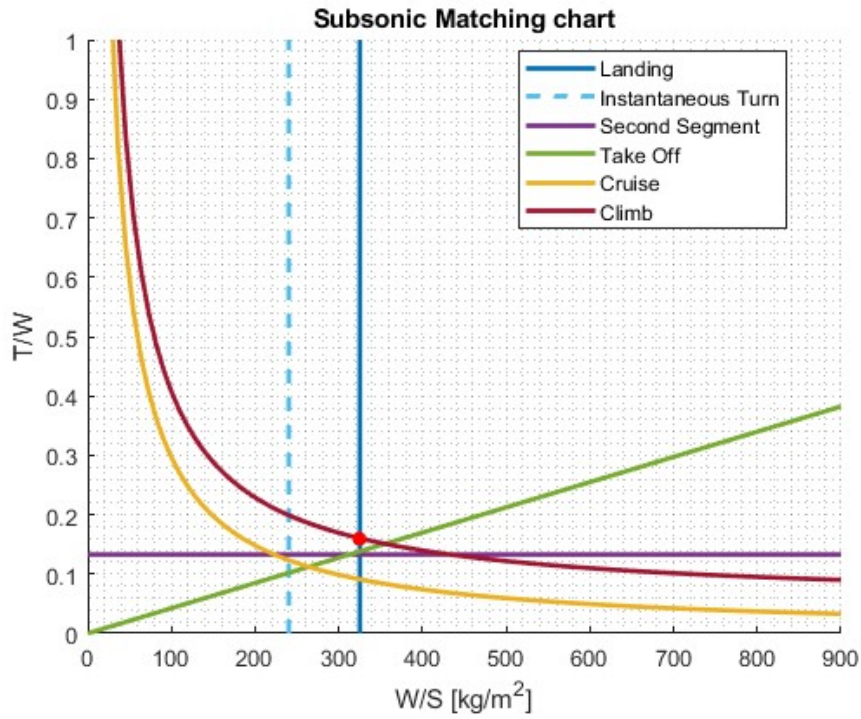


Figure 7.3: Subsonic Matching chart (Mach: 2, Pax:80)

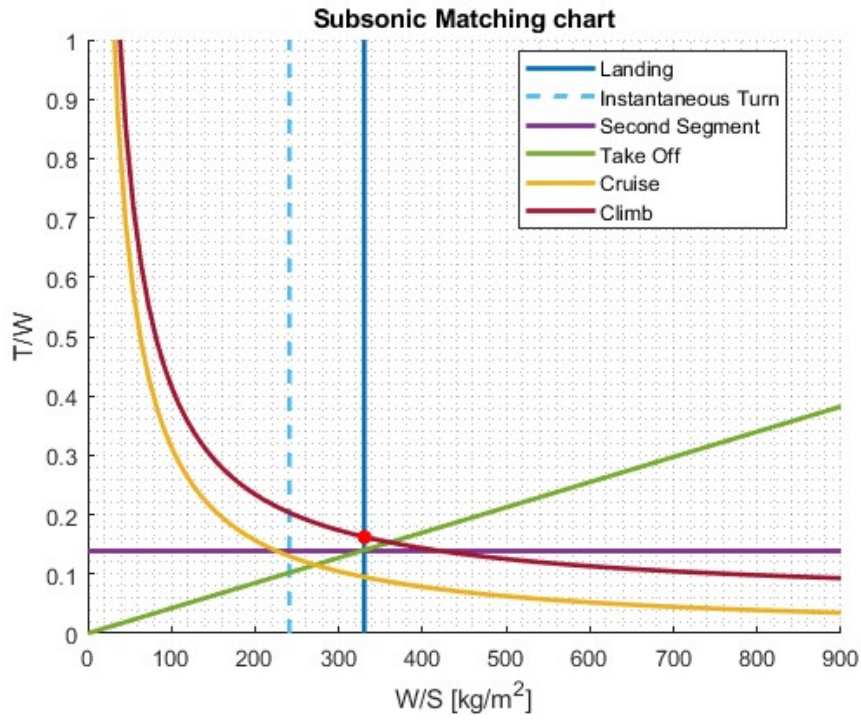


Figure 7.4: Subsonic Matching chart (Mach: 2, Pax:60)

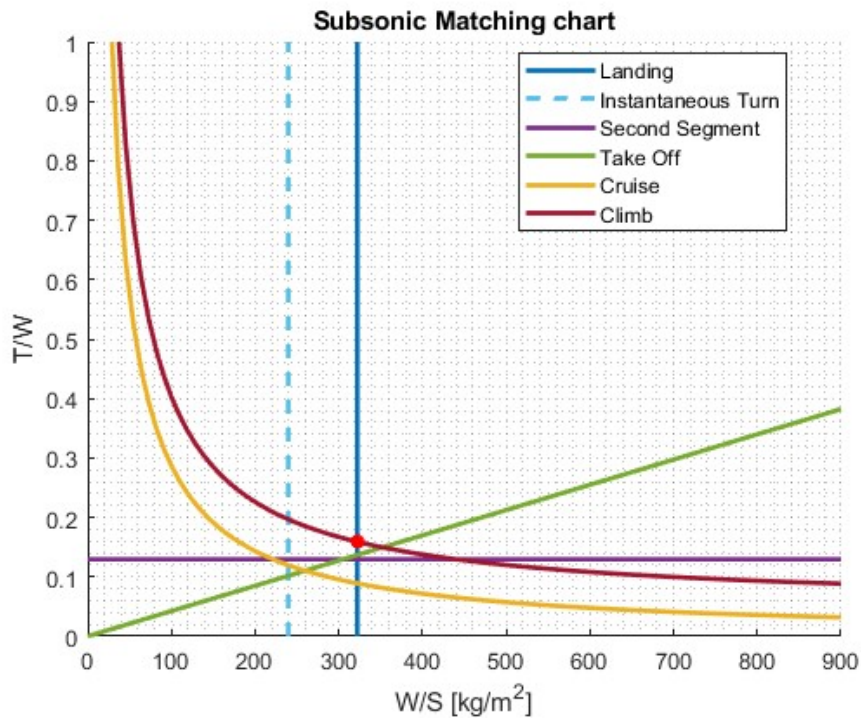


Figure 7.5: Subsonic Matching chart (Mach: 2, Pax:100)

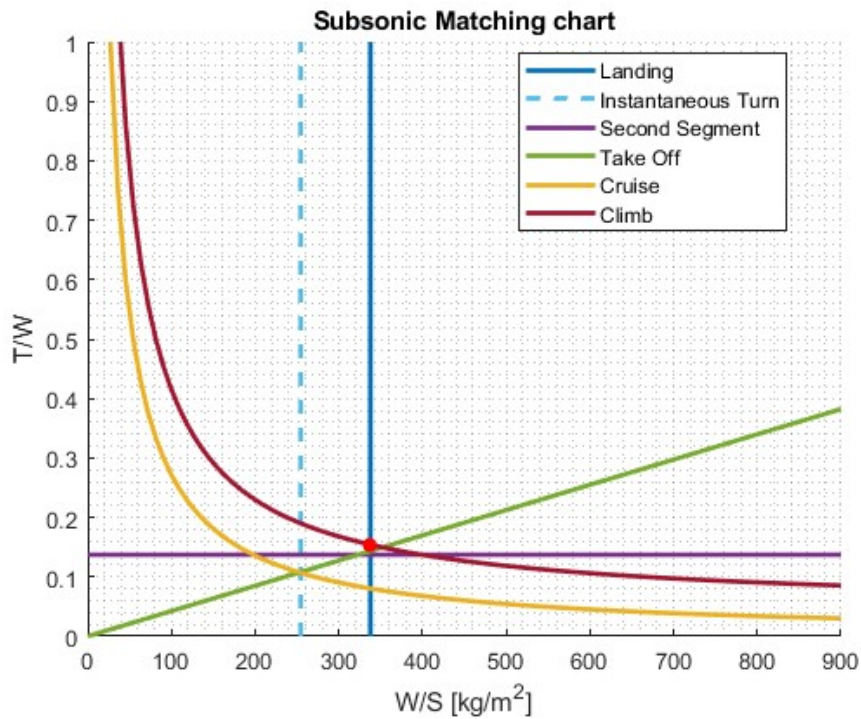


Figure 7.6: Subsonic Matching chart (Mach: 1.5, Pax:80)

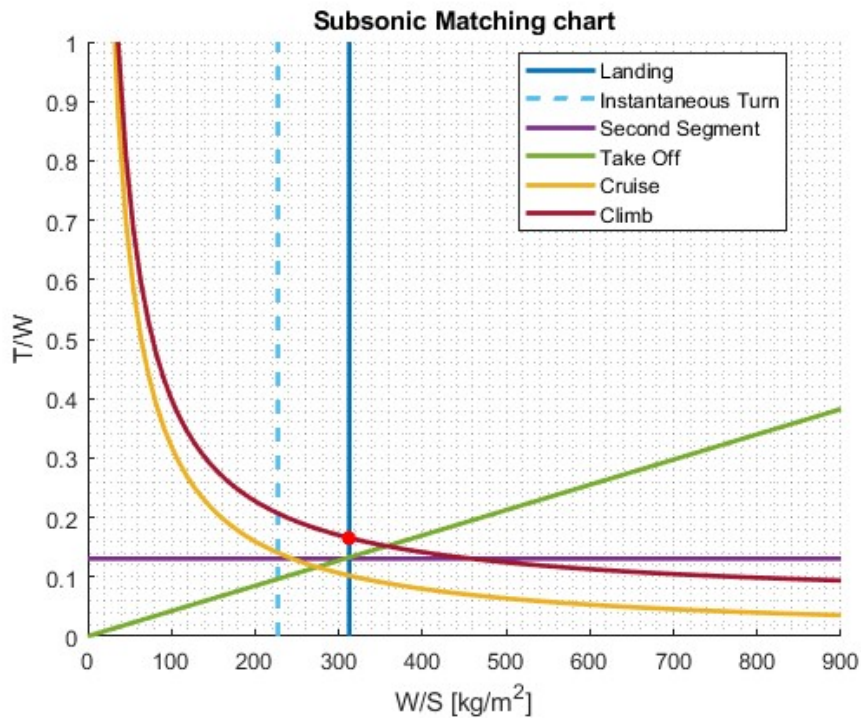


Figure 7.7: Subsonic Matching chart (Mach: 2.5, Pax:80)

In the subsonic regime, when varying the number of passengers, no visible changes in the matching chart are observed. However, as the Mach number increases, a higher wing loading requirement is evident, consequently leading to a reduction in the design Thrust-to-Weight ratio (T/W).

Supersonic

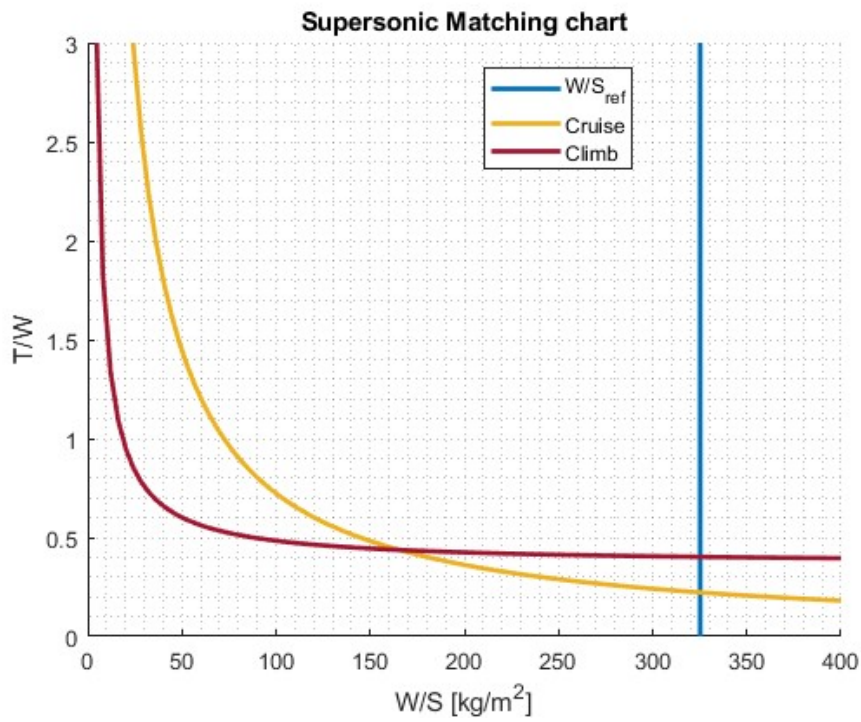


Figure 7.8: Supersonic Matching chart (Mach: 2, Pax:80)

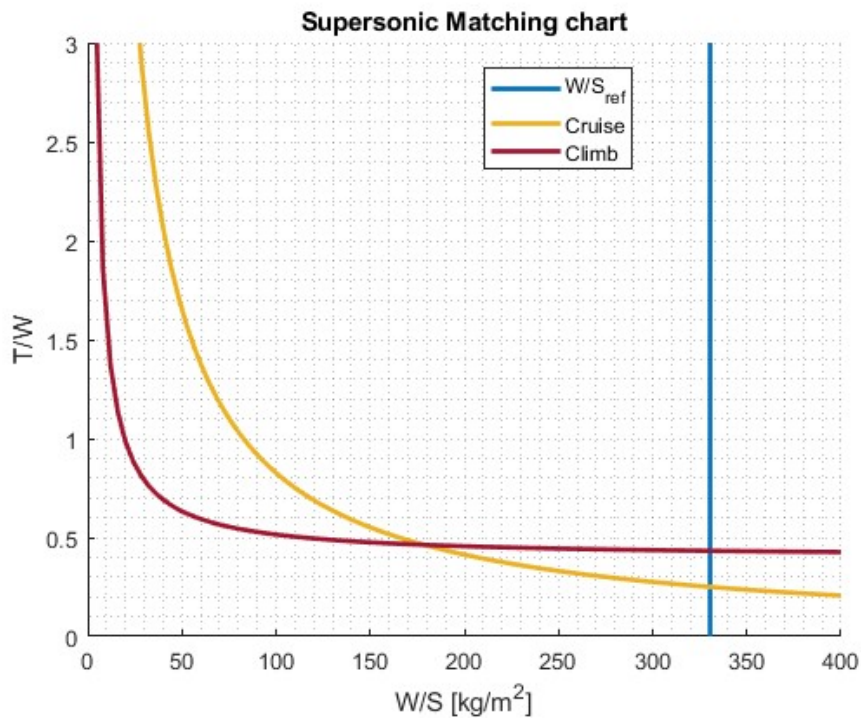


Figure 7.9: Supersonic Matching chart (Mach: 2, Pax:60)

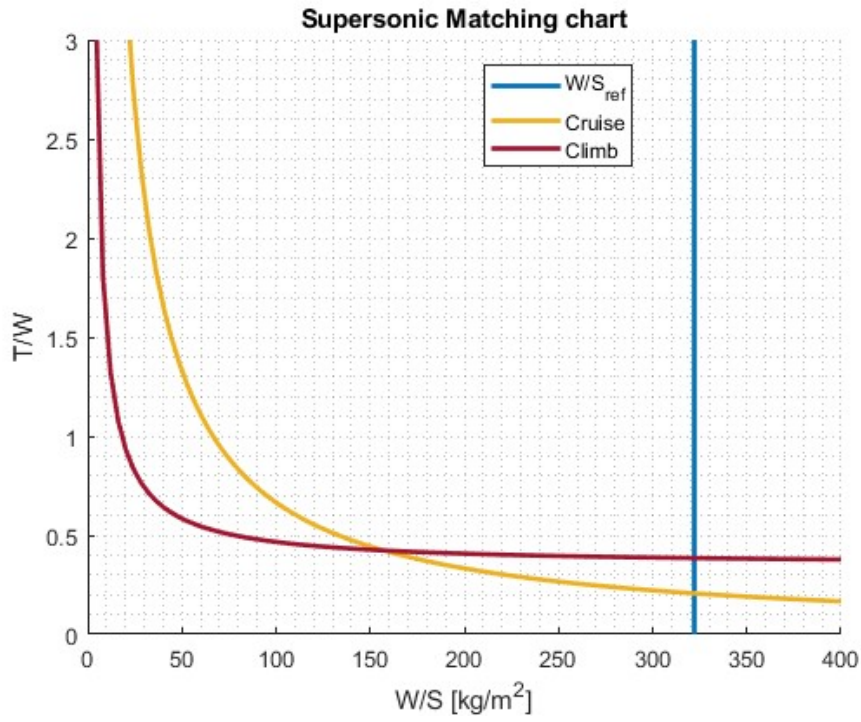


Figure 7.10: Supersonic Matching chart (Mach: 2, Pax:100)

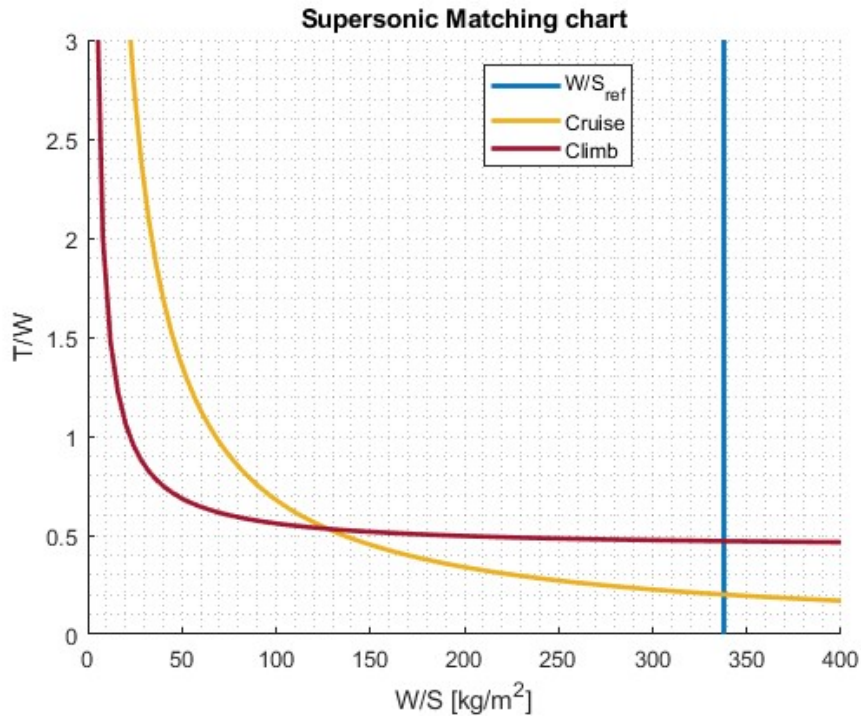


Figure 7.11: Supersonic Matching chart (Mach: 1.5, Pax:80)

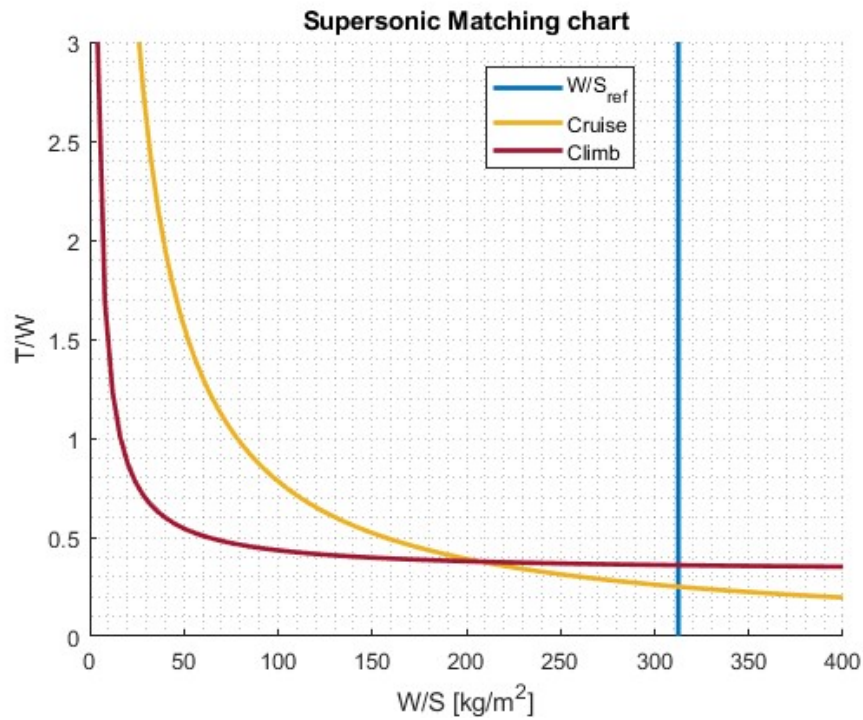


Figure 7.12: Supersonic Matching chart (Mach: 2.5, Pax:80)

In the supersonic regime, no noticeable changes are observed when varying the number of passengers. However, as the Mach number increases, there is an increase in wing loading, leading to a slight decrease in T/W , which is not very pronounced due to the shallow slope of the climb curve.

Chapter 8

Tank sizing

As previously explained, the disadvantage of using an unconventional fuel like LH2 is its low density, which results in enormous volumes required for storage. After calculating the necessary fuel in the previous section 6.1, we now seek the best locations for storage and optimal tank geometries to make the most of the available space. Since supersonic flight is a requirement, the wing profile will be slim, preventing the use of this space for storage as in conventional aircraft. Therefore, we will opt for a configuration where the tanks are located inside the fuselage, particularly between the passenger compartment and the cargo hold, further between the rear of the passenger compartment and tail. The motivation is that the tail must have a high aspect ratio to minimize aerodynamic resistance, so it cannot accommodate the fuel. Instead, it is used to house avionic equipment such as flight data recorders and cockpit voice recorders, along with all the necessary components.

8.1 Underfloor Tank Configuration

In the thesis [1], an analysis is conducted comparing three different tank geometry configurations in order to find the one that optimizes space the best. Among those analyzed are: One Circular Section, Two Circular Sections, and One Rounded Section. Naturally, given the shape of the fuselage, the last option is the one chosen.

The available volume for this tank takes into account the fact that, as will be seen later, in this section of the fuselage, we have a portion occupied by the passenger compartment and another designated for the cargo hold. The code then creates a loop to find an

appropriate tank height by increasing the fuselage diameter, as explained in the figure 8.1.

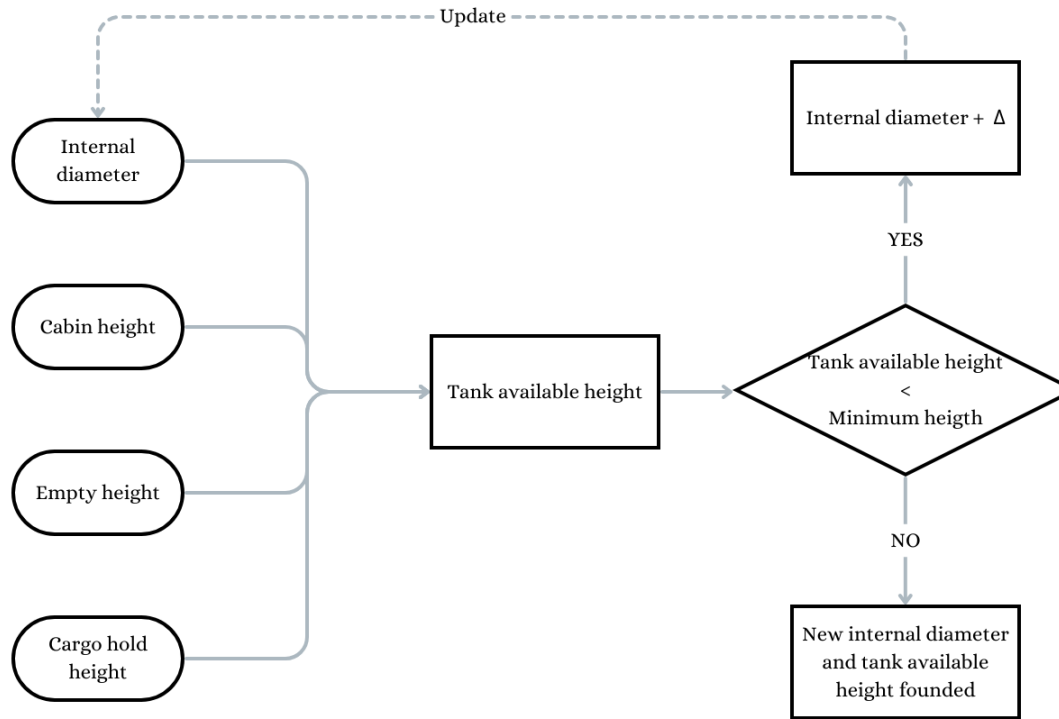


Figure 8.1: Available Tank Height and Internal Diameter Estimation

For this procedure, some assumptions are made:

- The fuselage section is divided in half, where the upper part contains the passenger compartment, and the lower part contains the tank and the cargo hold.

$$h_{cabin} = \frac{d_{internal}}{2} \quad (8.1)$$

- The height of the cargo hold is 50 cm.
- The empty space between the internal diameter of the fuselage and the cargo hold is evaluated using the formula:

$$h_{empty} = Margin [\%] * d_{internal} \quad (8.2)$$

where Margin is an input by user.

- The minimum tank height is fixed at 1.5 meters, and the available height is calculated as follows:

$$h_{available\ tank} = d_{internal} - (h_{cabin} + h_{cargo\ hold} + h_{empty}) \quad (8.3)$$

Once this cycle is completed, you obtain the two necessary pieces of information, and then you proceed with the sizing, taking into account the thicknesses of the material layers and insulation materials, assuming a maximum value of 8 cm. Subsequently, this data will be recalculated, and thanks to the convergence loop of the program, it will become more accurate, even though it is a good initial approximation.

The cross-sectional shape of this One Rounded Section Tank consists of a central rectangular part and two half-spheres on the right and left sides. Similarly, for the longitudinal section. The longer side of the rectangle that makes up the central part has the same dimension as the top of the hull, while the height of the same rectangle corresponds to the value found in the previously described cycle in the figure 8.1 and is equal to the diameter of the half-spheres positioned laterally. The two side spheres will increase the width of the rectangle, so it will be necessary to have a loop that checks that this height (and thus the diameter of the sphere) does not exceed the available width in the fuselage.

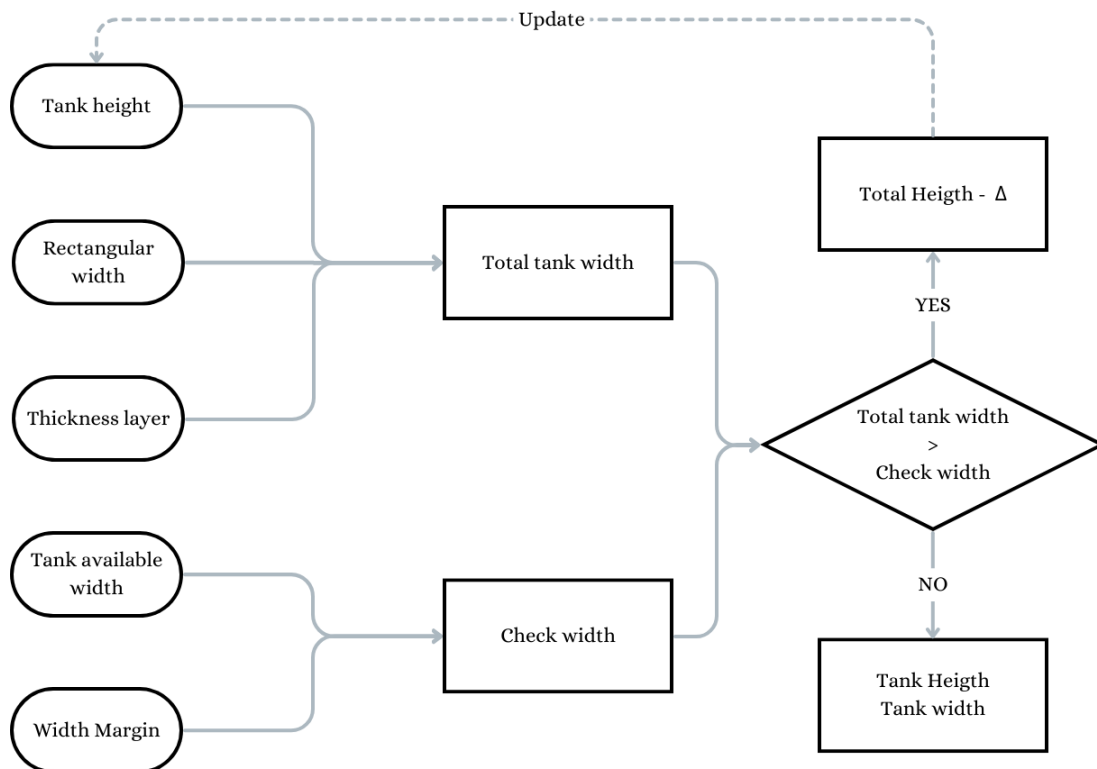


Figure 8.2: One Rounded Section Tank: Sizing Procedure

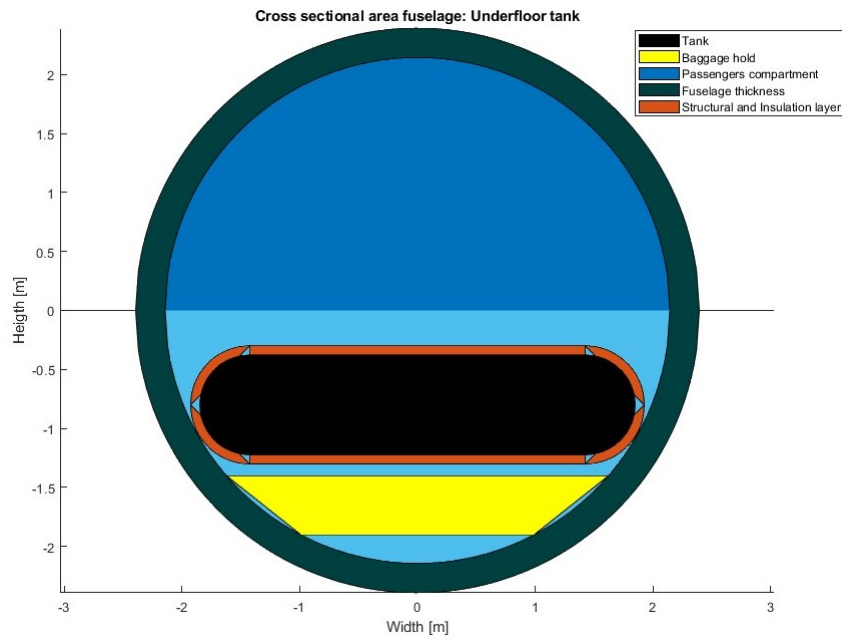


Figure 8.3: One Rounded Section Tank 2D

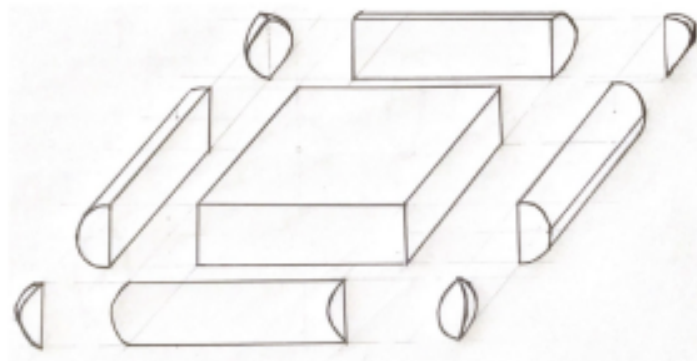


Figure 8.4: One Rounded Section Tank 3D [1]

In the figure 8.2, you can see the sizing procedure taking into account the limit imposed by the width measurement, while in Figure 8.3, you can observe the result obtained for the design configuration. In Figure 8.4, a 3D sketch of the tank has been drawn.

8.2 Rear Tank and Aircraft Length Definition

8.2.1 Rear Tank

To size the rear tank, it is necessary to know the remaining fuel once the underfloor tank is filled. The shape that optimizes space the best is a cylinder, assuming a continuous fuselage with a constant diameter between the tail and the passenger compartment. For sizing, the same pattern as shown in the figure 8.1 is used, but assuming that the cylinder is not centered with the fuselage center, but rather slightly higher. To calculate the tank's centering, the difference between the fuselage's inner diameter and the wing's height is calculated, and then divided by two to obtain the tank's centering measurement. Once the dimensions of the section are determined, the required length of the tank is found in order to accommodate the remaining fuel, taking into account structural margins and the thickness of the insulation layer. This defines the rear tank. In the figure 8.5, there is an example of the final configuration of the two tanks, in the case of configuration A (Please note the different scales of the axes).

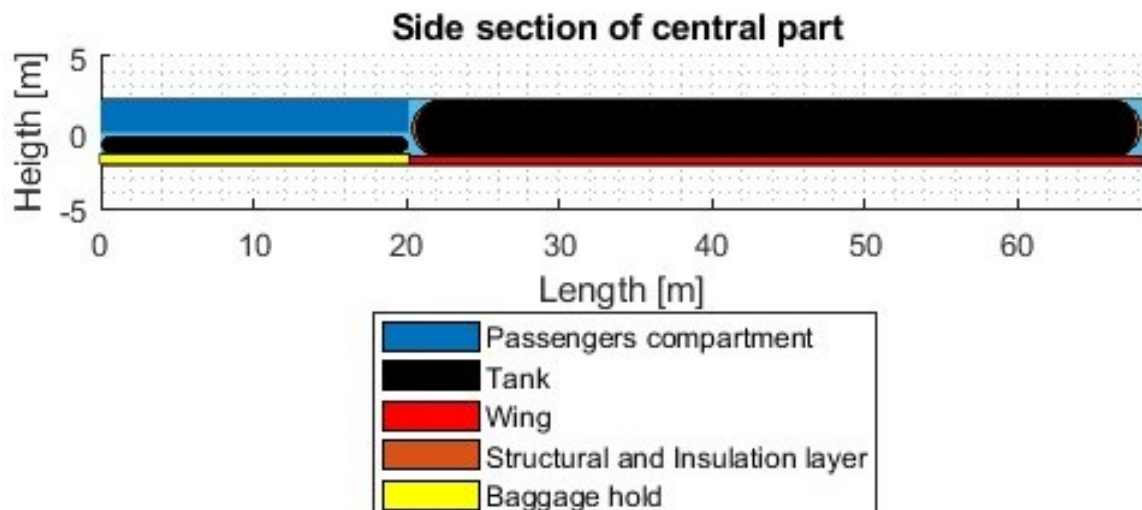


Figure 8.5: Tank configuration

8.2.2 Aircraft Length

The length of the aircraft is determined by various contributions, listed below:

- Front area: corresponds to the cockpit and the avionics bay immediately following

it; the calculation of the length of this part is done as follows, where μ represents the half-angle of the Mach cone.

$$L_{FA} = \frac{d_{external\ fuselage}}{2} * \frac{1}{\tan\frac{\mu}{2}} \quad (8.4)$$

$$\mu = \arcsin\frac{1}{M_{design}} \quad (8.5)$$

- Passenger compartment: this is the section dedicated to passengers, and the design parameters are specified in regulations and listed in a table 8.1 The number of rows is determined by dividing the number of passengers by 4 seats per row (narrow-body configuration).

$$L_{PC} = \#rows * L_{seats} + \#Galley/Toilet * L_{Galley/Toilet} + \#Emergency\ Exit * L_{Emergency\ Exit} \quad (8.6)$$

Regulation value	
L_{seats}	850 mm
$L_{Galley/Toilet}$	980 mm
$L_{Emergency\ Exit}$	610 mm
$\#rows$	20 - 15 - 25
$\#Galley/Toilet$	2
$\#Emergency\ Exit$	2

Table 8.1: Regulation value

- Rear tank bay: the size depends on the design of the rear tank, taking into account the available free space with the passenger compartment.
- Tail cone: the length of this part can be calculated using the following equation; the fitness ratio (FR) is chosen according to the image 8.6. The value taken for the fitness ratio is 2.

$$L_{TC} = FR * d_{external\ Fuselage} \quad (8.7)$$

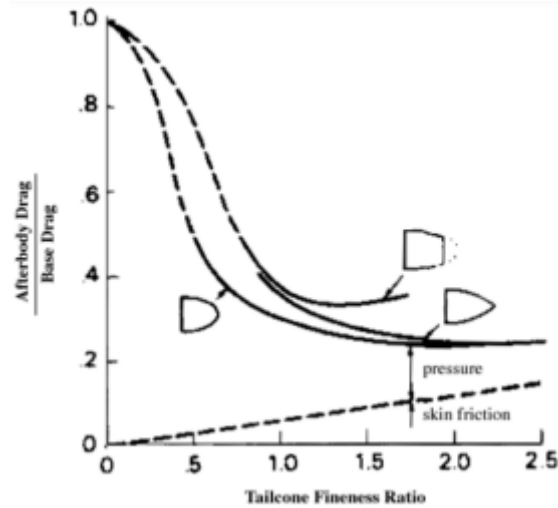


Figure 8.6: Fitness Ratio [19]

8.3 Layers Thickness of Structural and Insulation Material

Since LH2 is used as fuel, it is necessary to prevent boil-off and also design an insulating material that maintains the correct temperature inside the tank. Therefore, the calculation of both structural and insulation material thicknesses is carried out.

8.3.1 Structural design

The material for the tank structure must be chosen from materials that possess the following characteristics:

- It must have low liquid and gas permeability since one of the challenges with hydrogen is that its small atoms can permeate through the tank walls.
- It must be highly rigid.
- It must be low in density, lightweight, in order to optimize the total mass.

- It must have high fracture toughness so that the forces acting on it avoid inducing cracks, which could lead to safety issues.
- It must be highly resistant.

Considering the characteristics that need to be sought, the material must have the following parameters elevated:

- $\frac{\sigma_f}{\rho}$ Strength-limiting design with minimum mass
- K_{IC} Mode I fracture toughness
- $\frac{E}{\rho}$ Deformation-limiting design with minimum mass

The chosen materials that meet these parameters are:

- Continuous Carbon Fibre Reinforced Polymer [CFRP]: It provides high strength combined with very lightweight (first parameter listed above), albeit at a high production cost.
- Metals: It ensures strength with low acceptable density.
- Discontinuous Reinforced Metallic Composite: It is similar to CFRP but with the advantage of having very low gas permeability.

To find the design thickness, it is necessary to adopt an iterative cycle where the point of intersection between two curves determines the value. The two curves in question are one representing the material limit in terms of the limit stress to safety margin ratio, and the second is given by the following equation:

$$\frac{\sigma_f}{SM} \geq p_p * \left[\frac{a+c}{2t_{str}} * (1 + 2 * (1 + 3.6 * \frac{p_p}{E} * (\frac{a+c}{2t_{str}})^3) * \frac{a-c}{a+c}) + 0.5 \right] \quad (8.8)$$

where:

- $\frac{\sigma_f}{SM}$: It's the ratio between the limit stress and the safety margin; in the numerator, there is a material-dependent parameter, while in the denominator, there is a coefficient equal to 1.5.

- p_p : It is the maximum pressure value that a container can withstand before breaking, known as the burst pressure.

$$p_p = 2 * p_{ultimate} \quad (8.9)$$

$$p_{ultimate} = 1.5 * p_{limit\ design} \quad (8.10)$$

$$p_{limit\ design} = 1.1 * \Delta p \quad (8.11)$$

$$\Delta p = p_{max} - p_{atmosphere} \quad (8.12)$$

- c, a : They are the half minor axis and half major axis of tank section.
- E : is the Young modulus.

In the MATLAB program, once the user selects the material, this procedure is performed.

8.3.2 Insulation design

The desired characteristics in insulation material are:

- Low density to ensure lightness.
- Low thermal conductivity.
- Low thermal diffusivity.
- Low coefficient of heat transfer through radiation.

The task of the insulation material is to be able to deform in order to accommodate dimensional changes caused by thermal cycles, which are in turn induced by filling the tanks with LH2. Additionally, the insulation material must also prevent the condensation and solidification of atmospheric gases that may be present in the tank. This is because phenomena such as mechanical compression, impacts, vibrations, and more can result in reduced insulation effectiveness. In light of this, the most important parameters to look for in an insulation material are:

- K : Thermal conductivity. A low value of this parameter minimizes steady-state heat flow, while a low thermal diffusivity would lead to an increase in the time required for thermal energy to reach cryogenic temperatures.

- ρ : Density.

These conditions listed lead to the conclusion that materials with low mass or low density should be sought. In the program, two choices have been implemented:

- Silica Aerogels: In terms of thermal conductivity and density, they have values similar to materials belonging to the foam family. However, they are new technologies and are not yet well-characterized. Additionally, they have limitations in terms of mechanical properties.
- Combination of vacuum jacket and multilayer insulation (MLI): It proves to be an advantageous choice compared to aerogel since it has densities similar to foams but with a thermal conductivity two orders of magnitude lower than the same foam family. This choice therefore exhibits excellent properties. Furthermore, MLI has low thermal conductivity and reduced radiation heat transfer, as well as low density. All of this is enhanced by the vacuum layer, which has nearly zero thermal conductivity.

Both technologies are valid but come with significant costs, both in terms of installation and maintenance. For the second choice, it should be added that vacuum conditions around the tank imply an increase in their thickness to withstand the forces at play.

To find the value of the insulation material thickness, the heat transfer equation is used, taking into account only the conductive exchanges between the interior and exterior of the tank through the insulation and structural layers. Therefore, the following formula is used:

$$t_{ins} = 2 * \sqrt{\frac{k_{ins} * t_{fl} * (T_{int} - T_{LH2})}{h_{g,LH2} * \rho_{ins}}} \quad (8.13)$$

In this equation, it is noted that there is a dependence on the type of fuel, the type of insulation, external conditions, and the mission duration. Additionally, it is specified that the most critical case is analyzed, namely the "wet case," with the tanks completely full. In particular, the following parameters are considered:

- k_{ins} : Thermal conductivity of insulation material.
- ρ_{ins} : Density of insulation material.
- T_{LH2} : Temperature of cryogenic fuel.
- $h_{g,LH2}$: Heat of evaporation of cryogenic fuel.
- t_{fl} : Mission flight duration.
- T_{int} : Temperature of external interface of insulation layer.

8.3.3 Sizing Procedure

The sizing procedure, as shown in the figures 8.7 and 8.8 , is of significant importance because, first, the thickness of the insulation layer is determined by assuming suitable section dimensions for the tanks. Subsequently, the structural thickness is calculated, and then the exact dimensions are calculated. These final dimensions, thanks to the convergence cycle, will serve as input to recompute the insulation layer thickness and so on.

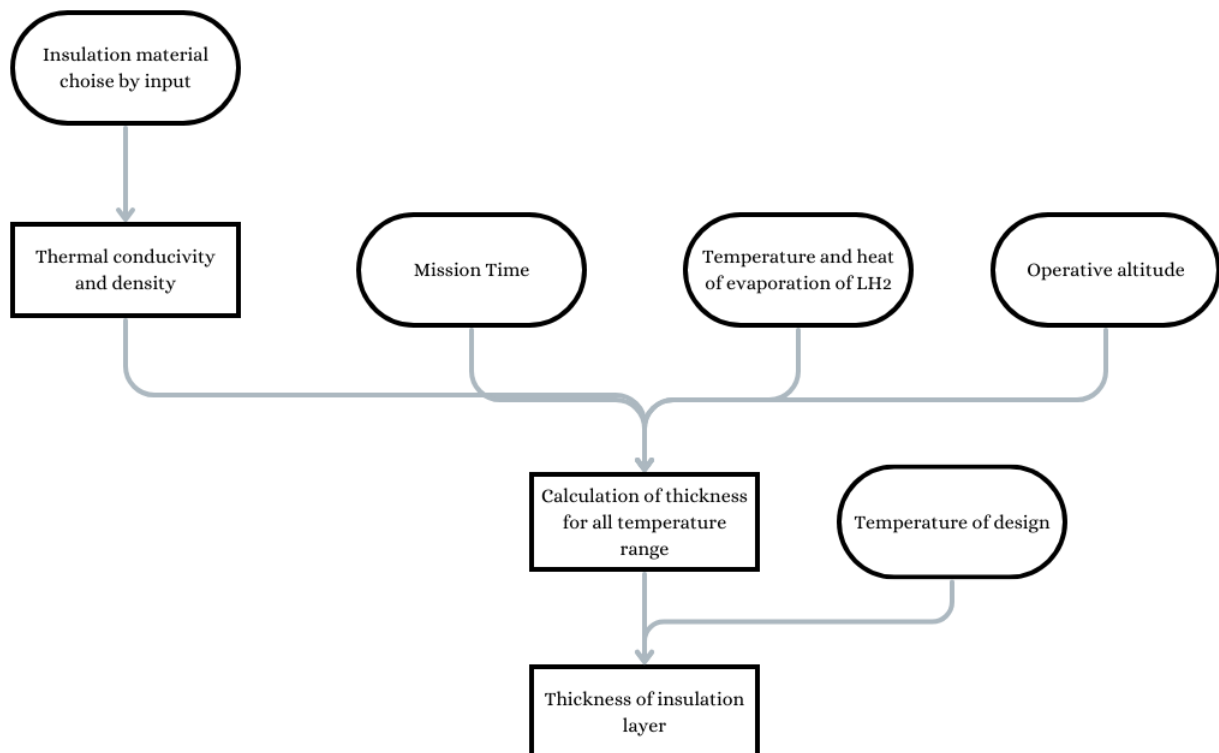


Figure 8.7: Sizing Layer Thickness Insulation Material

The figure 8.7 describes the procedure that the program follows for sizing the insulation material layer. The choice of material involves defining the parameters necessary for material calculation in the Excel file input. Input parameters for mission time, various LH2 parameters, and operating altitude are also provided. Afterward, an initial estimate of the insulation material thickness is made for all the temperatures in a range (-40°C to 30°C). Specifically, a vector of thickness values is created, varying with altitude and thus temperature. This is done to create a chart in case you want to see how a variation in degrees Celsius during sizing can affect the thickness of the insulation layer. Finally, the program returns the thickness corresponding to the input design temperature.

In the program, a maximum limit of 30 cm is set as the thickness to prevent sizing it in a way that would require reducing the diameter of the tanks, resulting in an increase in the length of the aircraft. In this case, we have three options:

- If all values in the vector are less than the available thickness, it means that for the entire temperature range (from sea level to supersonic cruise altitude), the maximum thickness adopted in the early stages is respected. In this case, the program chooses the design temperature, and the insulation material thickness is determined.
- If only some values in the vector are less than the available thickness, it means that only for a portion of the temperature range is the maximum thickness adopted in the early stages respected. In this case, the program selects the design temperature (the valid temperature range will be indicated by the program), and the insulation material thickness is determined.
- If none of the values are less than the available thickness, the program will request changing the material and close the program.

Please note that atmospheric pressure in the stratosphere is always calculated using the ISA (International Standard Atmosphere) formulas, as follows:

$$p_{stratosphere} = (22557.74 * e^{(-\frac{z[m]-11000}{6341.33})}) * 10^{-6} \quad (8.14)$$

Regarding the maximum pressure inside the tanks, it is set at 1.5 bar according to the reference. LH2 properties are set to -260C and 461.1MJ kg for temperature and

heat of evaporation respectively.

The figure 8.8 describes the procedure that the program follows. Initially, you are prompted to choose a material to configure the parameters necessary for sizing by Excel file for input. Then, the safety margin is set, the burst pressure is calculated using the maximum pressure inside the tanks and the external pressure, which is determined by the flight altitude. After that, the final structural thickness is evaluated. Finally, it is summed to the insulation thickness calculated earlier to determine the total thickness.

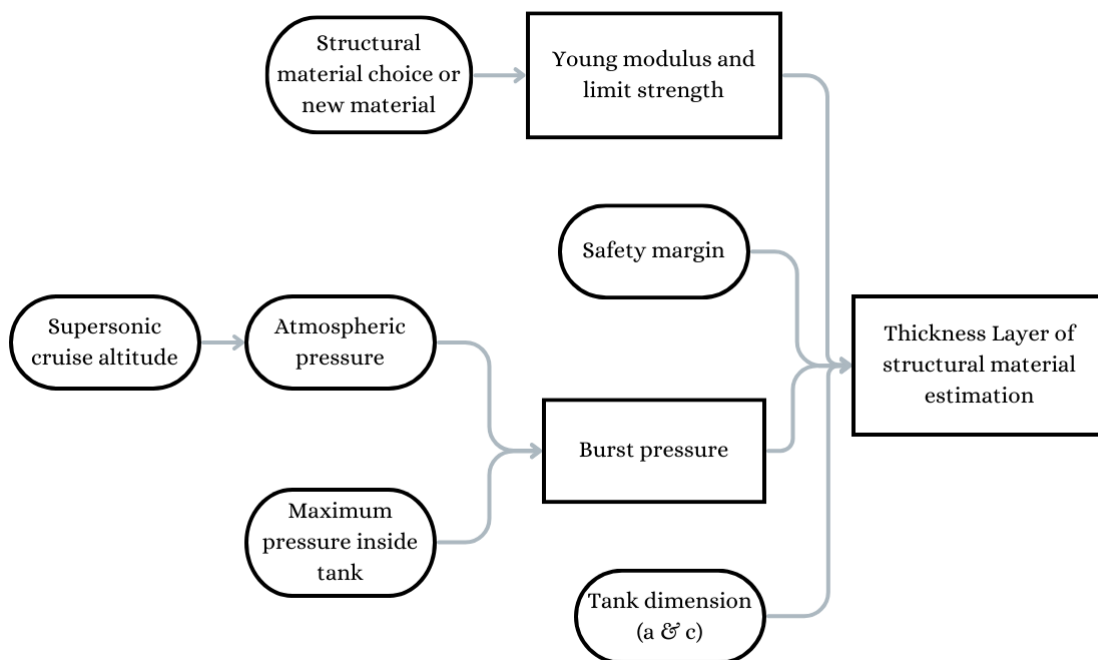


Figure 8.8: Sizing Layer Thickness Structural Material

8.4 Output data

Following various tests, it was found that the best structural material is Continuous Carbon Fibre Reinforced Polymer (CFRP), while the insulation material chosen is Vacuum Jacket + MLI. The design temperature selected is 30 degrees, as it represents a rather critical case and corresponds to when the aircraft is on the ground at the airport. The summarized data in the table 8.2 are derived from these choices.

		Tank sizing output				
		Design Point	B	C	D	E
Fuselage	Ext. diam.[m]	4.79	4.79	4.79	4.79	4.79
	Int. diam.[m]	4.29	4.29	4.29	4.29	4.29
Length	Front part [m]	8.93	8.93	8.93	6.27	11.4
	Center part [m]	66.74	64.84	68.19	52.01	80.52
	Pax comp. [m]	20.18	15.93	24.43	20.18	20.18
	Rear tank bay [m]	46.558	48.91	43.76	31.83	60.34
	Tailcone [m]	9.57	9.57	9.57	9.57	9.57
	Aircraft [m]	85.24	83.34	86.70	67.85	101.56
Pax Tank	Width [m]	3.78	3.78	3.78	3.78	3.78
	Height [m]	0.93	0.93	0.93	0.93	0.93
	Length [m]	19.90	15.70	24.11	19.90	19.90
	Struct. thick. [cm]	1.6	1.6	1.6	1.6	1.6
	Ins. thick. [cm]	2.34	2.34	2.34	2.34	2.34
	Total thick. [cm]	3.94	3.94	3.94	3.94	3.94
Rear Tank	Width [m]	3.61	3.61	3.61	3.61	3.61
	Height [m]	3.61	3.61	3.61	3.61	3.61
	Length [m]	46.05	48.37	43.28	31.46	59.70
	Struct. thick. [cm]	0.2	0.2	0.2	0.2	0.2
	Ins. thick. [cm]	2.34	2.34	2.34	2.34	2.34
	Total thick. [cm]	2.54	2.54	2.54	2.54	2.54

Table 8.2: Tank sizing output

Looking at the data, it is evident that the values for the external and internal diameters of the fuselage do not change with the configuration but have increased compared to the input data. This is because a minimum height has been assigned for the underfloor tank, and as a result, the found diameter is the minimum required to accommodate it.

Regarding the contributions to the length of various parts of the aircraft, it can be

observed that variations with changing passenger counts are minimal, primarily due to the addition of seat rows in the passenger compartment. Other parts may also vary but not significantly. However, when the Mach number varies, the total length varies considerably due to changes in the rear tank. Clearly, as the Mach number increases, more fuel is required. The following figures (from 8.11 to 8.15) illustrate the configuration of lengths as Mach number changes. It is emphasized that the wing design is consistent with the calculated dimensions, but its position is fictitious since the thesis does not include the wing design.

From the remaining part of the table, it is observed that with changes in configuration, the tanks vary only in length but not in cross-section. Below are the cross-sections of the tanks.

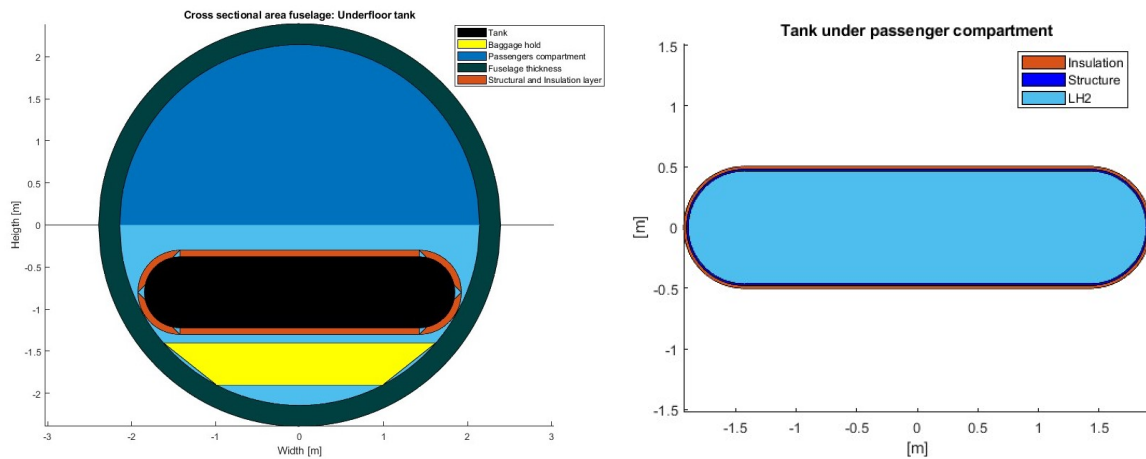


Figure 8.9: Section of tank under passenger compartment

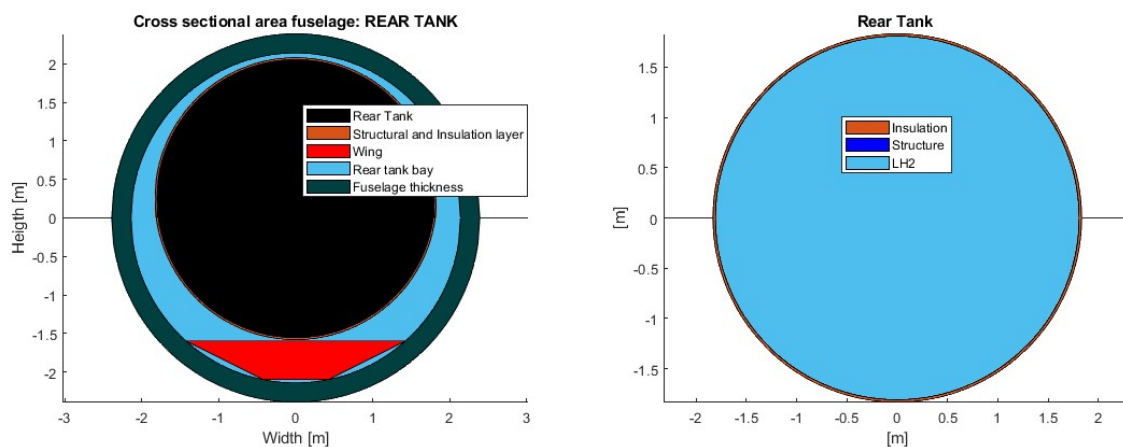


Figure 8.10: Section of rear tank

Furthermore, in these figures (8.9 and 8.10), you can appreciate the dimensioned thicknesses, which also do not vary with the configuration. As for the variation in tank length, the observations are the same as those made for the total length of the aircraft and can be observed in the following figures.

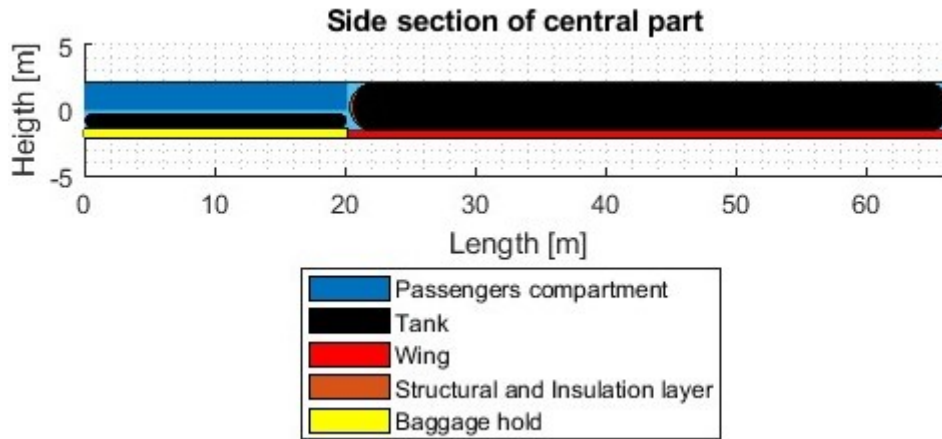


Figure 8.11: Configuration A: 80 pax and Mach 2

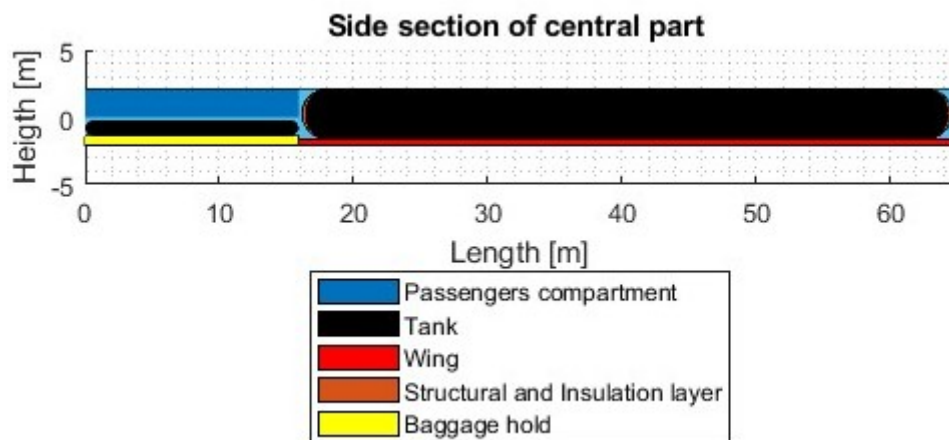


Figure 8.12: Configuration A: 60 pax and Mach 2

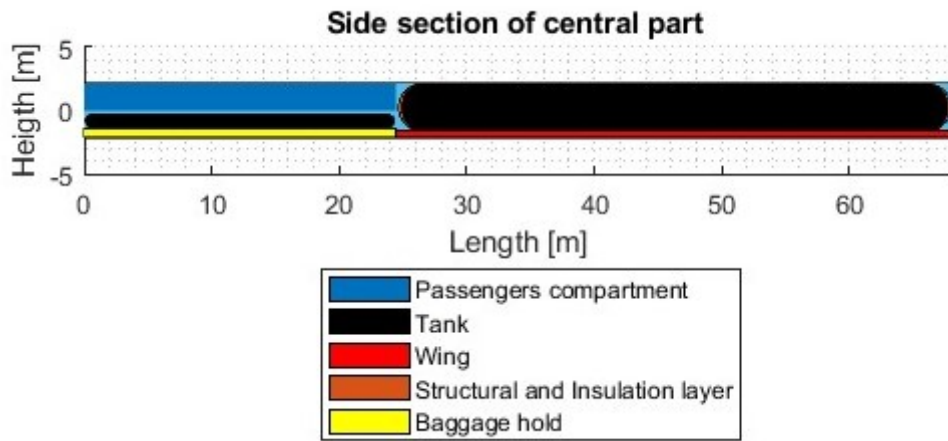


Figure 8.13: Configuration A: 100 pax and Mach 2

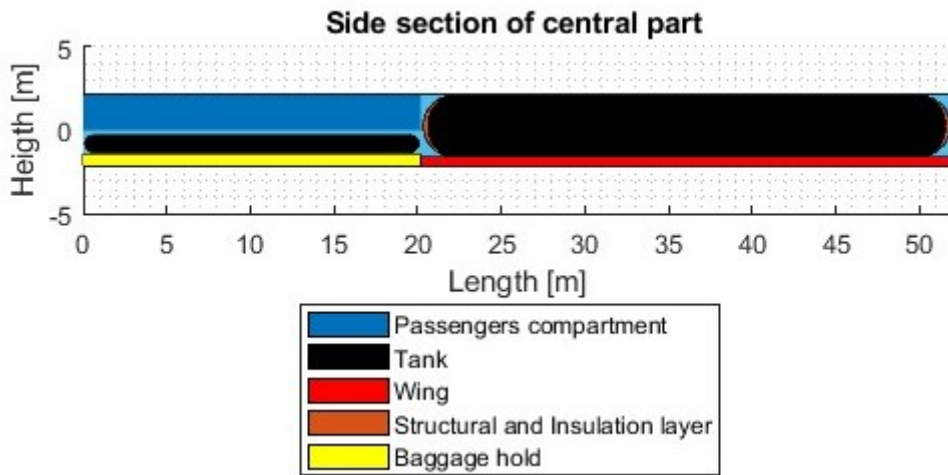


Figure 8.14: Configuration A: 80 pax and Mach 1.5

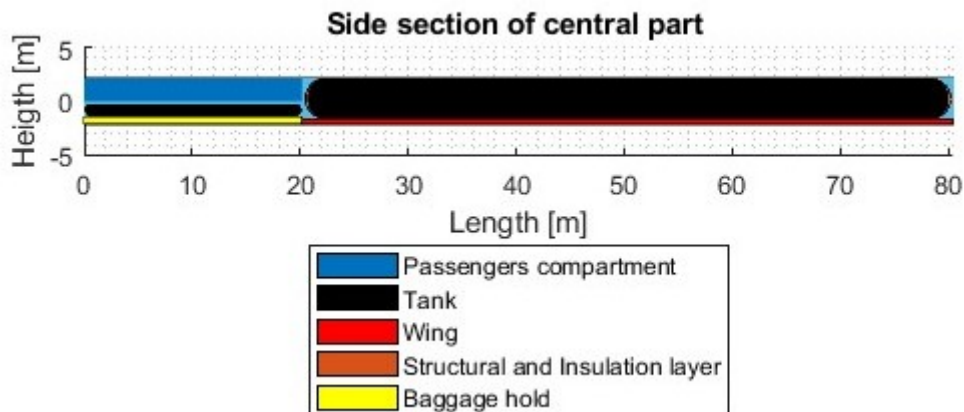


Figure 8.15: Configuration A: 80 pax and Mach 2.5

Finally, it is possible, through the program, to appreciate the variation in stress as the thickness changes for the structural part in the figures 8.16 and 8.17. Moreover, it is also possible to observe in the image 8.18 the variation in thickness of the insulating layer as the design temperature changes.

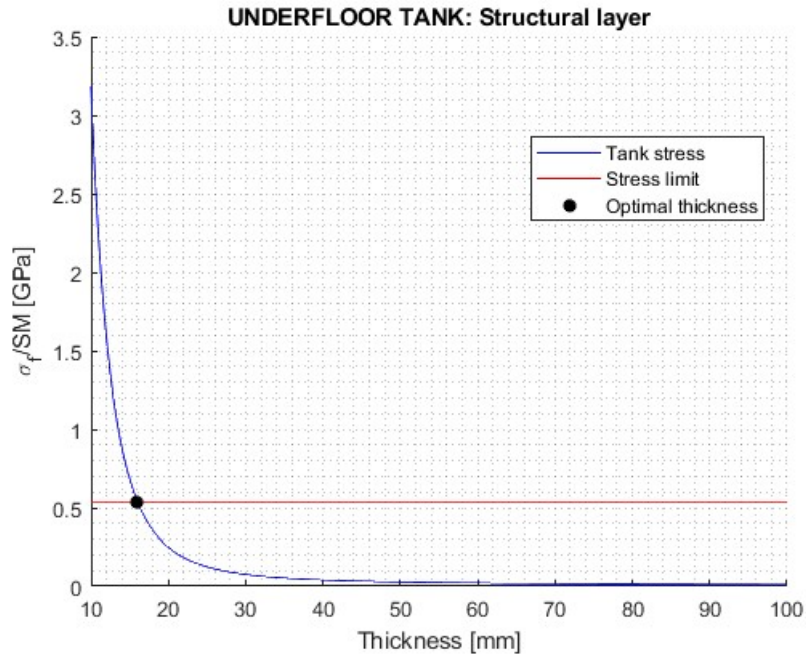


Figure 8.16: Structural layer underfloor tank

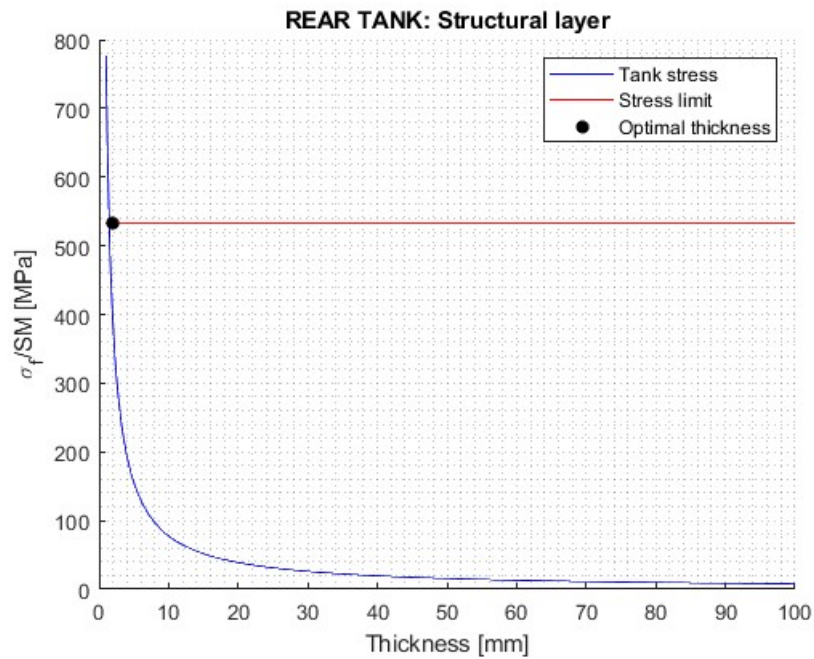


Figure 8.17: Structural layer rear tank

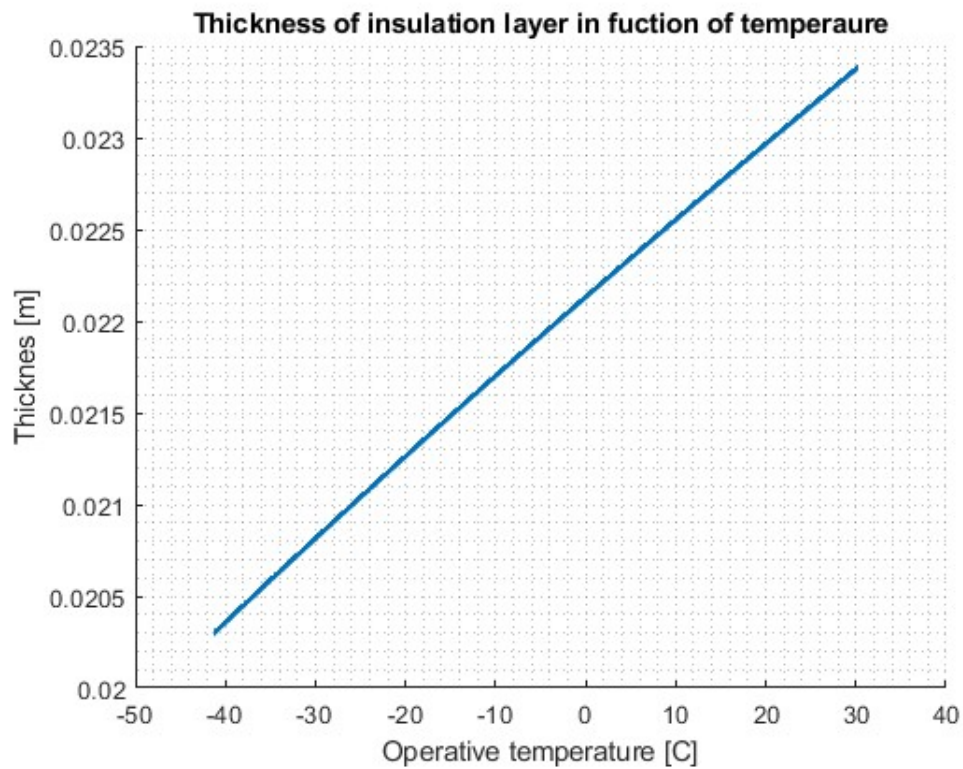


Figure 8.18: Insulation layer

8.5 End Convergence Loop

At this point, if the condition mentioned previously is satisfied, the loop ending and the program make the graphics that you see in the thesis.

Chapter 9

Aircraft center of gravity and comparison of configuration

9.1 Aircraft center of gravity

Once the iterative cycle is completed, the program proceeds with the final calculations, namely those related to the center of gravity. The latter will be approximate during the concept design phase since not all masses are available, such as the avionics component, the structural part of the wing, and so on. The only available masses are MTOW (Maximum Takeoff Weight), OEW (Operating Empty Weight), Payload, and fuel. Subsequently, the formula used is:

$$X_{CG \text{ aircraft}} = \frac{\Sigma(X_i * W_i)}{\Sigma(W_i)} \quad (9.1)$$

To find the position relative to the nose where these four available weights should be placed:

- OEW (Operating Empty Weight): It is considered to be at the midpoint of the aircraft's length.
- Payload: It is considered to be at the midpoint of the passenger compartment.
- Fuel: It is divided between the two fuel tanks based on their fuel load, with each portion positioned at the midpoint of the respective tank's length.

The center of gravity is also calculated by considering the condition of zero fuel, which means not taking into account the weight of the fuel but only the weight of the fuel tanks. This provides an initial approximation, recognizing that a significant contribution is missing at this stage, namely that of the wing and its aerodynamic center, making this calculation approximate in this phase of the project. In the table 9.1, the values of the center of gravity are shown for both the full load condition and the zero fuel condition, with the measurements considered starting from the nose.

Center of gravity					
	A (Design Point)	B	C	D	E
$CG_{max\ fuel}[m]$	41.53	40.75	42.12	32.64	49.92
$CG_{zero\ fuel}[m]$	41.27	40.52	41.84	32.74	49.31

Table 9.1: Center of gravity

9.2 Comparison of configuration

In this section, we will summarize the key aircraft data categorized by configuration, along with corresponding graphs and diagrams.

9.2.1 Configuration A: 80 pax and Mach 2

In the table 9.2, you can observe the design configuration, which is useful for comparison with results at the validity limits. Furthermore, in another figure 9.1, there is an overview of the aircraft dimensions.

Specifications		
	Unit	Configuration A
Payload	$[kg]$	9200
Propellant Mass	$[kg]$	46404
OEW	$[kg]$	151883
MTOW	$[kg]$	207487
Wing Surface	$[m^2]$	621.3
Wing Span	$[m]$	35.43
AR		2.02
Length	$[m]$	85.24
Fuselage external diameter	$[m]$	4.79
Mean Aerodynamic Chord	$[m]$	17.54
Mach		2
E_{sub}		22.33
E_{sup}		6.96
T/W_{design}		0.16
W/S_{design}		325.2

Table 9.2: Specifications of Configuration A

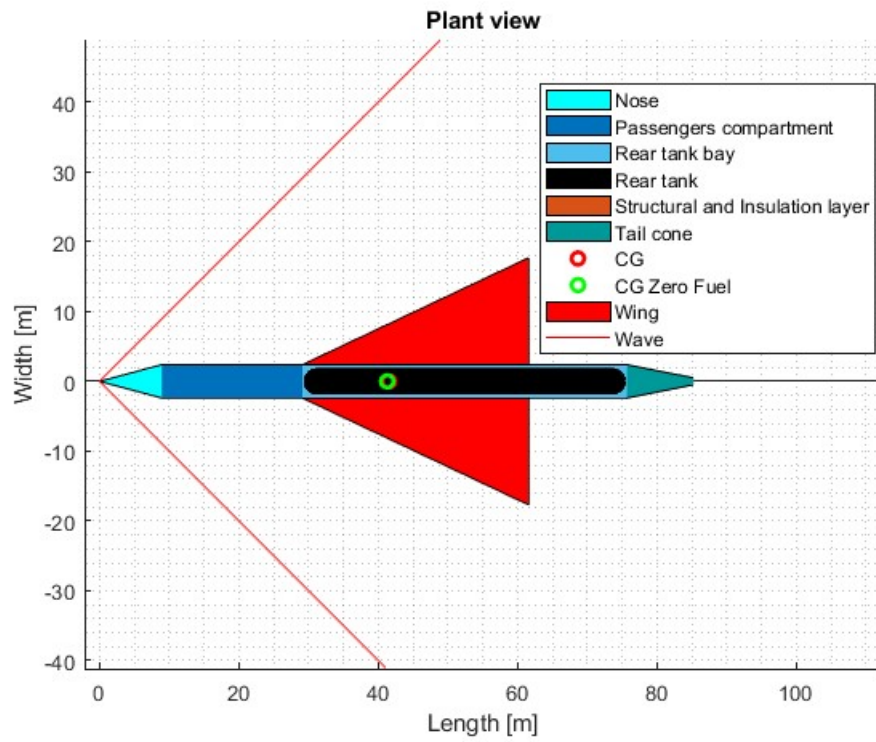


Figure 9.1: Overview configuration A

9.2.2 Configuration B: 60 pax and Mach 2

Specifications		
	Unit	Configuration B
Payload	[<i>kg</i>]	6900
Propellant Mass	[<i>kg</i>]	45128
OEW	[<i>kg</i>]	141994
MTOW	[<i>kg</i>]	194022
Wing Surface	[<i>m</i> ²]	568.44
Wing Span	[<i>m</i>]	34.58
AR		2.10
Length	[<i>m</i>]	83.34
Fuselage external diameter	[<i>m</i>]	4.79
Mean Aerodynamic Chord	[<i>m</i>]	16.44
Mach		2
E_{sub}		22
E_{sup}		6.33
T/W_{design}		0.16
W/S_{design}		330.45

Table 9.3: Specifications of Configuration B

In the table 9.3, it is noticeable that the data varies as the number of passengers decreases. There is a clear reduction in payload, fuel, OEW (Operating Empty Weight), and MTOW (Maximum Takeoff Weight). Other values also show a slight decrease, except for AR (Aspect Ratio), mean aerodynamic chord, and supersonic efficiency, which increase slightly. In the overview, there are no substantial differences observed.

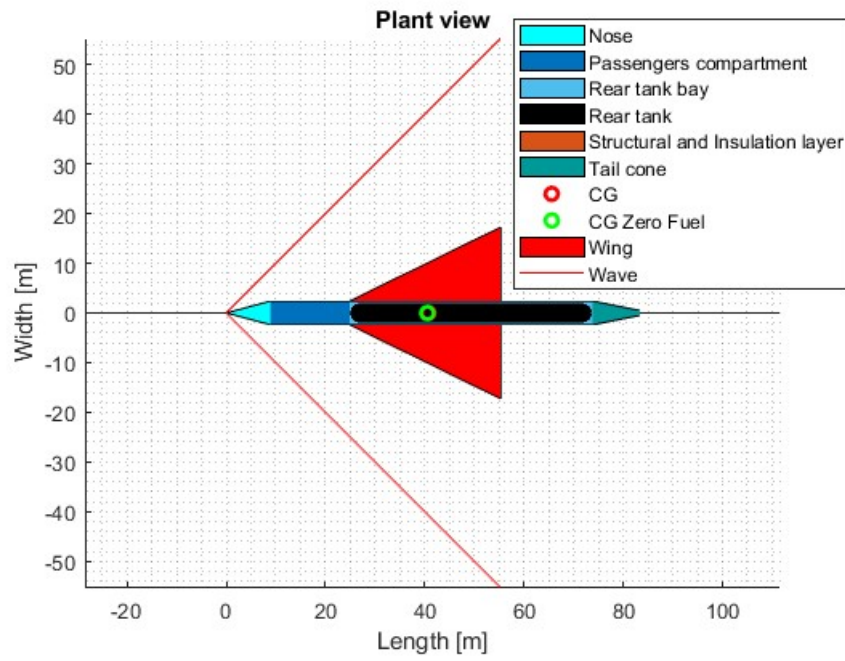


Figure 9.2: Overview configuration B

9.2.3 Configuration C: 100 pax and Mach 2

Specifications		
	Unit	Configuration C
Payload	[kg]	11500
Propellant Mass	[kg]	47361
OEW	[kg]	158325
MTOW	[kg]	217186
Wing Surface	[m ²]	655.60
Wing Span	[m]	36
AR		1.98
Length	[m]	86.7
Fuselage external diameter	[m]	4.79
Mean Aerodynamic Chord	[m]	18.21
Mach		2
E_{sub}		22.51
E_{sup}		7.37
T/W_{design}		0.16
W/S_{design}		322.12

Table 9.4: Specifications of Configuration C

For configuration C, similar observations can be made to those of configuration B, but with the directions of changes reversed. The data that decreased in configuration B now increase, and those that increased now decrease.

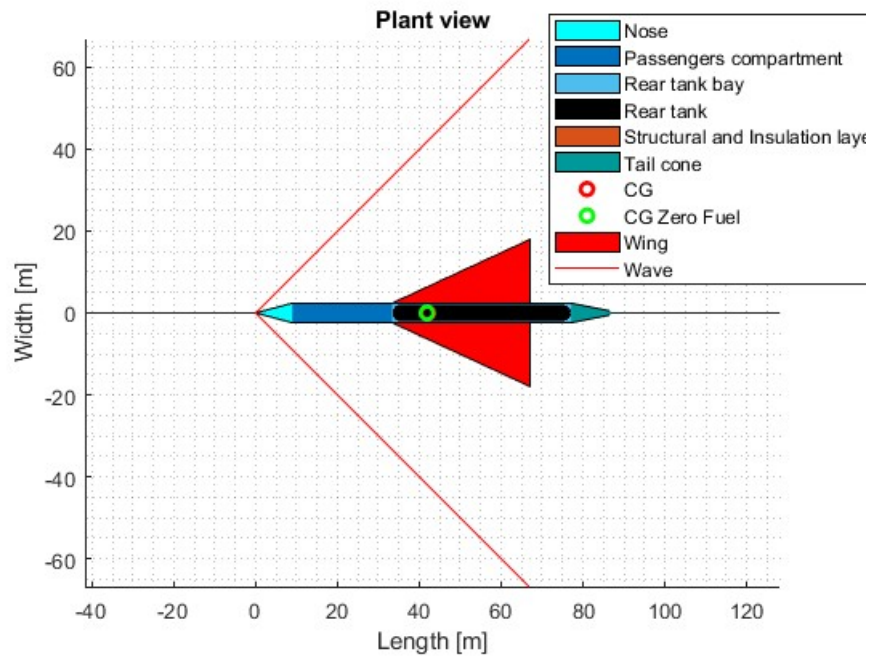


Figure 9.3: Overview configuration C

9.2.4 Configuration D: 80 pax and Mach 1.5

Specifications		
	Unit	Configuration D
Payload	[kg]	9200
Propellant Mass	[kg]	35822
OEW	[kg]	127008
MTOW	[kg]	172030
Wing Surface	[m ²]	494.33
Wing Span	[m]	28.19
AR		1.61
Length	[m]	67.84
Fuselage external diameter	[m]	4.79
Mean Aerodynamic Chord	[m]	17.54
Mach		1.5
E_{sub}		23.4
E_{sup}		6.61
T/W_{design}		0.15
W/S_{design}		337.81

Table 9.5: Specifications of Configuration D

From the table 9.5, it is observed that decreasing the Mach number to 1.5 results in a reduction in the required fuel and a decrease in weight from OEW to MTOW. The wing area slightly decreases with its consequences, and the total length of the aircraft decreases significantly.

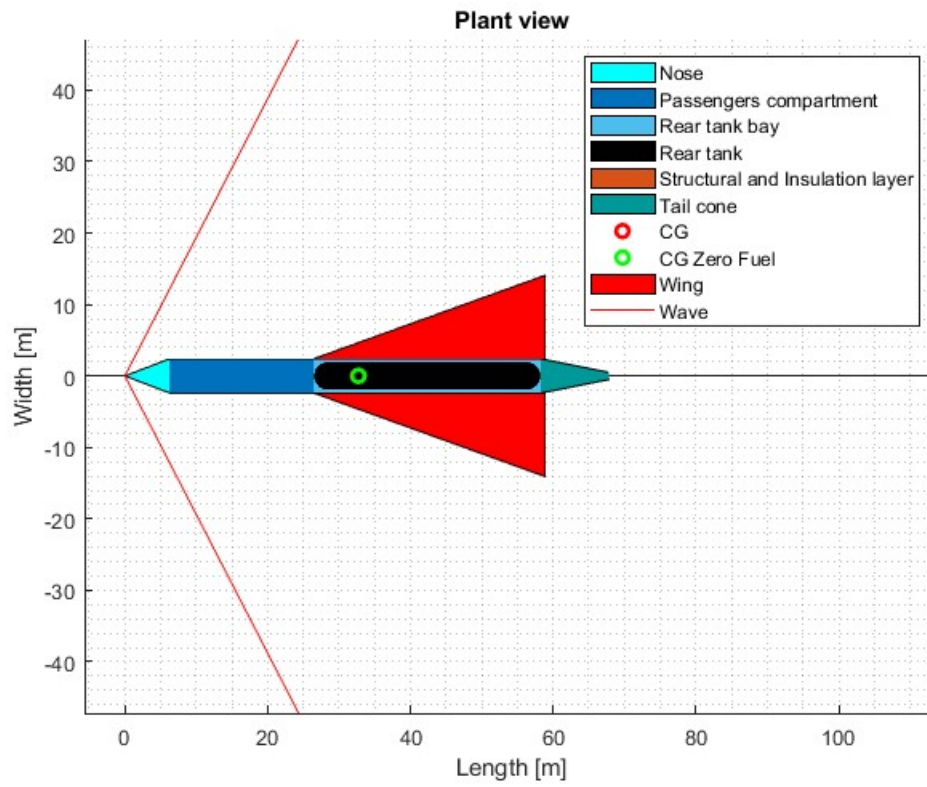


Figure 9.4: Overview of Configuration D

9.2.5 Configuration E: 80 pax and Mach 2.5

Specifications		
	Unit	Configuration E
Payload	[<i>kg</i>]	9200
Propellant Mass	[<i>kg</i>]	56307
OEW	[<i>kg</i>]	173402
MTOW	[<i>kg</i>]	238.91
Wing Surface	[<i>m</i> ²]	743.61
Wing Span	[<i>m</i>]	42.24
AR		2.4
Length	[<i>m</i>]	101.56
Fuselage external diameter	[<i>m</i>]	4.79
Mean Aerodynamic Chord	[<i>m</i>]	17.60
Mach		2.5
E_{sub}		21.59
E_{sup}		7.39
T/W_{design}		0.17
W/S_{design}		312.57

Table 9.6: Specifications of Configuration E

For configuration E, with an increase in Mach number to 2.5, it is observed that the dimensions increase significantly both in terms of length and weight.

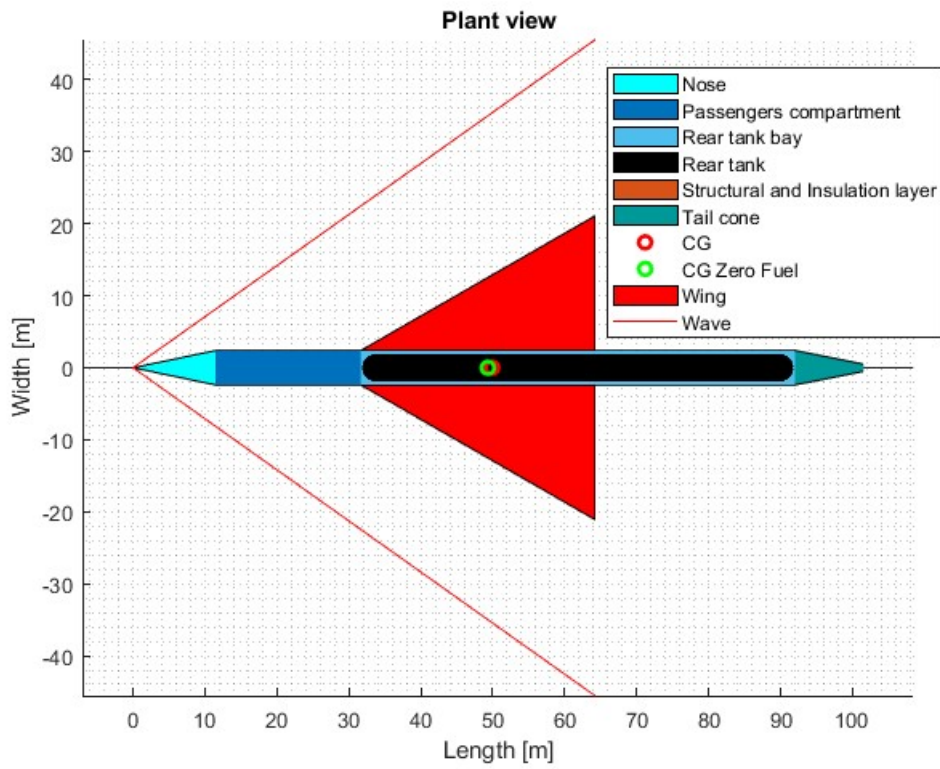


Figure 9.5: Overview of Configuration E

Chapter 10

Conclusion and future trend

The thesis objective has been achieved, as the creation of new methodology has led to obtaining good initial data for the continuation of aircraft design. The chosen operational method was that of a traditional aircraft, with appropriate modifications to various equations to extend their validity to LH2. In the preceding chapters, various results were analyzed step by step, revealing trends based on changes in high-level requirements. This is important because the values found at the design point are consistent with the new technology, and even when extending the validity range, the data quality remains good. There are certainly various aspects that can be improved in the future, with the aim of optimizing the results. First and foremost, detailed aerodynamic design could be implemented to determine the wing thickness in the first section near the fuselage, allowing for the installation of tanks in this wing box. This would reduce the volume of the rear tank and thus decrease the total length of the aircraft, a critical factor as Mach number increases.

Related to the aircraft's length, the design of the cockpit, tail, and avionics bays could be further explored. The equations used for these are quite basic and provide an estimate of the occupied length based on standard aircraft parameters. A more accurate study would yield more realistic measurements, thus optimizing the aircraft's length. The convergence loop can also be improved, as it currently considers only the main masses: payload, EOW (Empty Operating Weight), and fuel weight. It would be possible to select all avionic components and calculate their total weight, as well as create a preliminary

landing gear design to calculate its weight, thus providing MTOW (Maximum Takeoff Weight) with a value closer to reality. Similarly, once there are actual liquid hydrogen engines for aeronautical use, their weight could be added to the calculations.

In the future, the study on the engine should also be further explored because its characteristics have been derived from statistical analysis without using an existing one as a reference, due to its non-existence. It's important to remember that the Specific Fuel Consumption (SFC) has been estimated on a statistical basis and is not tied to a specific engine. This could result in different fuel consumption and, consequently, a different fuel weight, as seen. It is the fuel that predominantly defines the configuration due to the volume it occupies.

Finally, for the purpose of validating the methodology, it should be noted that configuration E is challenging to implement, primarily due to its considerable length. With the adjustments and observations just made, it could be made feasible, especially with the addition of optimization regarding the fuel tanks.

List of Figures

1.1	Projection of CO ₂ emissions from aviation (from [20])	5
1.2	Cost projection of landed costs at EU airports (from [20])	8
1.3	Cost comparison of H ₂ short-range aircraft versus kerosene and synfuel aircraft (from [20])	9
2.1	NASA Supersonic concept (from [5])	17
2.2	Lapcat A2	19
2.3	Twin Tail Boom Configuration (from [3])	20
2.4	Hydr.a. (from [2])	22
2.5	Operative Empty Weight parameters	28
3.1	Structure of the methodology	32
4.1	Mission profile with missed approach	40
5.1	$C_{L\alpha} = f(Mach)$ [15]	45
5.2	Skin roughness [15]	50
5.3	Interference Factor	52
5.4	Leading edge suction [15]	53
5.5	$K = f(Mach)$ [15]	54
5.6	$K = f(Mach)$ [15]	54
5.7	$C_D = f(Mach)$	61
6.1	Parameters for OEW	67
7.1	TOP [15]	75

7.2	Equilibrium equations in climb [13]	77
7.3	Subsonic Matching chart (Mach: 2, Pax:80)	81
7.4	Subsonic Matching chart (Mach: 2, Pax:60)	81
7.5	Subsonic Matching chart (Mach: 2, Pax:100)	82
7.6	Subsonic Matching chart (Mach: 1.5, Pax:80)	82
7.7	Subsonic Matching chart (Mach: 2.5, Pax:80)	83
7.8	Supersonic Matching chart (Mach: 2, Pax:80)	84
7.9	Supersonic Matching chart (Mach: 2, Pax:60)	84
7.10	Supersonic Matching chart (Mach: 2, Pax:100)	85
7.11	Supersonic Matching chart (Mach: 1.5, Pax:80)	85
7.12	Supersonic Matching chart (Mach: 2.5, Pax:80)	86
8.1	Available Tank Height and Internal Diameter Estimation	89
8.2	One Rounded Section Tank: Sizing Procedure	90
8.3	One Rounded Section Tank 2D	91
8.4	One Rounded Section Tank 3D [1]	91
8.5	Tank configuration	92
8.6	Fitness Ratio [19]	94
8.7	Sizing Layer Thickness Insulation Material	98
8.8	Sizing Layer Thickness Structural Material	100
8.9	Section of tank under passenger compartment	102
8.10	Section of rear tank	102
8.11	Configuration A: 80 pax and Mach 2	103
8.12	Configuration A: 60 pax and Mach 2	103
8.13	Configuration A: 100 pax and Mach 2	104
8.14	Configuration A: 80 pax and Mach 1.5	104
8.15	Configuration A: 80 pax and Mach 2.5	104
8.16	Structural layer underfloor tank	105
8.17	Structural layer rear tank	105
8.18	Insulation layer	106
9.1	Overview configuration A	111
9.2	Overview configuration B	113

9.3	Overview configuration C	115
9.4	Overview of Configuration D	117
9.5	Overview of Configuration E	119

List of Tables

2.1	Specifications of NASA Concept	17
2.2	Specifications of Lapcat A2	18
2.3	Specifications of Twin Tail Boom Configuration	20
2.4	Specifications of Hydr.a. (from [2])	21
2.5	Specifications of Low boom Concept	22
2.6	Requirements	23
2.7	Requirement	24
2.8	Mission profile	25
2.10	Fuel Weight	25
2.9	Aerodynamics	27
2.11	Operative Empty Weight	28
2.12	T/S Requirements Verification	28
2.13	T/W Requirements Verification	29
2.14	Tank sizing	29
4.1	$MTOW = f(Mach, Range)$ at Mach=2	36
4.2	$MTOW = f(Mach, Range)$ at Passengers=80	37
4.3	Other parameters at Mach=2	38
4.4	Other parameters at Passengers=80	38
5.1	Subsonic C_L first iteration	44
5.2	Subsonic C_L final iteration	44
5.3	Supersonic C_L first iteration	46
5.4	Supersonic C_L final iteration	46

5.5	E_{WD} [21]	56
5.6	Preliminary aerodynamics outputs	58
5.7	Subsonic lift output	58
5.8	Supersonic lift output	59
5.9	Subsonic drag output	59
5.10	Supersonic drag output	60
5.11	Aerodynamic efficiency	61
6.1	Constant weight ratio	68
6.2	Variable weight ratio	68
6.3	Operative empty weight	69
7.1	Wing Loading Requirements	79
7.2	Thrust to weight Requirements	80
8.1	Regulation value	93
8.2	Tank sizing output	101
9.1	Center of gravity	109
9.2	Specifications of Configuration A	110
9.3	Specifications of Configuration B	112
9.4	Specifications of Configuration C	114
9.5	Specifications of Configuration D	116
9.6	Specifications of Configuration E	118

Bibliography

- [1] Elena Sofia Abbagnato. Conceptual design methodology to size a supersonic passengers aircraft using lh2, 2021.
- [2] Buonpensiero Luca Enrico... Albert Mario. Hydr.a.lh2 supersonic aircraft. 2023.
- [3] Elena Sofia Abbagnato... Alberto Lorenzi, Carmelo Laudani. Green supersonic passenger transportation. *Politecnico di Torino*, 2019-2020.
- [4] G Daniel Brewer. *Hydrogen aircraft technology*. Routledge, 2017.
- [5] G Daniel Brewer and Ralph E Morris. Advanced supersonic technology concept study: Hydrogen fueled configuration, summary report. Technical report, NASA, 1975.
- [6] GD Brewer and RE Morris. Study of lh2 fueled subsonic passenger transport aircraft. Technical report, 1976.
- [7] Roberta Fusaro Davide Ferretto and Nicole Viola. A conceptual design tool to support high-speed vehicle design. *Politecnico di Torino*.
- [8] AAE (Academie de l'air et de l'espace Air and space academy). From concorde to new supersonic aircraft projects,aae. 2019.
- [9] Eli Dourado, Samuel Hammond, et al. Make america boom again: How to bring back supersonic transport. Retrieved from the Mercatus Research website: <https://www.mercatus.org/system/files/mercatus-dourado-supersonic-transport-v1.pdf>, 2016.
- [10] Reinhard Faass. Cryoplane: Flugzeuge mit wasserstoffantrieb. *Airbus Deutschland Cryoplane presentation*, 2001.

- [11] Nicole Viola Roberta Fusaro Davide Ferretto. Integrated aerospace system design course. *Politecnico di Torino*, 2022-2023.
- [12] Lapcat A2: https://en.wikipedia.org/wiki/Reaction_Engines_LAPCAT_A2.
- [13] Web site: <https://www1.grc.nasa.gov/beginners-guide-to-aeronautics/forces-in-a-climb/>.
- [14] Alain Picard and Laurent Madon. Mirage 2000 combat aircraft upgrade in dassault aviation: Solution for nwds system open and affordable. In *Proceedings of RTO Symposium on" Aircraft Update Programmes. The Economical Alternative*, 2000.
- [15] Daniel Raymer. *Aircraft design: a conceptual approach*. American Institute of Aeronautics and Astronautics, Inc., 2012.
- [16] Michael J Sefain. Hydrogen aircraft concepts and ground support. 2005.
- [17] Daniel Silberhorn, Georgi Atanasov, Jan-Niclas Walther, and Thomas Zill. Assessment of hydrogen fuel tank integration at aircraft level. In *Deutscher Luft-und Raumfahrtkongress*, 2019.
- [18] Clean Sky et al. Hydrogen-powered aviation: A fact-based study of hydrogen technology, economics, and climate impact by 2050. 2020.
- [19] Egbert Torenbeek. *Synthesis of subsonic airplane design: an introduction to the preliminary design of subsonic general aviation and transport aircraft, with emphasis on layout, aerodynamic design, propulsion and performance*. Springer Science & Business Media, 2013.
- [20] Hydrogen Joint Undertaking. Hydrogen powered aviation: A fact-based study of hydrogen technology, economics, and climate impact by 2050. 2020.
- [21] Nicole Viola, Roberta Fusaro, Oscar Gori, Marco Marini, Pietro Roncioni, Guido Saccone, Bayindir Saracoglu, Ali C Ispir, Christer Fureby, Thommie Nilson, et al. Stratofly mr3—how to reduce the environmental impact of high-speed transportation. In *AIAA Scitech 2021 Forum*, page 1877, 2021.

- [22] Andreas Westenberger. H2 technology for commercial aircraft. *Proceedings of the Advances on Propulsion Technology for High-Speed Aircraft, RTO, Rhode-Saint-Genese, Belgium*, pages 12–15, 2007.